6/IX-88

ISSN 0234-5366

ОБЪЕДИНЕННЫЙ
ИНСТИТУТ
ЯДЕРНЫХ
ИССЛЕДОВАНИЙ

JOINT INSTITUTE
FOR NUCLEAR
RESEARCH

N 4[30]-88

КРАТКИЕ СООБЩЕНИЯ ОИЯИ

JINR RAPID COMMUNICATIONS

Дубна 1988

Объединенный институт ядерных исследований

JOINT INSTITUTE FOR NUCLEAR RESEARCH

№4[30]-88

КРАТКИЕ СООБЩЕНИЯ ОИЯИ

JINR RAPID COMMUNICATIONS

сборник

COLLECTION

Дубна 1988

ОГЛАВЛЕНИЕ
CONTENTS

Preface 7

V.L.Aksenov
The Investigation of High Temperature Superconductors
at the Joint Institute for Nuclear Research
В.Л.Аксенов
Исследования высокотемпературных сверхпроводников
в Объединенном институте ядерных исследований 8

N.M.Plakida, V.Y.Yushankhaj
Antiferromagnetic Correlations in a Polar
Model for Oxide Superconductors
Н.М.Плакида, В.Ю.Юшанхай
Антиферромагнитные корреляции в полярной модели
оксидных сверхпроводников 14

V.L.Aksenov, S.Flach, N.M.Plakida
A Theoretical Study of Ultrasonic Anomalies
in $La_{2-x}Sr_xCuO_4$
В.Л.Аксенов, С.Флах, Н.М.Плакида
Микроскопическая теория акустических аномалий
в $La_{2-x}Sr_xCuO_4$ 22

T.Galbaatar, R.Rakauskas, J.Šulskus
Isotope Effect (O^{16} – O^{18}) in the Anharmonic Model
of High-T_c Superconductors
Т.Галбаатар, Р.Ракаускас, Ю.Шулскус
Изотопический эффект (O^{16} – O^{18}) в ангармонической
модели ВТСП 28

V.L.Aksenov, S.A.Sergeenkov
On the Phase Diagram of High-T_c Superconductive
Glass Model
В.Л.Аксенов, С.А.Сергеенков
О фазовой диаграмме в модели высокотемпературного
сверхпроводящего стекла 35

A.M.Balagurov, Hvan Chan Gen, V.A.Kudrjaschev,
G.M.Mironova, Nguyen Van Vuong, A.Pajaczkowska,
H.Shimchak, V.A.Trunov, Trinh Anh Kuan
Diffraction Stugy of Some High-T_c Superconductors with the Time-of-Flight Neutron Diffractometer DN-2
А.М.Балагуров, Хван Чан Ген, В.А.Кудряшев,
Г.М.Миронова, Нгуен Ван Вьюнг, А.Паячковска,
Х.Шимчак, В.А.Трунов, Чинь Ань Куан
Нейтронографические исследования некоторых высокотемпературных сверхпроводников на дифрактометре ДН-2 38

A.M.Balagurov, I.E.Graboj, A.R.Kaul, G.M.Mironova,
V.V.Moshchalkov, I.G.Muttik, Ja.A.Shapiro, M.E.Zalishchanskii
Neutron Scattering Study of $YBa_2Cu_3O_{6+\delta}$ $(0 < \delta < 0.8)$ Oxydes
А.М.Балагуров, И.Э.Грабой, А.Р.Кауль, Г.М.Миронова,
В.В.Мощалков, И.Г.Муттик, Я.А.Шапиро, М.Е.Залищанский
Нейтронографическое исследование структуры $YBa_2Cu_3O_{6+\delta}$ при $0 < \delta < 0,8$ 49

D.A.Korneev, L.P.Chernenko
On Determination of the Magnetic Field Penetration Depth in Oxide Superconductors by Polarized Neutrons Reflection
Д.А.Корнеев, Л.П.Черненко
Об определении глубины проникновения магнитного поля в оксидные сверхпроводники методом отражения поляризованных нейтронов 55

V.N.Duginov, I.E.Graboj, V.G.Grebinnik, I.I.Gurevich, A.R.Kaul,
B.F.Kirillov, E.P.Krasnoperov, A.B.Lazarev, B.A.Nikolsky,
V.G.Olshevsky, A.V.Pirogov, V.Yu.Pomjakushin, A.N.Ponomarev,
S.N.Shilov, V.A.Suetin, V.A.Zhukov
μSR-Investigation of the High-T_c Superconductor $HoBa_2Cu_3O_{7-\delta}$
В.Н.Дугинов, И.Э.Грабой, В.Г.Гребинник, И.И.Гуревич, А.Р.Кауль,
Е.Ф.Кириллов, Е.П.Красноперов, А.Б.Лазарев, Б.А.Никольский,
В.Г.Ольшевский, А.В.Пирогов, В.Ю.Помякушин, А.Н.Пономарев,
С.Н.Шилов, В.А.Суетин, В.А.Жуков
Исследование высокотемпературного сверхпроводника $HoBa_2Cu_3O_{7-\delta}$ μSR-методом 63

J.Wawryszczuk, T.Goworek, A.I.Ivanov, M.Lewandowski,
P.Mazurek, V.N.Rybakov, I.F.Uchevatkin, I.A.Yutlandov
Positron Annihilation in a High-Temperature Superconductor $YBa_2Cu_3O_{7-\delta}$

Я.Ваврыщук, Т.Говорек, А.И.Иванов, М.Левандовски,
П.Мазурек, В.Н.Рыбаков, И.Ф.Учеваткин, И.А.Ютландов
Аннигиляция позитронов в высокотемпературном
сверхпроводнике $YBa_2Cu_3O_{7-\delta}$ 67

A.S.Alexandrov, A.A.Astapov, V.M.Drobin, L.N.Zaitsev,
A.V.Kuznetsov, V.I.Lushchikov, E.I.Diachkov, E.A.Protasov,
G.P.Reshetnikov, V.V.Sikolenko, V.I.Smirnov, V.N.Trofimov,
S.V.Chernov, A.L.Shishkin
Effect of High Energy Radiation on Critical Parameters
of Superconducting Ceramics $YBa_2Cu_3O_7$
А.С.Александров, А.А.Астапов, В.М.Дробин, Л.Н.Зайцев,
А.В.Кузнецов, В.И.Лущиков, Е.И.Дьячков, Е.А.Протасов,
Г.П.Решетников, В.В.Сиколенко, В.И.Смирнов, В.Н.Трофимов,
С.В.Чернов, А.Л.Шишкин
Влияние излучений высокой энергии на критические параметры
сверхпроводящей керамики $YBa_2Cu_3O_7$ 73

И.Н.Гончаров, О.Е.Омельяновский
Намагниченность керамики $YBa_2Cu_3O_{7-x}$
после облучения релятивистскими ядрами углерода
I.N.Goncharov, O.E.Omelyanovsky
Magnetization of $YBa_2Cu_3O_{7-x}$ Ceramics after Irradiation
with Carbon Relativistic Nuclei 78

S.A.Korenev, D.Valentovič, V.I.Lushchikov
The Stabilization of High-Temperature
Superconductor $Y_1Ba_2Cu_3O_{7-\delta}$ Surface
С.А.Коренев, Д.Валентович, В.И.Лущиков
Стабилизация поверхности высокотемпературного
сверхпроводника $Y_1Ba_2Cu_3O_{7-\delta}$ 83

S.A.Korenev
The Emission Characteristics of $Y_1Ba_2Cu_3O_{7-\delta}$ Cathode
С.А.Коренев
Эмиссионные характеристики катода из $Y_1Ba_2Cu_3O_{7-\delta}$ 87

В.И.Дацков, Л.Миу, И.Н.Гончаров
Измерение критического тока кольцевых образцов
высокотемпературного сверхпроводника
бесконтактным методом
V.I.Datskov, L.Miu, I.N.Goncharov
The Measurement of Critical Current in HTSC Ring Probes
by the Noncontact Methods 91

V.M.Drobin, E.I.Dyachkov, V.N.Trofimov
Temperature Dependence of Critical Current and I-V Characteristics (IVC) in the $YBa_2Cu_3O_7$ (Y) and $Bi_2Sr_2CaCu_2O_8$(Bi) Ceramics
В.М.Дробин, Е.И.Дьячков, В.Н.Трофимов
Температурная зависимость критического тока и ВАХ керамик $YBa_2Cu_3O_7$ (Y) и $Bi_2Sr_2CaCu_2O_8$(Bi) 9

V.F.Bobrakov, B.V.Vasiliev, V.N.Polushkin
Squid Operating at Liquid Nitrogen Temperatures
В.Ф.Бобраков, Б.В.Васильев, В.Н.Полушкин
Сквид, работающий при азотной температуре. 10

PREFACE

This topical issue of Rapid Communications is devoted to the theoretical and experimental works in the field of high temperature superconductivity, which are being carried out at the Joint Institute for Nuclear Research. The main results obtained in the period of the 1987 year have been published in different scientific journals. Dr. V.L.Aksenov, Deputy Director of the Laboratory of Neutron Physics of JINR, refers to them in his paper. The results of the theoretical and experimental research obtained during the current year are reported in other papers included in the Communications.

The trend of this investigation is mainly defined by experimental facility the JINR has in performing condensed matter research by nuclear physics methods. The application of these methods may greatly promote the study to a better understanding of the mechanisms of superconductivity. The theoretical models elaborated and the methods being successfully developed on the basis laid as early as thirty years ago at the JINR open wide possibilities.

The Workshops on high temperature superconductivity held at Dubna in January and June, 1988 with the participation of socialist countries demonstrated high scientific potential of the Institutes of the Member-States of the JINR. The urgent task of today is to join our efforts in this most important field of modern research. I think that the JINR provides the physicists with a unique opportunity of doing that.

N.N.Bogolubov

Краткие сообщения ОИЯИ №4 [30] −88 JINR Rapid Communications No.4 [30]−88
УДК 538.945

THE INVESTIGATION OF HIGH TEMPERATURE SUPERCONDUCTORS AT THE JOINT INSTITUTE FOR NUCLEAR RESEARCH

V.L.Aksenov

This is a brief review of the performed at the JINR investigations in the field of high-temperature superconductivity physics and experimental methods exploited.

The investigation has been performed at the Laboratory of Neutron Physics, JINR.

Исследования высокотемпературных сверхпроводников в Объединенном институте ядерных исследований

В.Л.Аксенов

Дан краткий обзор проводимых в ОИЯИ исследований в области высокотемпературной сверхпроводимости и используемых экспериментальных методик.

Работа выполнена в Лаборатории нейтронной физики ОИЯИ.

The JINR program on high temperature superconductors (HTSC) in which all the Laboratories take part outlines five directions of investigation: the theory of mechanisms of superconductivity, the structure and dynamics of the lattice of HTSC, magnetic properties, the influence of irradiation on the HTSC properties, the development of SQUIDs and magnetometers on their base.

Theoretical studies are under way in the direction of the consequent consideration of strong electronic correlations /1, 2/ and strong anharmonic quasi-local lattice vibrations /3-6/ by the method suggested by N.N.Bogolubov in 1949 for the study of the polar model of metal (the Shubin-Wonsowsky model) and using the model description of the structural instability effect on superconducting pairing developed at Dubna at the end of the 70′s — beginning 80′s. Besides, the thermodynamic and dynamic properties of the superconducting glassy state characteristic for new superconductors are studied /7/. The first four papers of the Rapid Communications report on the result.

The experimental part of the program is determined essentially by the experimental apparatuses and nuclear physics methods developed at the JINR for the condensed matter research. First of all, this is particularly true for *the neutron scattering method*. The experiments which exploit such method are carried out at the Laboratory of Neutron Physics at the pulsed reactor IBR-2.

The IBR-2 reactor is one of the most advanced high flux reactors in the world. Its peak flux of thermal neutrons at the moderator surface is 10^{16} n cm^{-2} s^{-1}. At present there are no other neutron sources of such kind for scientific research in the USSR. In the nearest decade the reactor units and systems will be improved in order to increase the reactor mean power by 1.5 times, and reduce the reactor pulse in half, and obtain the thermal neutron flux of more than 10^{16} n cm^{-2} s^{-1}.

The HTSC investigations at the IBR-2 started in October, 1987. At that time the scientists got the possibility of using the reactor to conduct experiments after the planned replacement of the moving reflector. The first experiments were performed with lanthanum ceramics synthesized at the Baikov Institute of Metallurgy of the USSR Academy of Sciences. The inelastic incoherent neutron scattering spectra were measured at the KDSOG-M spectrometer on undopped and dopped by Sr (20 p.c.) lanthanum cuprate at temperatures of 10, 77 and 290 K. A new peak of the magnetic nature at about 6 meV was observed [8] at temperature below 290 K. Further experiments on samples with a strontium concentration of 10 and 30 p.c. confirm these results. The intensity of this peak increases with decreasing temperature and decreases with increasing strontium concentration. After the experiments have been accomplished the chemical composition was checked by neutron activation analysis, showing the amount of impurities (besides of Sr) below 0.5 p.c. Thus, the observed magnetic scattering seems to be intrinsic, possibly, due to short-order antiferromagnetic clusters.

The measurements on yttrium ceramics with different oxygen contents at temperatures between 10 and 290 K showed the appearance of additional magnetic scattering in the energy range from 15 to 40 meV of as yet unclear origin. These experiments were performed in collaboration with the Solid State Physics Institute of the USSR Academy of Sciences. The results are under preparation and will be published elsewhere.

The main advantage of the spectrometer KDSOG-M, i.e. the possibility of investigating the excitation spectrum at low temperatures and low transfer energies, was used in these experiments. Besides, the original property of the spectrometer is the fact that the spectrometer allows the simultaneous measurements of inelastic and quasielastic scattering. At present the mean thermal neutron flux on a sample, mounted in the spectrometer KDSOG-M is about 10^7 n $cm^{-2}s^{-1}$at a time resolution reaching 1 p.c. A higher resolution spectrometer, NERA-PR, the construction of which is nearly accomplished, will improve significantly the possibilities of measurements.

Interesting results were obtained at studying of the structure of the yttrium ceramics manufactured at the Moscow State University under changing oxygen content. Besides obtaining more detailed data on the structural phase transition, the existence of antiferromagnetic ordering at the oxygen content $x < 6.2$ was confirmed in these experiments. These results are presented in this issue of Rapid Communications. Other results of yttrium ceramics with iron substitution of copper and on bismuth ceramics are under preparation for the publication elsewhere. The measurements were performed with the diffractometer DN-2.

The DN-2 diffractometer permits the effective use of the wide spectrum of neutron wavelengths. This fact determines its advantages over the diffractometers at the stationary reactors in investigations requiring the detection of a great number of points of reciprocal space at low and middle momentum transfers and the high flux of neutrons at moderate resolution as well. The neutron flux on a sample is about 8×10^6 n $cm^{-2}s^{-1}$; a wavelength range, from 1.2 to 25 Å; and the interplanar spacing, from 0.6 to 120 Å, the resolution $\Delta d/d$ reaches 1 p.c. The diffractometer DN-2 may be efficiently used for the investigation of long-period structures ("new" bismuth compounds belong to this class also), superstructures, twins, domains and phase mixtures as well. The mentioned diffractometer is in fact the only one in the USSR, which can be used for the study of long-period structures in monocrystals.

At present the new diffractometer of high resolution (up to 0.05%), "super-SFINKS", is under construction at the IBR-2. This project is realized together with the Leningrad Institute of Nuclear Physics of the USSR Academy of Sciences (Gatchina) and the Reactor Laboratory of the Technical Centre in Finland. This project is the development of the "maxi-SFINKS" project for the high flux reactor "PIK", which is being constructed in Gatchina. It has undergone successful approbation as the "mini-SFINKS" diffractometer which is today under operation in Gatchina.

Besides the investigations mentioned above, test experiments were performed at the MURN spectrometer by the small-angle scattering method, and at the SPN-1 spectrometer by using polarized neutrons.

The method of spin relaxation of muons being developed at the Laboratory of Nuclear Problems for 15 years, gives unique possibilities for the study of magnetic properties of new superconductors on the microscopic level. The time spectrum of positrons from the positive muons decayed in matter is being measured during these experiments. Experimental data give information on the volume of superconducting phase in a sample, on the mean local magnetic field acting on a muon, on the magnetic field penetration depth and on the magnetic field distribution in vortices. Experiments carried out under various conditions, e.g. on a zero magnetic field cooled sample and on a magnetic field cooled sample with the following change of external parameters, present a more complete picture of new superconductors' behaviour in studies of a glassy state in particular.

The experiments on the study of the HTSC properties at the phasotron of the Laboratory of Nuclear Problems began last summer in collaboration with the Kurchatov Institute of Atomic Energy. Before that time, first measurements were conducted at the synchrocyclotron of the Leningrad Institute of Nuclear Physics (USSR AS) by a group of scientiscs of the Institute, the Kurchatov Institute and the Laboratiry of Nuclear Problems (JINR). This group of scientists was one of the first groups in the world applying the muon method to the study of the HTSC [9,10]. The results on the depth of magnetic field penetrating the sample and the existence of the superconductive glass phase are the most important ones.

The experiments are being carried out at the MUSPIN installation which has the muon beam intensity of 3×10^5 muon/μA with a momentum of 130 MeV/s and the beam polarization near to 80%. The counting rate of decay events with a target of 40 mm in diameter is 3×10^3 s^{-1}. The installation at the Leningrad Institute of Nuclear Physics has parameters near to those mentioned above. The measurements at the MUSPIN installation are being carried out at external fields (longitudinal and transverse) up to 0.7 T in the temperature range from 4.2 to 300 K. Further this interval is to be extended to the low temperature range.

This collection reports also on the work carried out at the Laboratory of Nuclear Problems by use of *positron annihilation.* Being the source of important information on the Fermi surface, this method will be further developed.

The JINR has unique possibilities for conducting investigations connected with the influence of *accelerated particle irradiation* on the HTSC physical properties. The main installation of the High Energy Physics Laboratory, the synchrophasotron with a proton energy of 9 GeV and the electrostatic generator of the Laboratory of Neutron Physics with a proton energy of 4 MeV may be used for irradiation, besides the mentioned phasotron for the proton acceleration to an energy of 680 MeV. The particle fluxes per cm^2/ hour are from 10^{15} to 10^{17} with a particle range in the medium from 10 to 10^4 μm. Some nuclei with energies up to 4 GeV per nucleon and a fluence from 10^6 to 10^{14} and a particle range above 10^4 um are being accelerated in the synchrophasotron as well. The accelerators of the Laboratory of Neutron Physics, the Laboratory of Nuclear Reactions and of the Institute Scientific Methodical Department (ISMD) produce the electrons with an energy from 2 to 40 MeV and a fluence of 10^{18}, a particle range being from 10^2 to 10^4 μm. The cyclotrons of the Laboratory of Nuclear Reactions used for the acceleration of ions with an atomic number from 2 to 84, with an energy from 1 to 20 MeV per nucleon and a fluence from 10^{13} to 10^{18}, and a particle range in medium from 3 to 100 μm have rather important potentialities. The first results of work at the synchrophasotron and at the installation of ISMD are presented in this collection. On the whole, it should be noted that this direction, important for further practical applications of the HTSC, is still the direction of unutilized potentialities.

A rather well developed cryogenic base of the JINR permits the conduction of *thermodynamic and electromagnetic investigations* necessary for the sample testing. Some results are presented here as well. Experience on conducting precision measurements enabled the scientists of the Laboratory of Neutron Physics to perform a very sensitive experiment on the study of the effect of the isotopic copper substitution on the temperature of the superconducting transition in yttrium ceramics /11/. Recently, the SQUID from yttrium ceramics working at liquid nitrogen temperature with sensitivity approximately equal to that of ordinary SQUIDs working at helium temperature, was manufactured at the Laboratory. The application of such SQUIDs is as yet delayed for the lack of conducting materials from HTSC.

In conclusion I would like to express hope that this compressed review of the JINR facilities and of some recent results /1-14/ together with other papers entering the given Rapid Communications will give its readers the idea of the JINR possibilities of investigation in the field of high temperature superconductivity and will promote to further scientific cooperation between the JINR Member States in this important branch of modern physics.

The author is very grateful to Academician N.N.Bogolubov and Professor A.N.Sissakian for stimulating discussions and support.

References

1. Bogolubov N.N., Aksenov V.L., Plakida N.M. Proc. of Int. Conf. on High Temperature Superconductors and Materials and Mechanisms of Superconductivity (Interlaken, 29 Feb. — 4 March 1988); Physica C, 1988, v.153, No.1.
2. Plakida N.M., Stasyuk I.V. JINR, E17-88-96, Dubna, 1988; (to be published in Int. Journal of Modern Physics B).
3. Aksenov V.L., Plakida N.M. Proc. of Int. Conf. on High Temperature Superconductors and Materials and Mechanisms of Superconductivity (Interlaken, 29 Feb. — 4 March 1988); Physica C, 1988, v.153, No.1.
4. Plakida N.M., Aksenov V.L., Drechsler S.L. — Europhys. Lett.,1987, v.4, No.11, p.1309-1314.
5. Plakida N.M., Drechsler S.L. — phys.stat.sol.(b), 1987, v.144, p.K113-K117.
6. Aksenov V.L., Flach S., Plakida N.M. — phys.stat.sol.(b), 1988, v.146, p.K1-K5.
7. Aksenov V.L., Sergeenkov S.A. JINR, E17-88-281, E17-88-354, Dubna, 1988. (submitted to Physica C).
8. Belushkin A.V. et al. — JETP Letters (in Russian), 1988, v.47, No.4, p.216-220.
9. Grebinnik V.G. et al. — JETP Letters (in Russian), 1987, v.46, Supplement, p.215-218.
10. Tarasov N.A. et al. — JETP Letters (in Russian), 1987, v.46, No.10, p.397-398.
11. Vasiliev B.V., Luschikov V.I., Sikolenko V.V. — JETP Letters (in Russian), 1988, v.47, No.5, p.276-278.

Received on May 7, 1988.

УДК 538.945

ANTIFERROMAGNETIC CORRELATIONS IN A POLAR MODEL FOR OXIDE SUPERCONDUCTORS

N.M.Plakida, V.Y.Yushankhaj

A planar tight-binding system of $Cu(3d^9)$ and $O(2p^6)$ electrons is considered in the framework of a polar model for metals. A second-quantized Hamiltonian is derived as a series expansion in powers of a small overlapping parameter, $\epsilon S \ll 1$, for $d(x^2 - y^2)$ and p_x-, p_y-orbitals. A generalized two-sublattice Hubbard model is obtained and treated perturbatively to the fourth order in ϵS. Various perturbative contributions are considered as effective spin Hamiltonians. Some comments on recent suggestions for the superconducting electron pairing due to antiferromagnetic Cu(3d) – O(2p) exchange are given.

The investigation has been performed at the Laboratory of Theoretical Physics, JINR.

Антиферромагнитные корреляции в полярной модели оксидных сверхпроводников

Н.М.Плакида, В.Ю.Юшанхай

В рамках полярной модели металла изучается двумерная система с сильной связью для электронов $Cu(3d^9)$ и $O(2p^6)$. Вторичноквантованный электронный гамильтониан представлен в виде ряда по степеням малого параметра перекрытия, $\epsilon S \ll 1$, для $d(x^2 - y^2)$ и p_x-, p_y-орбиталей. Получена обобщенная двумерная модель Хаббарда, которая исследуется в рамках операторной формы теории возмущений с точностью до четвертого порядка по ϵS. Установлено соответствие между различными вкладами теории возмущений и спиновыми гамильтонианами. Обсуждаются предложенные недавно механизмы сверхпроводящего спаривания электронов за счет антиферромагнитного Cu(3d) – O(2p) обмена.

Работа выполнена в Лаборатории теоретической физики ОИЯИ.

The existence of well-separated CuO_2 layers is a common and prominent structure peculiarity of new high-T_c superconductors. Now there is no doubt that it is just these layers that are the source of superconducting behaviour. We believe that the key electronic and magnetic properties of oxide superconductors can be understood in terms of a two-dimensional tight-binding model which includes only copper d-orbitals of $(x^2 - y^2)$ type overlapping oxygen p_x-, p_y-orbitals on a square network of Cu — O bonds. The objective of this paper is to derive an effective electron Hamiltonian for that planar system and to make its preliminary analysis. To carry it out, we follow the approach suggested by Bogolubov long ago[1,2] in developing the so-called polar model of metals[3]. This approach allows us, first, to represent the second-quantized Hamiltonian as an expansion in powers of a small overlapping parameter, $\epsilon S \ll 1$, of the Cu — O bond and, second, to employ a perturbation scheme in the operator form taking into account a strong degeneracy of the electron system examined. The general expressions derived will serve as a starting point for further studies of electronic and magnetic properties of layered superconducting compounds.

Consider a planar system with Cu ions at the square lattice points $\vec{f} = n\vec{a} + m\vec{b}$ and with two O ions per unit cell at the positions $\vec{g} = \vec{f} + \vec{r}$, $(\vec{r} = \vec{a}/2, \vec{b}/2)$. Let $\mathcal{H}_0$ be the one-particle electron Hamiltonian of the system. Then starting from the ionic Cu^{2+} (d^9) state at an $\vec{f}$-site and solving the Schrödinger equation $\mathcal{H}_0 | \Psi^{(\lambda)}_{\vec{f}}(\vec{r}) \rangle = \mathcal{E}^{(\lambda)} | \Psi^{(\lambda)}_{\vec{f}}(\vec{r}) \rangle$ for d-electrons one finds that $\lambda = (x^2 - y^2)$ is the d-orbital with the highest atomic energy $\mathcal{E}^{(x^2-y^2)} \equiv E_d$ and thus half-fulled (see, e.g.[4]). Further one adopts the fact that the wave function $\Psi_{\vec{f}}(\vec{r})$ of the $\lambda = (x^2 - y^2)$ type is overlapped through the $(pd\sigma)$-bond with four nearest oxygen orbitals: two of them $\Phi^{(x)}_{\vec{f} \pm \vec{b}/2}(\vec{r})$ are of the p_x-type and two $\Phi^{(y)}_{\vec{f} \pm \vec{b}/2}(\vec{r})$ are of the p_y-type These orbitals are of equal energy $\langle \Phi^{(a)}_{\vec{g}} | \mathcal{H}_0 | \Phi^{(a)}_{\vec{g}} \rangle = E_p$ and each of Cu — O bonds are characterized by the same overlap integral $\langle \Psi_{\vec{f}}(\vec{r}) | \Phi^{(a)}_{\vec{f} \pm \vec{r}}(\vec{r}) \rangle \equiv \epsilon S = \epsilon S^* \ll 1$. A chemical bond considered is largely ionic and its covalency degree is measured by the matrix element $\langle \Psi_{\vec{f}}(\vec{r}) | \mathcal{H}_0 | \Phi^{(a)}_{\vec{f} \pm \vec{r}}(\vec{r}) \rangle \equiv \epsilon SV \sim \epsilon S (E_d + E_p)/2$. All other atomic orbitals are assumed to exhibit much smaller overlaps for symmetry reasons and disregarded.

To obtain the second-quantized Hamiltonian of the system, we follow[1] and construct the set of orthogonalized atomic functions $\tilde{\Psi}_{\vec{f}}(\vec{r})$, $\tilde{\Phi}^{(a)}_{\vec{g}}(\vec{r})$ instead of the just introduced nonorthogonalized orbitals $\Psi_{\vec{f}}(\vec{r})$, $\Phi^{(a)}_{\vec{g}}(\vec{r})$. They can be written to the second order in (ϵS) as

$$\tilde{\Psi}_{\vec{f}}(\vec{r}) = (1 + \frac{3}{2}\epsilon^2 S^2)\, \Psi_{\vec{f}}(\vec{r}) - \frac{1}{2}\epsilon S \sum_{\pm \vec{r}'} \Phi^{(\beta)}_{\vec{f} + \vec{r}'}(\vec{r}) + \qquad (1)$$

$$+\frac{3}{8}\epsilon^2 S^2 \sum_{\pm\vec{r}'} \Psi_{\vec{f}+2\vec{r}'}(\vec{r}),$$

$$\tilde{\Phi}^{(\alpha)}_{\vec{f}+\vec{r}}(\vec{r}) = \Phi^{(\alpha)}_{\vec{f}+\vec{r}}(\vec{r}) - \frac{1}{2}\epsilon S[\Psi_{\vec{f}}(\vec{r}) + \Psi_{\vec{f}+2\vec{r}}(\vec{r})] + \tag{1}$$

$$+\frac{3}{8}\epsilon^2 S^2 \sum_{\pm\vec{r}'} [\Phi^{(\beta)}_{\vec{f}+\vec{r}'}(\vec{r}) + \Phi^{(\beta)}_{\vec{f}+2\vec{r}+\vec{r}'}(\vec{r})],$$

and possess the property $\langle\tilde{\Psi}_{\vec{f}}(\vec{r}) | \tilde{\Phi}^{(\alpha)}_{\vec{f}\pm\vec{r}}(\vec{r})\rangle = 0$. Now let us introduce the set of Fermi-operators $a^+_{\vec{j}\sigma}$ ($a_{\vec{j}\sigma}$) each of which creates (destroys) an electron with a spin σ in a state $|\Psi_{\vec{f}}(\vec{r})\rangle$ if $\vec{j}=\vec{f}$ and in $|\tilde{\Phi}^{(\alpha)}_{\vec{g}}(\vec{r})\rangle$ if $\vec{j}=\vec{g}$. Then the one-particle part of the electron Hamiltonian to the second order in ϵS can be represented in the form

$$\mathcal{H}_0 = E_d \sum_{\vec{f},\sigma} n_{\vec{f},\sigma} + E_p \sum_{\vec{g},\sigma} n_{\vec{g},\sigma} + \epsilon t_{fg} \sum_{<\vec{f},\vec{g}>,\sigma} (a^+_{\vec{f},\sigma} a_{\vec{g},\sigma} + \text{h.c.}) +$$

$$+\epsilon^2 t_{ff} \sum_{<\vec{f},\vec{f}'>,\sigma} a^+_{\vec{f},\sigma} a_{\vec{f}',\sigma} + \epsilon^2 t_{gg} \sum_{<\vec{g},\vec{g}'>,\sigma} a^+_{\vec{g},\sigma} a_{\vec{g}',\sigma}, \tag{2}$$

where $<\vec{i},\vec{j}>$ refers to neighbouring sites, and the hopping integrals can be expressed in terms of the above defined quantities as $\epsilon t_{fg} = \epsilon S[V-(E_d+E_p)/2]$, $\epsilon^2 t_{ff} = \epsilon^2 S^2[3/4\,E_d + 1/4\,E_p - V]$, $\epsilon^2 t_{gg} = \epsilon^2 S^2[3/4 E_p + 1/4 E_d - V]$. Proceeding to the interaction Hamiltonian one should consider the dependence of Coulomb matrix elements

$$V(\vec{i}\vec{j}/\vec{i}'\vec{j}') = \int d^3r_1 \int d^3r_2\, \overset{*}{\psi}_{\vec{i}}(\vec{r}_1)\, \overset{*}{\psi}_{\vec{j}}(\vec{r}_2)\, e^2/r_{12}\, \psi_{\vec{j}'}(\vec{r}_2)\, \psi_{\vec{i}'}(\vec{r}_1)$$

on mutial electron site positions $\vec{i},\vec{j},\vec{i}',\vec{j}'=\vec{f},\vec{g}$. The main contributions up to the second order in ϵS are due to

$$V(\vec{i}\vec{j}/\vec{i}\vec{j}) \sim 0(1),$$

$$V(\vec{i}\vec{j}/\vec{i}\vec{j}') \sim V(\vec{i}\vec{j}/\vec{i}'\vec{j}) \sim \epsilon S, \quad \text{if } (\vec{j},\vec{j}') = \text{n.n.} \text{ or } (\vec{i},\vec{i}') = \text{n.n.},$$

$$V(\vec{i}\vec{j}/\vec{i}\vec{j}') \sim V(\vec{i}\vec{j}/\vec{i}'\vec{j}) \sim \epsilon^2 S^2, \text{ if } (\vec{j},\vec{j}') = \text{n,n.n.} \text{ or } (\vec{i},\vec{i}') = \text{n.n.n.},$$

$$V(\vec{i}\vec{j}/\vec{i}'\vec{j}') \sim \epsilon^2 S^2, \quad \text{if} \quad (\vec{j},\vec{j}') = \text{n.n.} \quad \text{and} \quad (\vec{i},\vec{i}') = \text{n.n.}.$$

Here n.n. and n.n.n. mean the nearest-neighbour and the next-to-nearest-neighbour sites. As a result, the interaction Hamiltonian can be written as

$$\mathcal{H}_{int} = \mathcal{H}^{(0)}_{int} + \mathcal{H}^{(1)}_{int} + \mathcal{H}^{(2)}_{int},$$

$$\mathcal{H}^{(0)}_{int} = \frac{1}{2} \sum_{\vec{i},\vec{j};\sigma,\sigma'} V(\vec{i}\vec{j}/\vec{i}\vec{j})\, n_{\vec{i}\sigma} (n_{\vec{j}\sigma'} - \delta_{\vec{i}\vec{j}}\delta_{\sigma\sigma'}),$$

$$\epsilon \mathcal{H}^{(1)}_{int} = \sum_{\substack{<\vec{i},\vec{j}>=\text{n.n.}\\ \vec{\ell};\sigma,\sigma'}} V(\vec{i}\vec{\ell}/\vec{j}\vec{\ell})(n_{\vec{\ell}\sigma'} - \delta_{\vec{i}\vec{\ell}}\delta_{\sigma\sigma'})\, a^+_{\vec{i}\sigma} a_{\vec{j}\sigma},$$

$$\epsilon^2 \mathcal{H}^{(2)}_{int} = \sum_{\substack{<\vec{i},\vec{j}>=\text{n.n.n.}\\ \vec{\ell};\sigma,\sigma'}} V(\vec{i}\vec{\ell}/\vec{j}\vec{\ell})\, n_{\vec{\ell}\sigma'} a^+_{\vec{i}\sigma} a_{\vec{j}\sigma} + \tag{3}$$

$$+ \frac{1}{2} \sum_{\substack{<\vec{i},\vec{i}'>=\text{n.n.}\\ <\vec{j},\vec{j}'>=\text{n.n.}\\ \sigma,\sigma'}} V(\vec{i}\vec{j}/\vec{j}'\vec{j}')\, a^+_{\vec{i}\sigma} a^+_{\vec{j}\sigma'} a_{\vec{j}'\sigma'} a_{\vec{i}'\sigma}.$$

The Hamiltonian (2), (3) has a very complicated form to be treated. Further in this paper we restrict ourselves to the most strong on-site Coulomb repulsion $V(\vec{i}\vec{i}/\vec{i}\vec{i}) \equiv V_{d,p}$. In this case the Hamiltonian reduces to a generalized two-sublattice Hubbard model with hopping terms being considered as a perturbation $\mathcal{H} \to H = H_0 + \epsilon H_1 + \epsilon^2 H_2$, where

$$H_0 = E_d \sum_{\vec{f},\sigma} n_{\vec{f}\sigma} + E_p \sum_{\vec{g},\sigma} n_{\vec{g}\sigma} + \frac{1}{2} V_d \sum_{\vec{f},\sigma} n_{\vec{f}\sigma} n_{\vec{f}-\sigma} +$$

$$+ \frac{1}{2} V_p \sum_{\vec{g},\sigma} n_{\vec{g}\sigma} n_{\vec{g}-\sigma}, \quad H_1 = t_{fg} \sum_{<\vec{f},\vec{g}>,\sigma} (a^+_{\vec{f}\sigma} a_{\vec{g}\sigma} + \text{h.c.}), \tag{4}$$

$$H_2 = t_{ff} \sum_{<\vec{f},\vec{f}'>,\sigma} a^+_{\vec{f}\sigma} a_{\vec{f}'\sigma} + t_{gg} \sum_{<\vec{g},\vec{g}'>,\sigma} a^+_{\vec{g}\sigma} a_{\vec{g}'\sigma}.$$

We choose the parameters of the model to be such that, first, an initial undoped state belongs to a manifold L of state vectors $|\phi_0(\{N_{\vec{i}}\})>^{(\text{undop.})}$ with single occupied $\vec{f}$-sites and double occupied $\vec{g}$-sites, i.e. $|\phi_0(\{N_i\})>^{(\text{undop.})} = |\phi_0(\{N_f = 1, N_g = 2\})>$ and, second, doping creates holes at $\vec{g}$-sites rather than at $\vec{f}$-sites, i.e. $|\phi_0(\{N_i\})>^{(dop.)} = |\phi_0(\{N_f = 1, N_g = 2, 1\}>$. This is true when $(E_p + V_p) - E_d \equiv \mathcal{E} > 0$ and $(E_d + V_d) - (E_p + V_p) = V_d - \mathcal{E} > 0$. To be more definite, we assume also that ϵt_{fg}, $\epsilon^2 t_{ff}$, $\epsilon^2 t_{gg} << V_d$, $\mathcal{E}$, $V_d - \mathcal{E}$, and do not constrain a value of V_p. A similar model was proposed by Emery [5] and investigated by several authors [6,7].

Now we are interested in the ground state and low-lying excited states which clearly belong to the above-defined manifold L of single occupied $\vec{f}$-site states. Let us introduce the operator P projecting an arbitrary state vector $|\phi>$ of the system onto L, i.e. $P|\phi> = |\phi_0>$. Note that $H_0 P|\phi> = E_0 P|\phi>$ and thus the energy level E_0 is strongly degenerated. In its turn the projection operator $(1 - P)$ gives highly excited, polar, states of the system separated from the E_0-level by energies V_d, $V_d - \mathcal{E}$ and $\mathcal{E}$. To remove the degeneracy mentioned, we find an effective Hamiltonian $P\tilde{H}P$ which operates in the L subspace, instead of initial H (from (4)). The operator form of perturbation theory developed in [1-2] permits us to obtain the following expansion

$$P\tilde{H}P = P\tilde{H}_0 P + \sum_{n=1}^{\infty} \epsilon^n P\tilde{H}_n P . \tag{5}$$

The problem will be treated to the fourth order in ϵ. Let us introduce the operator $R = (H_0 - E_0)^{-1} \times (1 - P)$ which involves the excited polar states to the theory as virtual ones and write the necessary expressions

$$(1) \quad P\tilde{H}_0 P = P(E_d \sum_{\vec{f},\sigma} n_{\vec{f}\sigma} + E_p \sum_{\vec{g},\sigma} n_{\vec{g}\sigma} + \frac{1}{2} V_p \sum_{\vec{g},\sigma} n_{\vec{g}\sigma} n_{\vec{g}-\sigma}) P , \tag{6}$$

$$(\epsilon) \quad P\tilde{H}_1 P = PH_1 P , \tag{7}$$

$$\begin{aligned} (\epsilon^2) \quad & P\tilde{H}_2 P = P\tilde{H}_2^{(1)} P + P\tilde{H}_2^{(2)} P , \\ & P\tilde{H}_2^{(1)} P = -PH_1 RH_1 P , \quad P\tilde{H}_2^{(2)} P = PH_2 P , \end{aligned} \tag{8}$$

$$\begin{aligned} (\epsilon^3) \quad & P\tilde{H}_3 P = P\tilde{H}_3^{(1)} P + P\tilde{H}_3^{(2)} P , \\ & P\tilde{H}_3^{(1)} P = PH_1 RH_1 RH_1 P , \quad P\tilde{H}_3^{(2)} P = -PH_1 RH_2 P - PH_2 RH_1 P , \end{aligned} \tag{9}$$

$$(\epsilon^4) \quad P\tilde{H}_4 P = \sum_{i=1}^{4} P\tilde{H}_4^{(i)} P , \tag{10}$$

$$P\tilde{H}_4^{(1)}P = -PH_1RH_1RH_1RH_1P\,, \qquad P\tilde{H}_4^{(2)}P = -PH_2RH_2P\,,$$

$$P\tilde{H}_4^{(3)}P = PH_1RH_2RH_1P\,, \tag{10}$$

$$P\tilde{H}_4^{(4)}P = PH_1RH_1RH_2P + PH_2RH_1RH_1P\,.$$

Below we follow /1/ and treat various perturbative contributions (6)-(10) as exchange spin Hamiltonians. We present some principal results gained in this way without details.

One can see that $P\tilde{H}_1P = P\tilde{H}_3P = 0$ holds both in the undoped ($N_f = 1$, $N_g = 2$) and doped ($N_f = 1$, $N_g = 2,1$) system. Proceeding to even terms let us start with the former case. Then one can get

$$P\tilde{H}_2^{(1)}P = J'_{\vec{f}\vec{g}} \sum_{<\vec{f},\vec{g}>} \vec{S}_{\vec{f}}\vec{S}_{\vec{g}}\,. \tag{11}$$

Here $J'_{fg} = 2t_{fg}^2/(V_d - \mathcal{E})$ and $\vec{S}_i$ is the spin operator at an $\vec{i}$-th site. Since $<\phi_0|\vec{S}_{\vec{f}\vec{g}}|\phi_0>^{(\text{undop.})} = 0$ and $P\tilde{H}_2^{(2)}P = 0$, the second order contribution does not remove the spin degeneracy of $\vec{f}$-sites. The next approximation $\sim \epsilon^4$ yields

$$P\tilde{H}_4^{(1)}P + P\tilde{H}_4^{(2)}P = (J'_{ff} + J''_{ff}) \sum_{<\vec{f},\vec{f}'>} \vec{S}_{\vec{f}}\vec{S}_{\vec{f}'}\,, \tag{12}$$

where $J'_{ff} = 2t_{fg}^4/V_d(V_d - \mathcal{E})^2 > 0$, $J''_{ff} = 2t_{ff}^2/V_d > 0$; besides

$$P\tilde{H}_4^{(3)}P = I_{ff} \sum_{<\vec{f},\vec{f}'>} (S^+_{\vec{f}}S^-_{\vec{f}'} + S^-_{\vec{f}}S^+_{\vec{f}'})\,, \tag{13}$$

where $I_{ff} = t_{fg}^2 t_{ff}/(V_d - \mathcal{E})^2$ and the final term is $P\tilde{H}_4^{(4)}P = 0$. Thus, the behaviour of $\vec{f}$-sites electron spins is governed by the anisotropic Heisenberg Hamiltonian with exchange constants $J^z_{ff} = J'_{ff} + J''_{ff}$, $J^x_{ff} = J^y_{ff} = J^z_{ff} + I_{ff}$. In particular, concerning CuO_2 layers in the $La\,CuO_4$ compound /8/ one may deduce that the parameters of the model considered are such that they make an antiferromagnetic ground state preferable.

Now let us turn to the doped system. The second-order contribution now gives more complicated Hamiltonian forms:

$$P\tilde{H}_2^{(1)}P = (J'_{fg} + J''_{fg}) \sum_{<\vec{f},\vec{g}>} \vec{S}_{\vec{f}}\vec{S}_{\vec{g}} +$$

$$+ \frac{J'_{fg} + J''_{fg}}{2} \sum_{<\vec{f},\vec{g}\neq\vec{g}'>} (S^-_{\vec{f}} a^+_{\vec{g}\uparrow} a_{\vec{g}'\downarrow} + S^+_{\vec{f}} a^+_{\vec{g}\downarrow} a_{\vec{g}'\uparrow}) -$$

$$- \frac{J'_{fg}}{2} \sum_{<\vec{f},\vec{g}\neq\vec{g}'>} (n_{\vec{f}\downarrow} a^+_{\vec{g}\uparrow} a_{\vec{g}'\uparrow} + n_{\vec{f}\uparrow} a^+_{\vec{g}\downarrow} a_{\vec{g}'\downarrow}) + \tag{14}$$

$$+ \frac{J''_{fg}}{2} \sum_{<\vec{f},\vec{g}\neq\vec{g}'>} (n_{\vec{f}\uparrow} a^+_{\vec{g}\uparrow} a_{\vec{g}'\uparrow} + n_{\vec{f}\downarrow} a^+_{\vec{g}\downarrow} a_{\vec{g}\downarrow}),$$

$$PH_2^{(2)}P = t_{gg} \sum_{<\vec{g},\vec{g}'>} a^+_{\vec{g}\sigma} a_{\vec{g}'\sigma} . \tag{15}$$

Here $J'_{fg} = 2t^2_{fg}/(V_d - \mathcal{E})$, $J''_{fg} = 2t^2_{fg}/\mathcal{E}$, and $<\vec{f},\vec{g}\neq\vec{g}'>$ implies summation over pairs of $\vec{g}\neq\vec{g}'$ sites with a common intervening $\vec{f}$-site under summation too. Of course, one should keep in mind that derived expressions (14), (15) are applicable in the L subspace where $N_f = 1$, $N_g = 2{,}1$. The next fourth-order terms retain the spin forms (12), (13) provided that a small doping causes a weak renormalization of exchange constants. The derived expressions give us a starting point for further studies of electronic and magnetic properties of layered superconductors.

Emery [5], treating this model (with $\epsilon H_2 = 0$) actually on a similar perturbative basis, proposed a mechanism of superconducting pairing of O(2p) holes through O(2p) - Cu(3d) exchange. We note that the present formally strict approach excludes the virtual process underlying the antiferromagnetic pairing mechanism proposed by Emery. On the other hand, the qualitative suggestion made by Hirsh [6] seems to us very attractive. Hamiltonians (14), (15) and (12), (13) derived in this paper may serve as a quantitative basis in developing this suggestion.

The authors are greatly indebted to Academician N.N.Bogolubov for helpful discussions.

References

1. Bogolubov N.N. Lekcii z kvantovoj statistiti (in Ukranian). Kiev, Rad.Sk., 1949. L[illegible]s on Quantum Statistics,(Gordon and Breach, New York, 1967).

2. Bogolubov N.N., Tyablikov S.V. -- J.Exp.Theor.Phys., 1949, 19, p.251.
3. Shubin S.P., Wonsowsky S.V. — Proc. Roy. Soc., 1934, A145 p.159.
4. Weber W. -- Z.Phys., 1988, 70, No.3, p.323.
5. Emergy V.J. — Phys.Rev.Lett., 1987, 58, p.2794.
6. Hirsh J.E. -- Phys.Rev.Lett., 1987, 59, p.288; 1988, 60, p.379.
7. Jefferson J.H. — J.Phys.C: Solid St. Phys., 1988, 21, p.L193.
8. Vaknin D. et al. -- Phys.Rev.Lett., 1987, 58, p.2802.

Received on May 5, 1988.

УДК 538.945

A THEORETICAL STUDY OF ULTRASONIC ANOMALIES IN $La_{2-x}Sr_xCuO_4$

V.L.Aksenov, S.Flach, N.M.Plakida

A microscopical model for description of acoustic properties at structural phase transition in $La_{2-x}Sr_xCuO_4$ superconductors is proposed. Experimentally observed acoustic anomalies are described in the framework of the model.

The investigation has been performed at the Laboratory of Theoretical Physics, JINR.

Микроскопическая теория акустических аномалий в $La_{2-x}Sr_xCuO_4$

В.Л.Аксенов, С.Флах, Н.М.Плакида

Предложена микроскопическая модель, описывающая влияние структурного фазового перехода в лантановых оксидных сверхпроводниках на их упругие свойства. Дано объяснение наблюдаемым экспериментально акустическим аномалиям.

Работа выполнена в Лаборатории теоретической физики ОИЯИ.

Recently a number of investigations of ultrasonic attenuation and elastic constants in $La_{2-x}Sr_xCuO_4$ was done /1-5/. The measured anomalies in the sound velocity are expected to be caused by a structural phase transition (SPT) D^{17}_{4h} - D^{18}_{2h} at $T \neq T_0$ /4/ . This tetragonal-to-orthorhombic SPT results from the softening of the tilting mode (CuO_6 – octahedra rotations around (± 1, 1, 0)-axis) at the X-point of the Brillouin zone (BZ) denoted by wave vectors $\vec{q}_1$ and $\vec{q}_2$ /6/. A model for the microscopic description of this SPT was given in /6/. Thus, the strong $T_0(x)$ – dependence was proposed and a good agreement was reached with results of inelastic neutron scattering experiments /5/.

As was shown in /6/, the SPT can be described by the motion of oxygen ions using the Hamiltonian:

$$H = \sum_{\ell,k} \frac{m}{2} \dot{X}^2(\ell,k) + \frac{1}{4} \sum_{\ell,k} BX^4(\ell,k) +$$

$$+ \frac{1}{2} \sum_{\substack{\ell,\ell' \\ k,k'}} \phi_{kk'}(\ell,\ell') X(\ell,k) X(\ell',k') , \qquad (1)$$

where X(l, k) are the displacements of the k-th oxygen ion in the l-th unit cell along the z-axis (for details we refer to [6]).

Using the transformation

$$X(\ell, k) = \frac{1}{2}\frac{1}{\sqrt{2m}}[\vec{\xi}_k \times (\vec{R}(\vec{\ell} + a\vec{\xi}_k) - \vec{R}(\vec{\ell})]_z \tag{2}$$

with $\vec{\xi}_1 = (1, 0, 0)$, $\vec{\xi}_2 = (0, 1, 0)$ we introduce the octahedron rotation coordinates R_λ ($\lambda = 1, 2$). As a result explicit expressions of the soft-mode frequency Ω_0 at the X-point of BZ and of the order parameter $|\langle R_\lambda(\ell)\rangle|$ were given [6].

To introduce the deformation we follow the notations of [7-10] expanding the potential energy of the distorted lattice in terms of the localized strain tensor e_{ij}:

$$H_e = \frac{1}{2}\sum_{\ell,\alpha} M\dot{u}_\alpha^2(\ell) + \sum_\ell [\frac{1}{2}C_{11}\{e_{11}^2(\ell) + e_{22}^2(\ell)\} +$$

$$+\frac{1}{2}C_{33}e_{33}^2(\ell) + C_{13}\{e_{11}(\ell)e_{33}(\ell) + e_{22}(\ell)e_{33}(\ell)\} + \tag{3}$$

$$+C_{12}e_{11}(\ell)e_{22}(\ell) + \frac{1}{2}C_{66}e_{12}^2(\ell) + \frac{1}{2}C_{44}\{e_{12}^2(\ell) + e_{23}^2(\ell)\}].$$

C_{ij} are the elastic constants of the tetragonal lattice, M is the total mass of atoms in the unit cell. $u_\alpha(\ell)$ and $M\dot{u}_\alpha(\ell)$ are the position and momentum of the c.m. of the l-th unit cell, respectively. The elastic strains can be expressed by means of the normal coordinates $Q(\mu, \vec{q})$ of the μ-th acoustic branch with frequency $\omega(\mu, \vec{q})$, wave vector $\vec{q}$ and polarization vector $\vec{e}(\mu, \vec{q})$:

$$e_{ij}(\ell) = \langle e_{ij}(\ell)\rangle + u_{ij}(\ell), \tag{4-1}$$

$$u_{ij}(\ell) = -\frac{i}{2\sqrt{N}}\sum_{\mu,\vec{q}} e^{i\vec{q}\vec{\ell}}[q_i e_j(\mu,\vec{q}) + q_j e_i(\mu,\vec{q})]Q(\mu,\vec{q}), \tag{4-2}$$

$$\langle e_{11}(\ell)\rangle = \epsilon_1, \quad \langle e_{22}(\ell)\rangle = \epsilon_2, \quad \langle e_{33}(\ell)\rangle = \epsilon_3, \quad \langle e_{12}(\ell)\rangle = \epsilon_6. \tag{4-3}$$

The static deformation ϵ_i is taken into consideration in the long-wave length limit. The dynamical part of (3) becomes

$$H_e^d = \frac{1}{2M}\sum_{q,\mu} P(\mu,-\vec{q})P(\mu,\vec{q}) + \frac{1}{2}M\sum_{\mu,\vec{q}}\omega^2(\mu,\vec{q})Q(\mu,\vec{q})Q(\mu,-\vec{q}). \tag{5}$$

The interaction between optical (soft) and acoustic phonons can be written as

$$H_{R-e} = \sum_{\substack{\alpha,\beta,\gamma,\phi \\ \ell,k,k'}} g_{\alpha\beta\gamma\phi}(k,k')\, e_{\alpha\beta}(\ell)\, X_{\gamma}(\ell,k)\, X_{\phi}(\ell,k') \,. \tag{6}$$

We are interested only in the coupling to the tilting mode:

$$H_{R-e} = \sum_{\substack{\alpha,\beta \\ \ell,k,k'}} g_{\alpha\beta}(k,k')\, e_{\alpha\beta}(\ell)\, X(\ell,k)\, X(\ell,k') \,. \tag{7}$$

Because of the tetragonal symmetry of the lattice for $T > T_0$ there exist only three independent components of $g_{\alpha\beta}$:

$$\alpha_0 = g_{xx}(k,k) = g_{yy}(k,k)\,;\ \ \beta_0 = g_{zz}(k,k)\,;\ \ \gamma_0 = g_{xy}(1,2)\,. \tag{8}$$

Transforming (7) with the help of (6) one gets:

$$H_{R-e} = \frac{1}{8m} \sum_{\substack{\ell,\ell' \\ \lambda,\lambda'}} W_{\lambda\lambda'}(\ell)\, \sigma_{\lambda\lambda'}(\ell,\ell')\, R_{\lambda}(\ell)\, R_{\lambda'}(\ell') \,, \tag{9-1}$$

with

$$W_{\lambda\lambda'}(\ell) = \begin{cases} \alpha_0 \{ e_{xx}(\ell) + e_{yy}(\ell) \} + \beta_0 e_{zz}(\ell)\,, & \lambda = \lambda', \\ \gamma_0\, e_{xy}(\ell)\,, & \lambda \neq \lambda', \end{cases} \tag{9-2}$$

$$\sigma_{\lambda\lambda'}(q) = \begin{cases} 2\,(1 - F_{\lambda}(q))\,, & \lambda = \lambda', \\ 1 - F_{\lambda}(q) - F_{\lambda'}(q) + F_{\lambda}(q)\, F_{\lambda'}(q)\,, & \lambda \neq \lambda', \end{cases} \tag{9-3}$$

$$F_x(q) = \cos q_y a\,, \qquad F_y(q) = \cos q_x (a)\,. \tag{9-4}$$

From eq. (9) one can obtain the correct $\epsilon \cdot R^2$ interaction in the phenomenological Landau expansion of the free energy /10/, where ϵ are components of stress tensor. Here we are interested only in the so-called resonant part of (9) producing a jump in the sound velocity at T_0 :

$$H_{res} = \frac{iR}{8m\sqrt{N}} \sum_{\mu,\vec{q}} Q(\mu,\vec{q}) \sum_{\ell,\lambda,\lambda'} M_{\lambda\lambda'}(\mu,\vec{q})\,\sigma_{\lambda\lambda'}(\vec{q}+\vec{q}_1)\, e^{i\vec{\ell}(\vec{q}+\vec{q}_1)} \cdot r_{\lambda}(\ell) \qquad (10)$$

with

$$M_{\lambda\lambda'}(\vec{q},\mu) = \begin{cases} (\alpha_0 \vec{q}_{\perp} + \beta_0 \vec{q}_z) \cdot \vec{e}(\mu,\vec{q}) , & \lambda = \lambda', \\ \gamma_0 \,(q_x e_y(\mu,q) + q_y e_x(\mu,q)) , & \lambda \neq \lambda', \end{cases} \qquad (11)$$

$$R = |\langle R_{\lambda}(\ell)\rangle| , \quad r_{\lambda}(\ell) = R_{\lambda}(\ell) - \langle R_{\lambda}(\ell)\rangle .$$

This resonant part vanishes in the tetragonal phase ($R = 0$). In the case of $T < T_0$ the equation of motion of the acoustic commutator Green's function $D(\mu, \vec{q}, \omega)$ becomes:

$$D(\mu,\vec{q},\omega) = [\,\omega^2 - \omega^2(\mu,\vec{q}) - \Sigma(\mu,\vec{q},\omega)\,]^{-1} . \qquad (12)$$

Neglecting the terms $\langle Q(\mu,\vec{q})\, r_{\lambda}(\ell)\rangle$, the mass operator Σ can be expressed by the commutator Green's function $G_{\lambda\lambda'}(\vec{q}, \omega)$ of the tilting mode:

$$\Sigma(\mu,\vec{q},\omega) = \frac{4R^2}{(16m)^2} [\, \sum_{\lambda'} M_{\lambda\lambda'}(\mu,\vec{q})\, \sigma_{\lambda\lambda'}(\vec{q}-\vec{q}_1)]^2 \cdot \sum_{\lambda\lambda'} G_{\lambda\lambda'}(\vec{q}-\vec{q}_1,\omega) . \qquad (13)$$

In the long-wave length limit of acoustic phonons [1-4] we can approximate $\vec{q} - \vec{q}_1 \approx -\vec{q}_1$.

The corresponding acoustic frequencies satisfy the inequality $\omega(\mu, \vec{q}) \ll \Omega_0(T)$. Using

$$G_{\lambda\lambda'}(\vec{q}_1,\omega) = [\, -\Omega_0^2(T) + \omega^2\,]^{-1} \cdot \delta_{\lambda\lambda'} ,$$

(see [8]) one can calculate the new frequency poles of $D(\mu, \vec{q}, \omega)$ and consequently the renormalized frequencies. The lower frequency corresponding to the modified acoustic energy is

$$\tilde{\omega}^2(\mu,\vec{q}) = \omega^2(\mu,\vec{q}) - \frac{a_{\mu}(\vec{q})}{\Omega_0^2} , \qquad (14)$$

with

$$a_{\mu}(\vec{q}) = \frac{8R^2}{(16m)^2} [\, \sum_{\lambda'} M_{\lambda\lambda'}(\mu,\vec{q})\, \sigma_{\lambda\lambda'}(\vec{q}_1)\,]^2 .$$

To compare (14) with the experiments /1-4/ one has to integrate $a_\mu(\vec{q})$ over all $\vec{q}$-directions as soon as only ceramic samples were used. In the case of longitudinal sound it follows:

$$a_L(q) = \frac{1}{2}\left(\frac{R}{3m}\right)^2 (2a_0 + \beta_0)^2 q^2, \tag{15-1}$$

and in the case of transverse sound:

$$a_T(q) = \frac{1}{2}\left(\frac{R}{m}\right)^2 \gamma_0^2 q^2. \tag{15-2}$$

Using $\eta_0^2(T) = 32\Gamma_0 R^2(T)$ for $T < T_0$ (see /6/) one gets (even in the case of a second order SPT as in La_2CuO_4) for the changed sound velocity $\tilde{S}_\mu$:

$$\tilde{S}_L = [S_L^2 - \frac{1}{9}\frac{1}{B}(2a_0 + \beta_0)^2]^{1/2}, \tag{16-1}$$

$$\tilde{S}_T = [S_T^2 - \frac{1}{B}\gamma_0^2]^{1/2}. \tag{16-2}$$

The change in S_μ is finite as predicted by experiments. The jump height is determined by the anharmonicity of the oxygen-Z-vibrations $B = 64\Gamma_0 \cdot m^2$ and the interaction parameters a_0, β_0 and γ_0 .

Let us discuss the influence of Sr-doping. Besides of changes in the electronic structure, there is a strong dependence of $S_\mu^2 - \tilde{S}_\mu^2$ on x_{Sr} with its maximum near x = 0.15. As was shown in /6/, there will be no noticeable B(x)-dependence, but according to (16) an increase of γ_0 with x_{Sr} up to $x \approx 0.15$ and its drastic decrease for $x > 0.15$ is to be expected. Together with the fact that S_T (for $T > T_0$) has its minimum at $x \approx 0.2$ we conclude the Sr-doping causes (besides a decrease of T_0 — see /6/) a remarcable softening of the elastic constants $C_{ij} \sim S_\mu$ in the tetragonal phase (up to $x \approx 0.2$) and furthermore an increase of the interaction strength between the deformation and the optical soft mode (up to $x = 0.15$). In summary these effects lead to a softening of the elastic constants of 50% at low temperatures for $0.15 < x < 0.2$. Thus, the possible role of the SPT in $La_{2-x}Sr_xCuO_4$ is to cause a softening of the lattice in the orthorombic phase. Note, that the change in the sound velocity (16) is independent of temperature. This is also an unexplained experimental fact /1-4/ suggesting our model to be valid over a wide temperature range. Another interesting fact is the wide temperature range of 60K-150K, where the change

$S_T \to \tilde{S}_T$ takes place. This may be caused by additional slow-relaxation dynamics. As was mentioned in [6], there are indications of nonvanishing long-time correlations $L_{\lambda\lambda} = \lim_{t \to \infty} \langle r_\lambda (t) r_\lambda \rangle \neq 0$ near the SPT, causing central peak and precursor cluster fluctuations (see [12]). It is easy to show in the case of $L \neq 0$ that there exists a resonant part in (9) even for $T > T_0$, which has the same form as (10) where the order parameter R^2 is replaced by L.

Summarizing, a model for the microscopic description of anomalous lattice behaviour in $La_{2-x}Sr_x CuO_4$ is presented. The SPT can "switch on" a remarcable softening of the elastic moduli. This softening may change through crystal fields inner properties of some excitations in the crystal, e.g. the frequency of excitons connected with d-d-excitations (see [13]). Thus, the interaction of such excitations with electrons is changed.

References

1. Horie Y., Fukami T., Mase S. — Solid State Comm., 1987, 63,p.653.
2. Bishop D.J., Gammel P.L. — Phys.Rev., 1987, B35, p.8788.
3. Fossheim K., Laegrid T. et al. — Solid State Comm., 1987, 63, p.531.
4. Yoshizaki R., Hikata T. et al. — J.J.Appl.Phys., 1987, 26, Suppl.26-3.
5. Birgeneau R.J., Chen C.Y. et al. — Phys.Rev.Lett., 1987, 59, p.1329.
6. Aksenov V.L., Flach S., Plakida N.M. — phys.stat.sol.(b), 1988, 146.
7. Feder J., Pytte E. — Phys.Rev., 1970, B1, p.4803.
8. Pytte E. — Phys.Rev., 1970, B1, p.924.
9. Konwent H., Plakida N.M. — Acta Phys.Pol., 1983, A63, p.755.
10. Plakida N.M., Shakhmatov V.S. — Physica C, 1988, C153 in print.
11. Fossheim K. — Physica Scripta, 1982, 25, p.665.
12. Aksenov V.L., Bobeth M., Plakida N.M., Schreiber J. — J.Phys., 1987, C20, p.375.
13. Weber W. — J.Phys. B., Z.Phys., 1988, 70, p.323.

Received on May 6, 1988.

Краткие сообщения ОИЯИ №4 [30]-88 *JINR Rapid Communications No.4 [30]-88*
УДК 538.945

ISOTOPE EFFECT (O^{16} – O^{18}) IN THE ANHARMONIC MODEL OF HIGH-T_c SUPERCONDUCTORS

T.Galbaatar, R.Rakauskas , J.Šulskus*

The results of a numerical simulation are presented for the oxygen isotope effect in the high-T_c oxides by solving the Schrödinger equation for a local vibrational mode of oxygen ions in a double well anharmonic potential of the form $-Ax^2/2+Bx^4/4$.

The investigation has been performed at the Laboratory of Theoretical Physics, JINR.

Изотопический эффект (O^{16}– O^{18}) в ангармонической модели ВТСП

Т.Галбаатар, Р.Ракаускас, Ю.Шулскус

Представлены результаты моделирования кислородного изотопического эффекта в высокотемпературных сверхпроводниках, полученные численным решением уравнения Шредингера для квазилокальной моды движения атомов O^{16}, O^{18} с потенциалом вида $Ax^2/2 + Bx^4/4$.

Работа выполнена в Лаборатории теоретической физики ОИЯИ.

The recent discovery of new cuprate oxide superconductors having transition temperatures T_c up to 114K /1-3/ have caused an immense activity in research of the mechanism(s) responsible for the superconductivity, in particular, whether it is mediated by phonons or not; a question which is still open. However, the recent experimental observations of the oxygen isotope effect in the LaSrCuO and YBaCuO systems /4/ indicate that phonons play a certain role in the formation of superconductivity. Thus, in the light of the new high-T_c superconductors the isotope effect becomes an important issue with respect to testing any theory intending to explain such high T_c's.

Calculations of the electronic structure /5/ demonstrate overlapping of the 3d states of copper with the 2p states of oxygen indicating the importance of the Cu-O chain for such high T_c's. It was shown /6/ that interactions of electrons with the high frequency Cu-O

**Vilnius V.Kapsukas University, 232054 Vilnius, Lith.SSR.*

bond-stretching mode can produce strong electron-phonon coupling leading to T_c around 40K. However, the pure phonon mechanism in the harmonic approximation fails to explain experimentally observed 90K in the YBaCuO system /9/ . Structural studies of the high-T_c cuprate oxides have revealed features as evidence of structural instabilities and the existence of soft modes in LaSrCuO system. The investigation of the phonon behaviour of $YBa_2Cu_3O_7$ by neutron inelastic scattering shows larger phonon density states in lower frequency modes rather than in high frequency ones /6/ which turned out to be in agreement with theoretical calculations /9/ of the phonon spectra for large coupling constant λ_s. As it was demonstrated earlier within the anharmonic model of the high-T_c superconductors /10/ large values of λ_s can be obtained as a result of interaction of electrons with the so-called soft bond-bending mode, related to the highly anharmonic vibrations of oxygen ions of the CuO_6 octahedron, due to the high susceptibility of the lattice χ_s . This idea has been backed up by the observation of unusual large Debye-Waller factors in $YBa_2Cu_3O_7$ /13/. In this paper we suggest for the vibration of the oxygen ions a double-well anharmonic model potential

$$U(x) = -Ax^2/2 + Bx^4/4 + A^2/4B , \tag{1}$$

where A and B are both positive and related through

$$U_0 = A^2/4B \qquad \text{and} \qquad x_0 = (A/B)^{1/2} \tag{2}$$

to real physical quantities, the central barrier height U_0 and it's average width x_0, respectively, thus $2x_0$ being the distance between the two minima of the potential. Units are used where $h = k_B = 1$. By introducing the dimensionless coordinate and energy

$$\xi = x/x_0 \qquad \text{and} \qquad E_n = E_n'/U_0 \tag{3}$$

one obtains the Schrödinger equation in the following form

$$-d^2\phi(\xi)/d\xi^2 + 1/\beta^2[(1-\xi^2)^2 - E_n]\phi(\xi) = 0 , \tag{4}$$

which was numerically solved for a broad set of the dimensionless parameter $\beta = \omega_0/4U_0$, where $\omega_0 = \sqrt{\frac{2A}{m}}$ is a characteristic frequency; and m, the reduced mass of the Cu-O-Cu cluster, thus a complete replacement of O^{16} by O^{18} in the cluster is simulated through decreasing β by 5%. The cluster approach is motivated by the fact that superconductivity has been observed in crystalline as well as in ceramic states. The eigenvalues E_n and eigenfunctions ϕn of the anharmonic oscillator are calculated as well as the matrix elements of the dipole moment ξ_{01} and the mean square amplitude of vibrations Q^2. The obtained anharmonic eigenfunctions ϕ_n are expanded in terms of the eigenfunctions $u_j(x)$ of the harmonic oscillator

$$\phi_n(x) = \sum_{j=0}^{N_{max}} a_j u_j(x) , \tag{5}$$

where N_{max} is fixed by the condition that $\sum_{j=0}^{N_{max}} a_j^2$ be unity within the given accuracy.

A study of the convergence accuracy of (5) indicates that it improves from 0.25% to better than 0.0001% when the number of the expansion coefficients is increased from 40 to 100. This demonstrates the strong effect of the anharmonicity on the eigenfunctions. The behaviour of the energy spectrum is illustrated in Fig. 1 in terms of $\Lambda_{1,2}/\epsilon_{01}$.

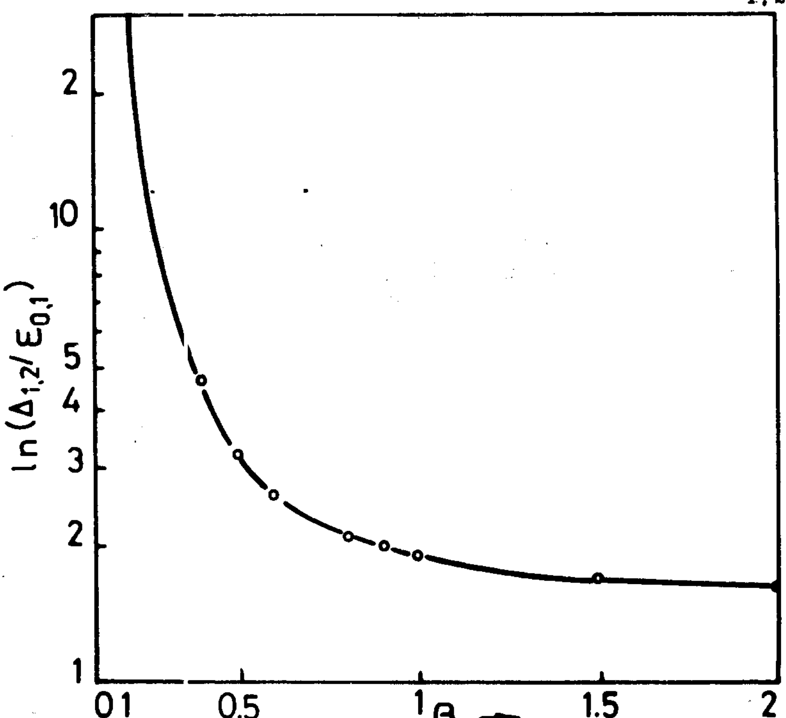

Fig. 1.

Here is

$$\Delta_{1,2} = E_2 - E_1 \, . \tag{6}$$

There, one can see two features of the above ratio demonstrating for higher levels weak and for lower ones strong anharmonicity. The same effect is observed in the dependence of the mean square amplitude of vibration (Table 1) on the anharmonicity, too, calculated by

$$Q^2 = \langle n \,|\, \xi^2 \,|\, n \rangle \, . \tag{7}$$

We found that while for larger β it steadily increases with temperature, for lower values of β an oscillating behaviour is observed.

The values of β can be estimated by the relation $\Omega_{01} = (E_1 - E_0) U_0 = \epsilon_{01} U_0$. We reckon the frequency Ω_{01}, in the case of the soft bond bending mode at range 10-30 meV. Then, for values of $\beta \sim 0.2\ U_0$ becomes very large (~1000 meV) which is unphysical. In the region $\beta = 0.4 \div 0.8\ U_0$ takes values between 10-150 meV, thus values of β in this range can be considered as physically meaningful. As one can see from Fig. 1 in this region the application of a two level approximation is allowed. According to /10/ the coupling constant is given by

$$\lambda_s = N(0) \langle J_s^2 \rangle \chi_s \, , \tag{8}$$

Table 1

The mean-square amplitude of vibration Q^2 (dimensionless) for different values of β. Underneath the corresponding eigenvalues E_n (dimensionless) are given.

β / n	0	1	2	3	4	5	6	7	8
0.125	0.951	0.932	0.753	0.785	0.452	0.718	0.717	0.815	0.897
E_n	0.242	0.243	0.681	0.689	0.985	1.09	1.30	1.53	1.77
0.42	0.650	0.922	0.801	1.08	1.24	1.38	1.54	1.65	1.79
E_n	0.631	0.842	1.79	2.71	3.84	5.12	6.51	8.00	9.57
0.6	0.594	1.01	1.04	1.31	1.53	1.69	1.89	2.04	2.27
E_n	0.777	1.33	2.82	4.48	6.41	8.58	10.88	13.37	15.99
0.84	0.597	1.13	1.29	1.59	1.68	2.07	2.32	2.51	2.73
E_n	0.982	2.12	4.51	7.26	10.41	13.89	17.64	21.64	25.85

where N(0), J_s and χ_s denote the density of states at Fermi level E_F, the deformation potential and the static susceptibility of the lattice, respectively. The latter is described in a two-level approximation by

$$\chi_s = \frac{2x_0^2 \xi_{01}^2}{\Omega_{01}} \, \mathrm{th}\,(\Omega_{01}/2T) \,, \tag{9}$$

where $x_{01} = x_0 \xi_{01}$ is the matrix element of the dipole moment between the states ϕ_0 and ϕ_1. This expression can be derived from the spectral representation

$$\chi_s = Z^{-1} \sum_{n,m} e^{-\beta E_n} \frac{1 - e^{-\beta(E_m - E_n)}}{(E_m - E_n)/U_0 - \omega/U_0} <m \,|\, \xi \,|\, n>^2 \,, \tag{10}$$

where $Z = \Sigma\, e^{-\beta E_n}$, in the static limit $\omega = 0$ by considering the two lowest levels, only. We studied the convergence of (10) taking into account up to four levels. As one can see from Table 2 it is convergent, thus the application of the two-level approximation is justified.

Table 2

The static susceptibility χ (dimensionless) calculated by taking into account 2,3 and 4 levels, respectively for three different values of β at T = 92K.

β	χ_s		
	n = 2	n = 3	n = 4
0.2	262.191	262.199	262.208
0.5	3.236	3.249	3.251
1.0	0.711	0.719	0.720

The transition temperature has been calculated by the general relation

$$T_c = \Omega_{01} \, f(\lambda_s, \mu^*) \,, \tag{11}$$

where Ω_{01} is the frequency of the phonon mode under consideration, $f(\lambda_s, \mu^*)$ is given for the weak and strong coupling cases by the McMillan /11/ and the Allan-Dynes /12/ formulas, respectively, μ^* is the

Coulomb pseudopotential. Differentiating (11) with respect to the isotopic mass one obtains the following relation for the relative shift in T_c

$$\delta T_c = dT_c / T_c = -a\, dm/m , \tag{12}$$

where

$$a = 0.5\,\left(1 + \frac{\beta\, d\epsilon}{\epsilon\, d\beta}\right)\left(1 - \frac{\lambda}{f}\frac{df}{d\lambda} - \frac{\mu^{*2} df}{f\, d\mu^*}\right) . \tag{13}$$

The isotope effect thus depends on λ_s and μ^* through the second term while the first term gives the effect of the anharmonicity on the value of a. To calculate the coupling constant we estimate x_0, $N(0)$ and J_s^2 in the following ranges: $x_0 = (0.1 \div 0.3)$ Å, $N(0) = (1 \div 3)$ states/eV and $J_s^2 = (0.5 \div 1)$ (eV/Å)^2. As is shown in Fig. 2 in the anharmonic case even an inverse isotope effect is possible for $T_c < 33$K, while in the narrow region 34-35K a nearly zero or heavily suppressed one is observed. At T_c slightly above 36K a lies in the range 0.1-0.2, depending on β; thus, it is in agreement with experimental observation for the LaSrCuO system. However, for higher T_c we found normal isotope effect with a trend of a to increase with temperature and then to saturate at 0.3-0.4, which is in contradiction with the up-to-date observed trend of a to decrease. We conclude from our numerical calculation that in the anharmonic model the phonon mechanism permits one to obtain an agreement with the experimentally observed isotope effect in the LaSrCuO system ($a \sim 0.1$-0.2) whereas it is not the case for the YBaCuO system. This may be an indication that higher energy levels have to be taken into account, otherwise a nonphonon mechanism should be considered.

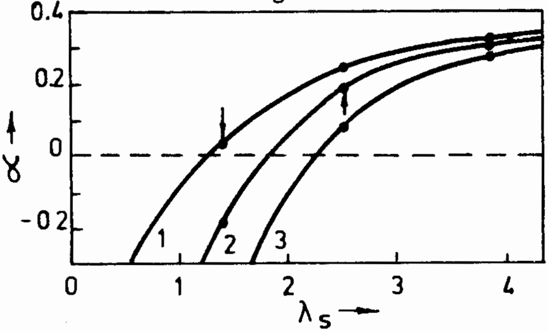

Arrows $T_c \approx 35$K

$\beta = 0.4$, $1 - \mu^* = 0$; $2 - \mu^* = 0.1$; $3 - \mu^* = 0.2$.

Fig. 2.

Finally, we would like to express our gratitude to Dr. N.M.Plakida for pointing out the problem and helpful discussions and Prof. M.G.Meshcheryakov for supporting the work.

References

1. Bednorz J.G., Müller K.A. — Z.Phys., 1986, B64, p.189.
2. Wu M.K. et al. — Phys.Rev.Lett., 1987, 58, p.908.
3. Chu C.W. et al. — Phys.Rev.Lett., 1988, 60, p.941.
4. Learey K.J. et al. — Phys.Rev.Lett., 1987, 59, p.1236.
5. Mattheiss L.F. — Phys.Rev.Lett., 1987, 58, p.1028.
6. Liu J.Q. et al. — Intern.J.Mod.Phys., 1987, B1, p.513.
7. Krumhansl J.A., Schrieffer J.R. — Phys.Rev., 1975, B11, p.3535.
8. Weber W. — Phys.Rev.Lett., 1987, 58, p.1371.
9. Weber W., Mattheiss L.F. — Phys.Rev., 1988, B37, p.599.
10. Plakida N.M. et al. — Intern.J.Mod.Phys., 1987, B1, p.1071.
11. McMillan W.L. — Phys.Rev., 1968, 167, p.331.
12. Allan P.B., Dynes R.C. — Phys.Rev., 1975, B12, p.905.
13. Caponi J.J. et al. — Europhys.Lett., 1987, 3, p.1301.

Received on May 23, 1988.

Краткие сообщения ОИЯИ №4 [30]-88 *JINR Rapid Communications No.4 [30]-88*
УДК 537.312.62

ON THE PHASE DIAGRAM OF HIGH-T_c SUPERCONDUCTIVE GLASS MODEL

V.L.Aksenov, S.A.Sergeenkov

The transition temperature T_c and isothermic magnetization are calculated as functions of applied magnetic field in the frame of the 2-D XY Josephson glass model. Three characteristic regions are shown to be distinguishable in the H-T plane: the diamagnetic region, region of superconducting glass and region of Josephson spin glass. The results are in quantitative agreement with experimental data and the results of numerical simulations for "new" superconductors.

The investigation has been performed at the Laboratory of Neutron Physics, JINR.

О фазовой диаграмме в модели высокотемпературного сверхпроводящего стекла

В.Л.Аксенов, С.А.Сергеенков

В двумерной XY модели джозефсоновских спинов вычислена зависимость температуры фазового перехода T_c и изотермической намагниченности от внешнего магнитного поля H при $0 \le H < \infty$. Показано, что на плоскости (T, H) имеются три области, различающиеся характером зависимости T_c от H: диамагнитная область, область сверхпроводящего стекла и область джозефсоновского спинового стекла. Результаты качественно согласуются с данными экспериментов и численного моделирования для "новых" сверхпроводников.

Работа выполнена в Лаборатории нейтронной физики ОИЯИ.

Many of the experimental results on the glassy behaviour of high-T_c superconductors can be explained in the 2-D disordered Josephson spin lattice model /1/. The phase diagram in the plane H-T was studied both numerically (up to fields $H \lesssim H_c^u$) /2/ and by analytical methods (for $H > H_c^u$) /3/. This paper presents the generalization to arbitrary magnetic fields. The obtained phase boundary $T_c(H)$ is shown in the upper part of the figure.

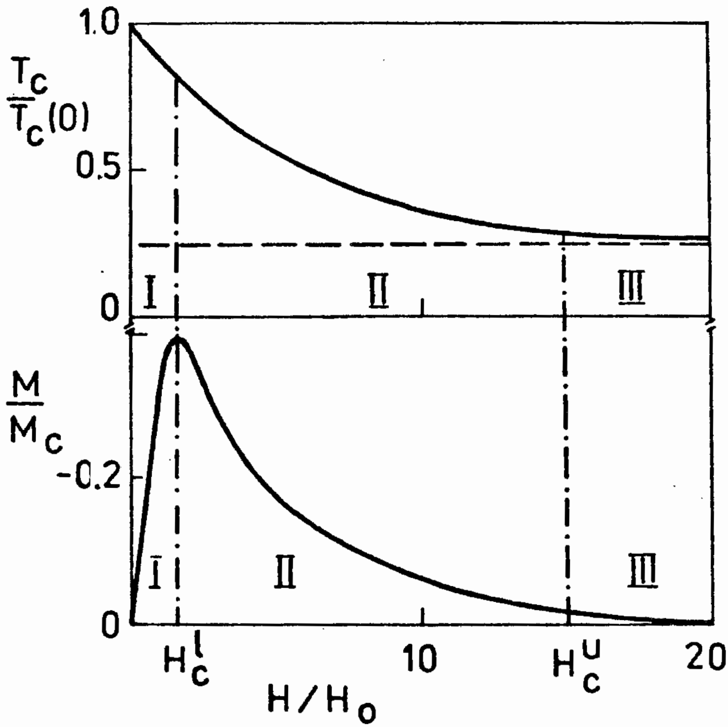

One may distinguish three characteristic regions in the field dependence of T_c:

I. $H < H_c^{\ell}$ (quasireversible diamagnetic region)

$$\frac{T_c(0) - T_c(H)}{T_c(0)} = \frac{2}{\sqrt{3}} \left(\frac{H}{H_0}\right)^2 , \tag{1}$$

where

$$H_c = \frac{3}{4} H_0 , \quad H_0 = \frac{\phi_0}{2S} , \quad T_c(0) = \frac{1}{2} JN ,$$

and $S = \pi\sigma$ is a mean-square area of the superconducting cluster.

II. $H_c^u > H > H_c^{\ell}$ (region of superconductive glass: AT line)

$$\frac{T_c(0) - T_c(H)}{T_c(0)} = \sqrt[3]{\frac{6}{\sqrt{3} \cdot H_0^2}} \cdot H^{2/3} , \tag{2}$$

where $H_c^u = 15\, H_0$.

III. $H > H_c^u$ (region of Josephson spin glass: strong frustration)

$$T_c(H) = T_c(\infty)\left(1 + \frac{3NH_0^2}{2H^2}\right), \quad T_c(\infty) = \frac{1}{2} J\sqrt{N}. \tag{3}$$

The phase diagram obtained is consistent with [1] at $H \lesssim H_c^u$ and with [2] at $H > H_c^u$. The lower part of the picture shows the field dependence of the isothermal magnetization M. In the diamagnetic region (I) it has a linear character, in the SCG phase (II) the nonlinear effects become essential, and, at last, in the region of the JSG phase (III) the magnetization rapidly tends to zero (when $H \to H_c^u$) indicating the strong suppression of the superconducting transition temperature T_s in contrast with the glassy temperature $T_c(H)$ (see the figure).

The glassy transition, as is well-known, is connected with the dynamic transition from the ergodic to the nonergodic state. The non-ergodicity parameter of the model $L_{ij} = \lim \overline{\langle S_i^*(t)\, S_j\rangle} \sim T(\chi_{FC} - \chi_{ZFC})$ is calculated, and its temperature dependence versus $T/T_c(H)$ is shown to have a universal character (a dynamic "temperature-field". scaling). The estimations for La ceramics [3] with $T_c(0) = 28K$, $H_0 = 0.05T$ give the mean value of the superconducting cluster area $S \simeq 0.02\,\mu^2$ and Josephson energy $J \simeq 3.5K$ in reasonable agreement with commonly used estimates. On the whole the experimental data for field-cooled and zero field-cooled measurements confirm the obtained phase diagram. Nevertheless, further experimental study of the magnetic field dependence of T_c under transition from the SCG phase to the JSG phase is of interest.

R e f e r e n c e s

1. Morgenstern I. et al. – Z.Phys.B, 1987, 69, p.33.
2. Vinokur V.M. et al. – ZhETF, 1987, 93, p.343.
3. Müller K.A. et al. – Phys.Rev.Lett., 1987, 58, p.1143.

Received on April 22, 1988.

Краткие сообщения ОИЯИ №4 [30]-88 *JINR Rapid Communications No.4 [30]-88*
УДК 538.911/945

DIFFRACTION STUDY OF SOME HIGH-T_c SUPERCONDUCTORS WITH THE TIME-OF-FLIGHT NEUTRON DIFFRACTOMETER DN-2

A.M.Balagurov, Hvan Chan Gen, V.A.Kudrjaschev[1], G.M.Mironova, Nguyen Van Vuong, A.Pajaczkowska[2], H.Shimchak[2], V.A.Trunov[1], Trinh Anh Kuan

The results of neutron diffraction experiments performed on high-T_c superconductors of the 1-2-3 type by using the time-of-flight diffractometer are discussed. The test experiment on $YBa_2Cu_3O_{7-\delta}$ after profile refinement of the data has given us a well-known structure. The final profile R-factor is 2.7%. Neutron diffraction on $YBa_2Cu_3O_7$ and $GdBa_2Cu_3O_7$ single crystals has been measured with the aim to reveal possible long-period modulation of the atomic structure. The diffraction patterns from these crystals do not involve any additional peaks commensurate with the main structure. The incommensurate peaks are also absent, the lowest limit for the period of modulation is as high as 400Å. The structure of $YBa_2(Cu_{1-x}Fe_x)_3O_{7-\delta}$ has been determined at x=0,0.06 and 0.10. Some indications of occupying (2q) positions in the centre of octahedra with Fe atoms have been received. The (1a) positions on Cu-O chains contain both Fe-atoms and vacancies.

The investigation has been performed at the Laboratory of Neutron Physics, JINR.

Нейтронографические исследования некоторых высокотемпературных сверхпроводников на дифрактометре ДН-2

А.М.Балагуров и др.

Обсуждаются результаты структурных экспериментов с ВТСП типа 1-2-3, проведенных на нейтронном дифрактометре по времени пролета: тестовый эксперимент с $YBa_2Cu_3O_{7-\delta}$, поиск длиннопериодной модуляции структуры монокристаллов $YBa_2Cu_3O_7$ и $GdBa_2Cu_3O_7$ и эксперимент с $YBa_2(Cu_{1-x}Fe_x)O_{7-\delta}$. Обработка нейтронограмм, полученных на хорошо аттестованном порошке $YBa_2Cu_3O_{7-\delta}$, привела к значениям структурных пара-

---

[1] *The Institute of Nuclear Physics of USSR AS, Gatchina*

[2] *The Institute of Physics, Warsaw*

метров, совпадающим с известными из литературы. Величина R-фактора по профилю составила 2,7%. В монокристаллических образцах никаких признаков дополнительных пиков от периодов, соизмеримых с основной структурой, не обнаружено вплоть до $d \cong 40\text{Å}$. Признаки несоизмеримой синусоидальной модуляции структуры отсутствуют вплоть до $d \leq 400\text{ Å}$. Для соединения с медью, частично замещенной железом, получены указания на заполнение железом позиций (2q) в центре усеченных кислородных октаэдров и наличие как атомов железа, так и вакансий в позициях (1a) на цепочках Cu-O вдоль оси кристалла.

Работа выполнена в Лаборатории нейтронной физики ОИЯИ.

The crystal structure of the high-temperature superconductors is intensively analysed now in all neutron centres of the world. Therefore, it is inevitable and even desirable to repeat identical experiments in order to obtain reliable results. New unusual information may be received on the spectrometers having the unique parameters. One of such spectrometers is the neutron time-of-flight diffractometer DN-2 /1/ at the pulsed reactor IBR-2. It has been designed for long-period crystal structure investigations, so the diffraction pattern is measured in the range of long d-spacing which is hard-to-reach for conventional diffractometers. Another unique feature of DN-2 is extremely small exposition time needed for data collection, so it permits carring out the real time diffraction investigations of noncyclic transient phenomena /2/.

In the present work some results of the first diffraction experiments with high-T_c SC ceramics and single crystals on the DN-2 are given.

1. The Features of the Experimental Method and Data Processing

Time-of-flight neutron diffraction data on the diffractometer DN-2 are collected using the one-dimensional position detector lying in horizontal plane. In such a case two-dimensional spectra are measured with scanning of wavelength and scattering angle. An available wavelength range of 1.2-20Å being combined with a scattering angle variation of 10°-160° permits one to have the d-spacing range of 1.6-100 Å. At the same time, the resolution ($\Delta d/d$) of DN-2 is not very high and in the best case it makes up 1% at $2\theta \geq 140°$ and $d \geq 3$ Å. Such poor resolution as well as some features of wavelength distribution of an incident neutron beam are not suitable for the precise powder diffraction study. But it does not preclude from a Rietveld profile analysis [3] of HTS ceramics due to their relative large unit cell and high symmetry. Certainly, in our case the Rietveld method gives temperature factors of atoms much worse than at conventional diffractometers, as the range of small d-spacing is inaccessible. But at the same time, including in the fitting only the reflections with $d \geq 1.4$ Å makes it possible to have no effect of uncertainties in thermal factors on other structure parameters. We use the version of the Rietveld method described in Ref. /4/.

2. The Test Experiment on $YBa_2Cu_3O_{7-\delta}$

The well-known sample of high-T_c superconductor $YBa_2Cu_3O_{7-\delta}$ having $T_c = 91K$ and $\Delta T = 3.7K$ was chosen for the test experiment. Earlier the refinement of the sample structure was done in Ref./5/ with the mini-SFINKS diffractometer. The main purpose of our measurements was to check the sensitivity of structure parameters, determined in Ref. /5/, by the fit covering the range from 0.9 to 2.0 Å if the range is shifted to $1.4 \leq d \leq 3$ Å.

The sample was carefully ground powder of 5.5 g, placed into a cylinder of diameter 8 mm made from Ti-Zr alloy with $b_{coh} = 0$. In order to reveal possible parasitic phases the measurements at low scattering angles (30° and 60°) were performed. It was shown that up to $d \leq 16$ Å there were no additional diffraction peaks. For profile analysis the data were measured with maximum resolution at $2\theta = 150°$ for about 10 hours. Data handling was done over the range of $1.4 \leq d \leq 3$ Å, which included 44 diffraction maxima compatible with the symmetry of the lattice (see Fig. 1.).

The results obtained after refinement of occupancy factors and coordinates of Cu- and O-atoms are shown in Table 1. These results agree well with the data from Ref. /5/.

One can see that the results of independent neutron diffraction experiments given in Refs. /5/ and /6/ are practically the same for coordinates of atoms, but the thermal parameters differ by a factor of 2.5. In order to test the influence of this difference on our results the fitting has been done with the varied occupancy of 04 and z-coordinate of Cu2; the other parameters are taken from /5/ or /6/ and are fixed. It is shown in Table 2 that both n(04) and z(Cu2), R-factors and χ_n are practically constant for these two cases. Only the parameter A_{12} which corrects the form of the effective spectrum of neutrons ($f_{cor} = d^{A_{12}-1}$) has marked change.

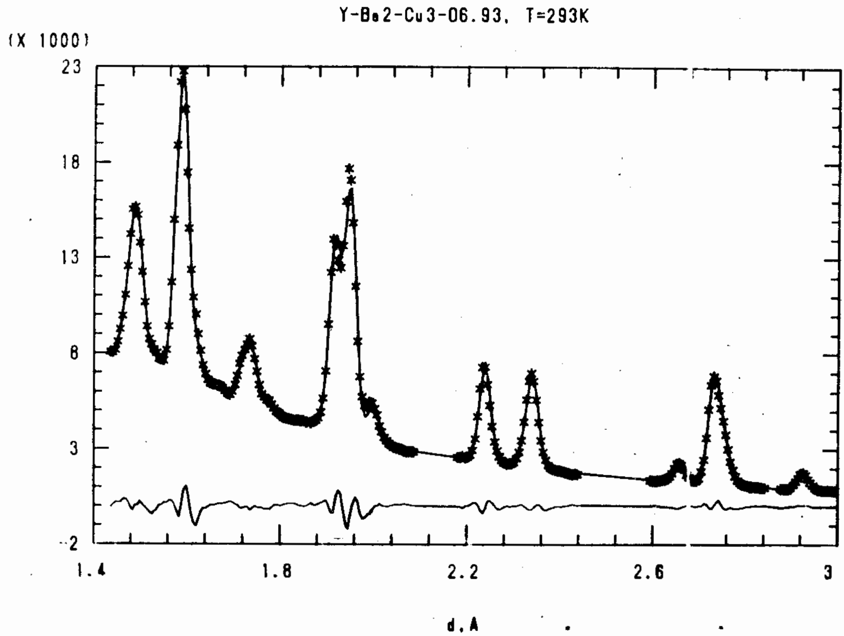

Fig. 1. The observed (stars) and calculated (solid line) neutron profile intensities for $YBa_2Cu_3O_{7-\delta}$ with the difference marked below. The total number of points are 245, R = 2.7%, the expected agreement index R_e = 1.8%.

Table 1

The results (agreement indexes, atom positions and occupancies) for an orthorhombic Pmmm$YBa_2Cu_3O_{7-\delta}$. The thermal parameters and z-coordinate of Ba are taken from Ref./5/ and are fixed. R-factors in %, $\chi_n = (\chi^2/m)^{1/2}$, m is a degree of freedom.

R_p	R_b	R_w	χ_n	n(Cu1)	n(Cu2)	z(Cu2)
2.7	7.3	4.9	3.61	1.02(2)	2.02(2)	0.356(2)

z(01)	z(02)	z(03)	n(04)
0.155(1)	0.372(3)	0.383(3)	0.97(3)

In conclusion, the analysis of data from $YBa_2Cu_3O_{7-\delta}$ gives, firstly, an excellent fit between 1.4 and 3 Å and shows, secondly, that the results are week functions of the variation of thermal parameters. In some limits the change is completely compensated by a common corrective factor.

Table 2

The results of fitting for set parameters from Ref./5/ (1) and Ref. '6/ (2). Only z(Cu2) and n(04) were varied. The attempt to fit n(05) was also made (3).

	R_p	R_b	R_w	χ_n	Z(Cu2)	n(O4)	n(O5)	A_{12}
(1)	2.7	7.4	4.9	3.61	0.3566(5)	0.974(30)	----	0.57(3)
(2)	2.7	7.4	4.9	3.59	0.3563(5)	0.967(30)	----	0.68(3)
(3)	2.7	7.4	4.8	3.58	0.3563(5)	0.925(40)	0.07(4)	0.58(3)

3. The Search for the Long-Period Modulations

We have measured neutron diffraction from $YBa_2Cu_3O_7$ and $GaBa_2Cu_3O_7$ single crystals to have evidence for possible long-period modulation of the atomic structure both commensurate and incommensurate with the main period. The single crystals were prepared by melting initial materials with Cu excess, and had superconducting properties (T_c = 70-75K). We did not separate the single crystals from a crucible and therefore, had the plates of good quality with the area of ~ 20 mm^2, large enough for the experiment. But on the other hand, the diffraction pattern could be measured near $\vec{c}^*$-direction only.

All reflections from a (001)-plane up to the twelfth order ones have been measured on both crystals at room and liquid nitrogen temperature (Figs. 2 and 3). The commensurate modulation of the structure must give additional maxima either between diffraction orders or at $d > d_{00}$. But no evidences of such peaks were found. On the other hand, the incommensurate modulation of the sinusoidal type must give satellites near main peaks. If the modulation vector has the $\vec{c}^*$-direction, then the gap between the satellite position d_s and the main peak position d_0 is $\Delta d = d_0^2/d_s$. The rough minimum estimations of d_s may be obtained for the (001) reflex. The width of this reflex makes one possible to see some additional peaks if $\Delta d \gtrsim 0.3$ Å . From this it follows that if an incommensurate modulation exists, its period will be more than 400 Å .

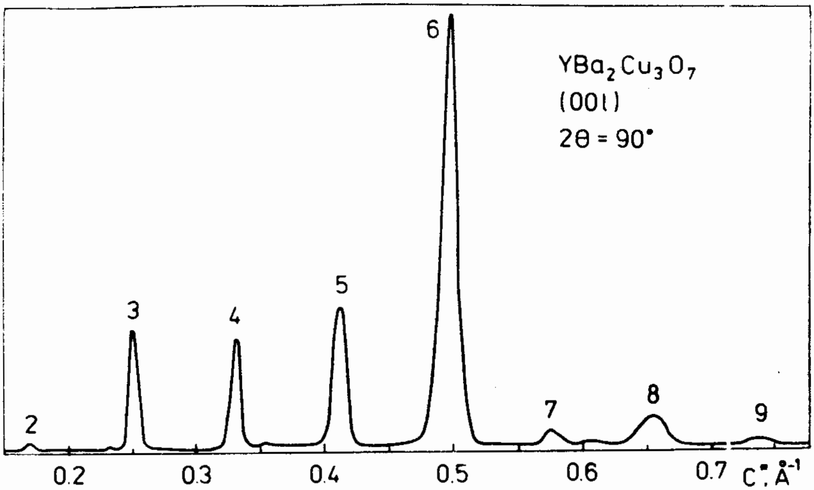

Fig. 2. The orders of the reflection from (001) plane of the $YBa_2Cu_3O_7$ *single crystal.*

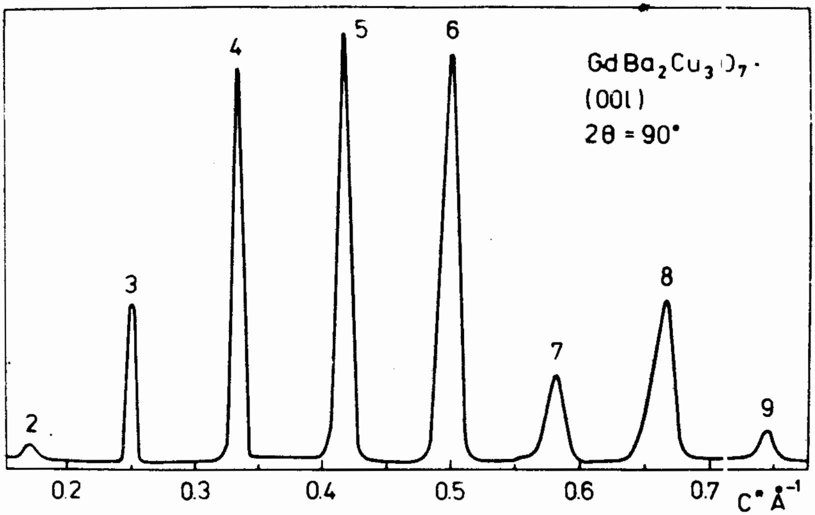

Fig. 3. The same as in Fig. 2 for the $GdBa_2Cu_3O_7$ *single crystal.*

4. On the Substitution of Copper for Iron

The problem of substitution of copper in 1-2-3 ceramics for a neighbouring elements of the 4th period from iron to gallium and silver is discussed in many papers /7 – 12/. There is detailed information on the modification of T_c, symmetry and lattice parameters in

$YBa_2(Cu_{1-x}Fe_x)_3O_{7-\delta}$ depending on x /8,10,11/. But at the same time, there is no reliable data on the possibility of the favourable substitution of one of the nonequivalent structure position (1a) and (2q) of copper for iron.

Our experiments were performed on three samples of $YBa_2(Cu_{1-x}Fe_x)_3O_{7-\delta}$ with x = 0.0, 0.06 and 0.10, which were prepared with standard ceramics technique at the Institut of Physics, Warsaw. Diffraction patterns were measured at $2\theta = 154°$ for about 2-4 hours. The initial values of parameters for profile analysis were taken from Ref./8/. The typical parts of diffraction pattern, where one can see the transition from orthorombic symmetry for x = 0 to a tetragonal one for x = 0.06 and x = 0.10, are shown in Fig. 4. The results of data analysis (R-factors and the values of varied parameters) are given in Table 3. For the sample without iron the two versions are given. They are different by the thermal parameter values, but one can see that the occupancies stay in both cases invariable. For the x = 0.06 sample the two versions of data processing are given too: for $a \neq b$ and $a = b$ cases. In the second case there is the insignificant increasing of R-factors; the structure parameters have not changed.

Table 3

The results for $YBa_2(Cu_{1-x}Fe_x)_3O_7$ with x = 0.0, 0.6 and 0.10. The sets (1) and (2) for 0% Fe are differentiated by thermal factors: (1) — from Ref. /5/, (2) — from Ref./13/.

	0% Fe		6% Fe		10% Fe
	1	2	$a \neq b$	$a = b$	$a = b$
R_p	6.0	5.8	5.7	5.9	6.9
R_w	8.0	7.8	7.5	7.8	9.5
χ_n	1.94	1.88	1.47	1.53	2.58
a,Å	3.816	3.817	3.861	3.862	3.864
b,Å	3.881	3.882	3.874	3.862	3.864
c,Å	11.663	11.665	11.641	11.631	11.618
n_e (1a)	1.02(1)	1.00(1)	0.92(2)	0.91(2)	0.96(2)
n_e (2q)	1.97(2)	1.98(2)	2.05(2)	2.06(2)	2.06(2)
z_{Cu} (2q)	0.360(1)	0.359(1)	0.363(2)	0.362(2)	0.362(2)
n(O4)	0.92(2)	0.89(2)	0.97(2)	0.98(2)	1.00(2)

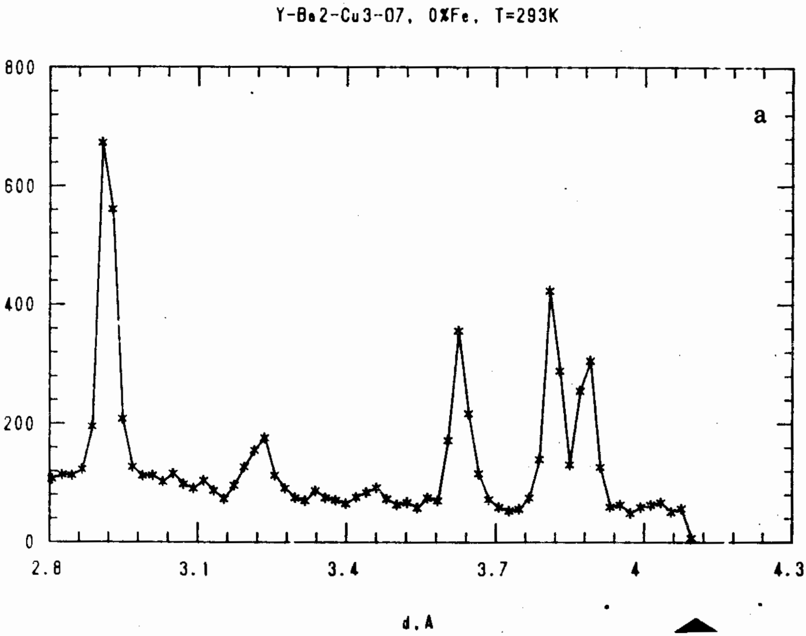

Fig. 4. The typical part of diffraction pattern for the Fe contained samples: a – 0%, b – 6%, c – 10%.

It should be noted that tetragonalization occurres with an increase of Fe content and is accompanied by a decrease of the value $g = c/3 - (a+b)/2$, where a, b and c are the lattice parameters. It is known that in the case of the falling of 04 occupancy from 1 to 0 in pure $YBa_2Cu_3O_7$ the lattice becomes also tetragonal, but the g-value increases.

Given in Table 3 occupancies of copper are normalized on the coherent scattering amplitude $b_{Cu} = 0.772 \cdot 10^{-12}$cm. For $x = 0$ they are in good agreement with multiplicity of positions (1a) and (2q), where the atoms Cu1 and Cu2 are situated. To determine the concentration of impurity in these positions, one must know the probabilities of the substitution. Initially assuming equiprobable substitution of Cu for Fe both in (1a) and (2q) and having in mind that $b_{Fe} = 0.954 \cdot 10^{-12}$cm, one can have for $x = 0.10$ $n(1a) = 1.024$ and $n(2q) = 2.047$. The experimental value n_e (1a) is essentially less than 1.024, while n_e (2q) is equal to 2.047 in the limit of errors. This fact allows one to assume that the (2q)-position is filled in by Fe-atoms in the right concentration, while in the (1a)-position there are some number of vacancies. One can calculate the occupancies of (1a) and (2q) positions for Cu, Fe and vacancies (see Table 4) taking into account the possibi-

Y-Ba2-Cu3-O7, 6%Fe, T=293K

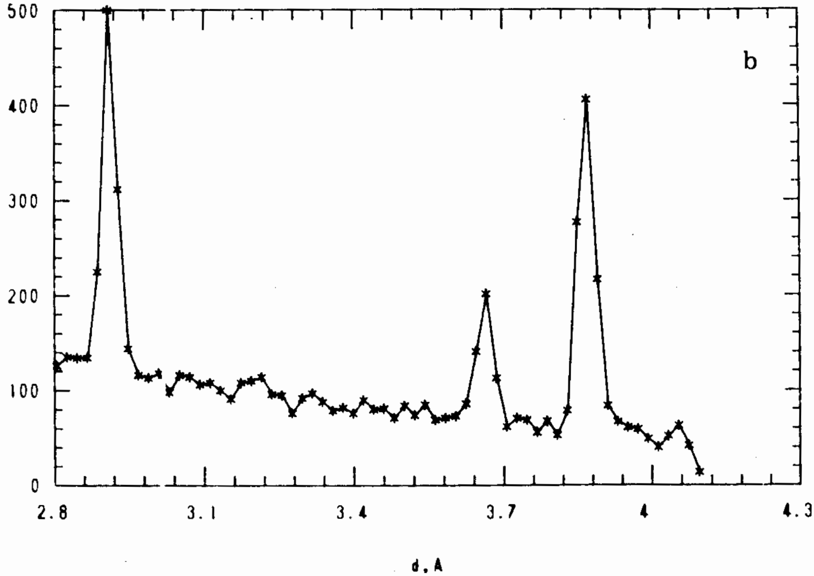

Y-Ba2-Cu3-O7, 10%Fe, T=293K

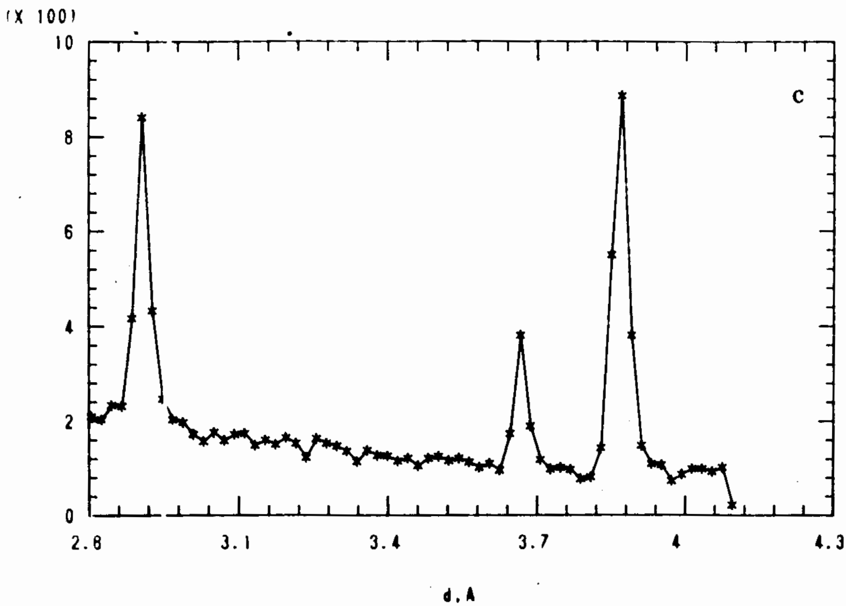

Table 4

The occupancies of (1a) and (2q) sites by Cu and Fe atoms and vacancies. The calculation was made assuming that n_{Cu} = $= k(1 - x)$, $n_{Fe} = kx$.

	(1a)		(2q)	
x	0.06	0.10	0.06	0.10
n_e	0.92	0.96	2.05	2.06
k	0.91	0.94	2.02	2.01
n_{Cu}	0.85	0.85	1.90	1.81
n_{Fe}	0.05	0.09	0.12	0.20
n_{vac}	0.10	0.06	-0.02	-0.01

lity of vacancies and assuming that Cu and Fe are present in the samples in right concentration, i.e. $n_{Cu} \sim (1 - x)$ and $n_{Fe} \sim x$. It is obvious, that Table 4 is correct only for a (2q) position due to $n_{vac} = 0$. For the (1a) position the experimental value n_e can be explained by various ways: one can decrease n_{Fe}, simultaneously increasing n_{Cu} and n_{vac}. In this sense, the values of n_{Fe}(1a) given in Table 4 are the upper limit. It should be noted that n_{Fe} both for (1a) and (2q) positions are practically equal to the iron concentration in initial composition. The visible decrease of Cu1 is still obscure though there is information of such kind in other papers. For example, in the $YBa_2Cu_3O_{6.6}$ single-crystal structure analysis by X-Ray /13/ it was reported that n_{Cu}=(1a) = = 0.862.

5. Conclusions

The results of the present paper confirm the good possibilities of structure investigations of high-T_c superconductors with the TOF-diffractometer DN-2. The Rietveld method gives reliable information about the positional parameters and occupancies of atoms. The oxygen content is determined with the accuracy of (0.02-0.03) atom per unit cell. Including in the fitting of data the diffraction peaks with d-spacing greater than 1.4 Å makes the correlations between thermal and occupancy parameters not so important.

A likely explanation of our measurements on $YBa_2(Cu_{1-x}Fe_x)_3O_7$ can be done if one concludes that Fe impurities are present in both Cu1 and Cu2 site in accordance with 1/3 and 2/3 probabilities. Simultaneously the vacancies (6-10%) are present in Cu1 site. The search for long-period modulations of single crystal structures of $YBa_2Cu_3O_7$ and $GdBa_2Cu_3O_7$ has not given any evidences of additional diffraction peaks. We have found that the lowest limit of possible incommensurate modulation is as high as 400 Å.

The authors are indebted to V.L.Aksenov for encouragement and helpful discussions.

References

1. Balagurov A.M. et al. JINR, 3-84-291, Dubna, 1984.
2. Mironova G.M. JINR, P13-88-326, Dubna, 1988.
3. Albinati A, Willis B.T.M. — J.Appl.Cryst., 1982, 15, p.361.
4. Balagurov A.M. et al. JINR, P14-87-744, Dubna, 1987.
5. Antson O.K. et al. — Sol.St.Comm., 1987, 64, p.757.
6. Capponi J.J. et al. — Europh.Lett., 1987, 3, p.1301.
7. Maeno Y. et al. — Nature, 1987, 328, p.512.
8. Zhou X.Z. et al. — Phys.Rev.B., 1987, 36, p.7230.
9. Mehbod M. et al. — Phys.Rev. B, 1987, 36, p.8819.
10. Kistenmacher T.J. et al. — Phys.Rev.B, 1987, 36, p.8877.
11. Oda J. et al. — Jap.J.Appl.Phys., 1987, 26, p.L1660.
12. Tomy C.V. et al. — Sol.St.Comm., 1987, 64, p.889.
13. Tonnikov V.N. et al. — Pis'ma v JETF, 1987, 46, p.457.

Received on June 29, 1988.

Краткие сообщения ОИЯИ №4 [30]–88 *JINR Rapid Communications No.4 [30]–88*
УДК 538.911/945

NEUTRON SCATTERING STUDY OF $YBa_2Cu_3O_{6+\delta}$ ($0 < \delta < 0.8$) OXYDES

A.M.Balagurov, I.E.Graboj*, A.R.Kaul*, G.M.Mironova, V.V.Moshchalkov*, I.G.Muttik*, Ja.A.Shapiro*, M.E.Zalishchanskii

Neutron scattering study of $YBa_2Cu_3O_{6+\delta}$ ($\delta = 0 \div 0.8$) compounds is performed. For $\delta = 0.08$ we observed tetragonal crystal structure with lattice parameters a=3.840 Å and c=11.737 Å and an additional diffractional peak which may be considered as (1/2 1/2 1) magnetic reflection. Any other magnetic reflections corresponding to AF structure suggested earlier have not been found within the limits of the experimental resolution and intensity.

The investigation has been performed at the Laboratory of Neutron Physics, JINR.

Нейтронографическое исследование структуры $YBa_2Cu_3O_{6+\delta}$ при $0 < \delta < 0{,}8$

А.М.Балагуров и др.

Проведено нейтронографическое исследование структуры $YBa_2Cu_3O_{6+\delta}$ при $\delta = 0{,}08$, 0,36, 0,48 и 0,68. Только при $\delta = 0{,}08$ решетка кристалла является тетрагональной с а= 3,840 Å и с= = 11,737 Å, и на нейтронограмме присутствует дополнительный пик, который можно интерпретировать как отражение (1/2 1/2 1) от антиферромагнитной структуры. Других магнитных пиков с интенсивностями, превышающими статистическую ошибку, не обнаружено.

Работа выполнена в Лаборатории нейтронной физики ОИЯИ.

The possibility of the AF ordering in oxygen deficient $YBa_2Cu_3O_{6+\delta}$ compounds at temperatures T < 500 K has been recently confirmed in neutron scattering experiments [1,2]. Low intensity and very limited number of the magnetic reflections made impossible the reliable determination of magnetic structure, the effective Cu moment and even its orientation with respect to crystal structure. Measurements of magne-

---

*Moscow State University

tic scattering in $YBa_2Cu_3O_{6+\delta}$ on polarized neutrons showed the presence of magnetic fluctuations up to $\delta = 0.59$ [3]. Taking into account the importance of the interconnection of magnetic and superconducting properties in $YBa_2Cu_3O_{6+\delta}$ compounds we need additional data to know exactly the magnetic structure.

In earlier experiments carried out with the help of crystal spectrometer one of the obstacles was connected with the strong higher harmonic contribution (mainly $\lambda/2$) into the measured integral intensity. We used the time-of-flight diffractometer where this contribution is absent and, therefore, we hoped to determine more correctly the magnetic reflection intensity. Also we aimed to check the absence of the long range antiferromagnetic order in $YBa_2Cu_3O_{6+\delta}$ compounds with $\delta > 0.2$.

Oxygen deficient $YBa_2Cu_3O_{6+\delta}$ samples were prepared by quenching them from different annealing temperatures $T = 350 \div 950$ C into liquid nitrogen [4]. The oxygen content was determined by the wet chemical analysis and also from Rietveld fitting of the diffraction patterns.

Time-of flight diffractometer DN-2 [5] and pulsed reactor IBR-2 were used to register neutron diffraction patterns which were recorded by the position detector with the sensitive area of about 150 cm^2 and the angular resolution of 19′. The time-of-flight and interplane spacing relative resolution of DN-2 makes up 1% for d = 3 Å and $2\theta = 150°$. We looked for the magnetic reflections up to d = 20 Å for several scattering angles of 90, 40 and 30°.

The refinement of neutron diffraction patterns measured with high resolution at $2\theta = 150°$ was performed using the Rietveld method adapted to the DN-2 [6]. This diffractometer is designed for measurement of the medium and large d-spacing, so we cannot determine the thermal parameters of atoms independently. But including in the fitting the reflections with $d \gtrsim 1.4$ Å only makes the correlations between thermal parameters and occupancy more less.

Parameters derived from neutron scattering data are given in the Table. The oxygen content was found from the neutron diffraction pattern fitting in the range of $1.4 \div 3$ Å (Fig.1). The δ value determined both by the wet chemical analysis and from neutron scattering data are in good agreement for samples No.2-4. For sample No.1 there is certain discrepancy between these two methods, δ_c is appreciably greater than δ_r and is not in accordance with low T_c. It may be caused by the existence of sharp dependence of T_c in the range $\delta = 0.7 \div 0.8$.

We do not show here the final results of Rietveld refinement as they agree well with the data from earlier neutron experiments [7], which showed that samples prepared in the above described manner

Table

Characteristics of the samples under study

Sample	T_a,K	T_c,K	δ Chem.	δRietv.	R,%	$g1 \cdot 10^2$	$g2 \cdot 10^3$
1	873	58	0,83	0.68 (2)	5.4	4.1	7.8
2	923	40	0.51	0.48 (2)	4.2	4.7	5.7
3	973	<20	0.41	0.37 (2)	2.6	5.7	4.3
4	1213	0	<0.20	0.08 (1)	7.3	7.2	0.0

T_a is the annealing temperature, T_c is the temperature of phase transition (the middle point of resistive curve), δ_c and δ_r are the 04 oxygen content determined by the chemical analysis and from Rietveld fitting. R – the profile R-factor, $g1 = c/3 - (a+b)/2$ and $g2 = (b-a)/(b+a)$ are the parameters of the deviation from the ideal perovskite structure and the orthorhombic distortion of the tetragonal lattice.

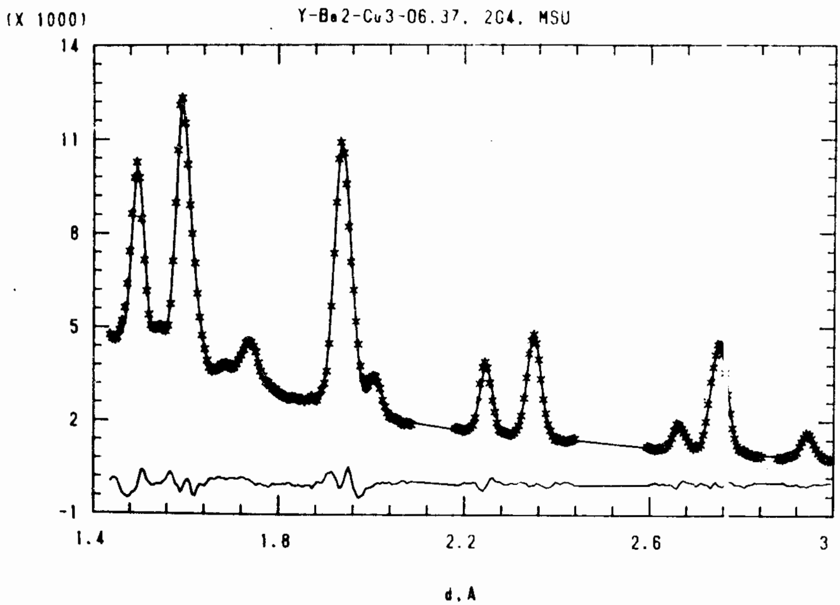

Fig.1. Observed (dots) and calculated (solid line) diffraction profile from sample No.3. The difference curve is shown in the bottom. The total of 245 experimental points were processed with R-factor over profile being 2.6%, weighted R_w-factor 3.4% and expected R_e = 2.1%.

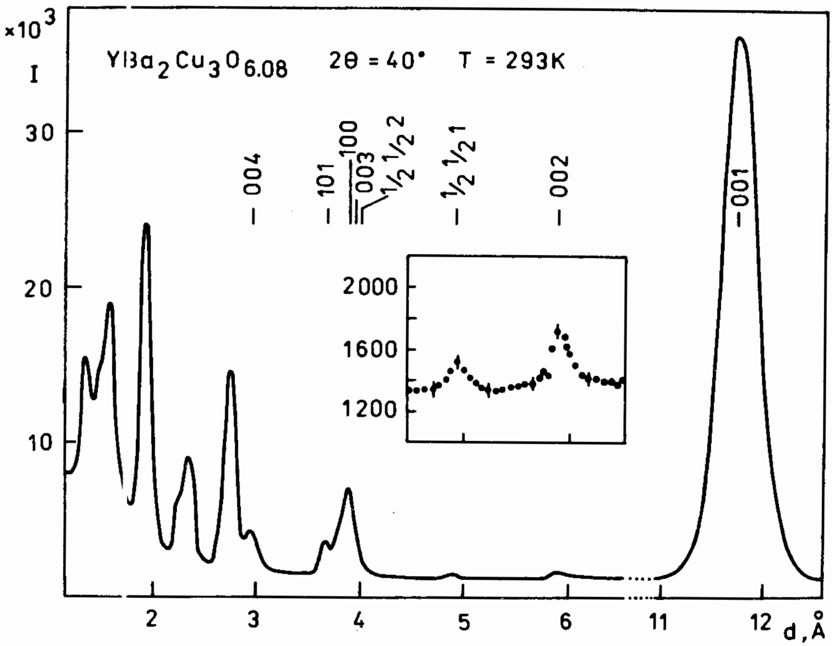

Fig.2. Diffraction spectrum from sample No.4 measured at 2θ=40°. A peak at d= 4.93 Å is clearly observable. It may be considered as (1/2 1/2 1) magnetic reflection from the AF structure.

really become oxygen deficient and variation of δ correlates with the (b - a)/(b + a) value. After annealing at 970 K the diffraction pattern shows a pure single tetragonal phase with 04 removed from (1e) positions.

As is shown in Ref. /1, 2/ the AF ordering in $YBa_2Cu_3O_{6+\delta}$ for $\delta \leq 0.15$ leads to the unit cell doubling along a and b axes, i.e. permits the enhancement of magnetic peaks of the (1/2 1/2 ℓ) type (if Miller indices are used for nuclear cell). In experiments /1, 2/ the peaks (1/2 1/2 1) and (1/2 1/2 2) with d equal about 5Å and 4 Å, respectively, were observed to have approximately equal intensities.

A carefull check undertaken in the vicinity of d = 5 Å has revealed an additional weak reflection (d = 4.93 Å) in sample No.4 only (Fig.2). The lattice parameters for this sample were measured under good resolution (2θ = 90° and 150°), being a = b = 3.840 Å and c = 11.737 Å* and

---

**In Ref. /1/ : a = b = 3.857 Å and c = 11.855 Å, in Ref. /2/ : a = b = 3.843 Å and c = 11.756 Å.*

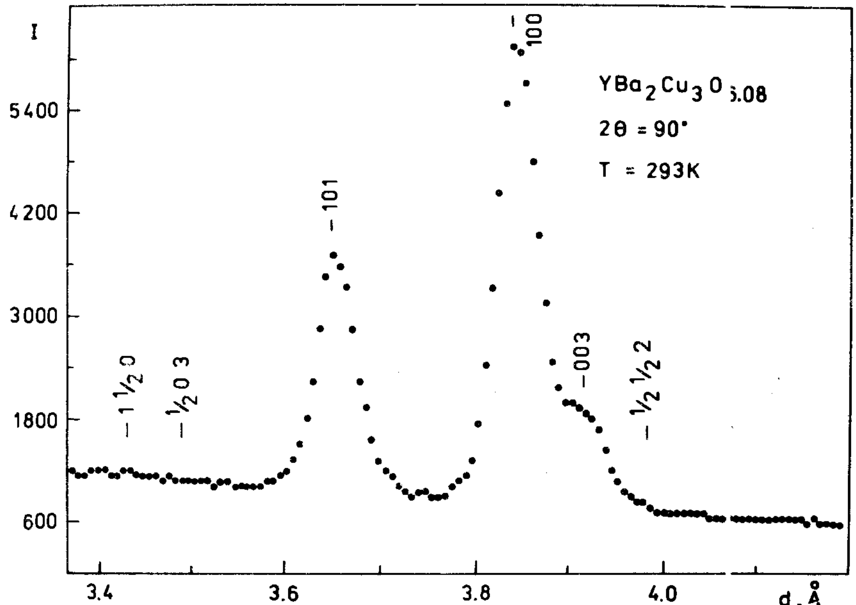

Fig.3. Diffraction spectrum from sample No.4. In the vicinity of d =3.99 Å the (1/2 1/2 2) magnetic reflection must occur, but its intensity does not exceed the statistical error.

corresponding to calculated (1/2 1/2 1) magnetic peak position. No other magnetic peaks were found within the limits of experimental resolution and intensity. Namely $I_{\frac{1}{2}\,\frac{1}{2}\,2}$ (d = 3.99 Å) = 38 ± 54 (fig.3), while $I_{\frac{1}{2}\,\frac{1}{2}\,1}$ (d = 4.93 Å) = 1053 ± 123. Corrections for the effective spectrum, Lorentz factor and absorption have small influence on the intensity ratio for these two peaks and so it appears to be equal to ~20 at least.

Rietveld profile refinement of the data from No.4 sample gave $\delta = 0.08$ (R = 7.3%) showing only a modest correspondence with the tetragonal P4/mmm structure. Many peaks especially those occurring in the range of d = 3 Å have some additional intensity.

Thus the performed experiments have not demonstrated any signs of AF long range ordering in $YBa_2Cu_3O_{6+\delta}$ compounds for $\delta \geq 0.36$. For $\delta = 0.08$ the additional peak appears and it may be considered as a magnetic reflection (1/2 1/2 1) from tetragonal AF lattice with doubled a and b. In contrast to Refs.[1,2] no other additional reflections have been observed in our experiments. Therefore, one should consider with care the models suggested in Refs.[1,2] and a new thorough search for magnetic peaks is necessary.

The authors would like to express their gratitude to V.L.Aksenov, V.I.Lushchikov and Yu.M.Ostanevich for usefull discussions.

References

1. Tranquada J.M. et al. – Phys.Rev.Lett., 1980, 60, p.156.
2. Rossat-Mignod J. et al. – Physica C, 1988, 152, p.19.
3. Mezei F. et al. KFKI-1988-15/e, Budapest, 1988.
4. Kaul A.R., Graboj I.E., Tret'jakov Yu.D. "Superconductivity", issue I, ed. Ozhogin V.I., Moscow, MSU, 1987.
5. Balagurov A.M. et al. JINR, 3-84-291, Dubna, 1984.
6. Balagurov A.M. et al. JINR, P14-87-744, Dubna, 1987.
7. Hewat A W. et al. – Sol. St. Commun. 1987, 64, p.301.

Received on June 17, 1988.

Краткие сообщения ОИЯИ №4 [30]-88 *JINR Rapid Communications No.4 [30]-88*
УДК 538.945 + 539.125.5

ON DETERMINATION OF THE MAGNETIC FIELD PENETRATION DEPTH IN OXIDE SUPERCONDUCTORS BY POLARIZED NEUTRONS REFLECTION

D.A.Korneev, L.P.Chernenko

The $R_+(k_\perp)$, $R_-(k_\perp)$ reflection coefficients are calculated for $YBa_2Cu_3O_7$ film sprayed on $SrTiO_3$ ($k_\perp$ is a normal to the surface component, of a wavevector of neutrons) using the quantum mechanical model describing the reflection of neutrons from the surface of a thin superconducting film. The dependence of $S(k_\perp)=R_+(k_\perp)/R_-(k_\perp)$ on the depth of magnetic field penetration into a superconductor Λ, on the external magnetic field H, and on a film thickness d is analysed. The possibility is motivated of carrying out experiments on determination of Λ under condition compared favourably with those under which the experiments with ceramic samples of high temperature superconductor have been conducted.

The investigation has been performed at the Laboratory of Neutron Physics, JINR.

Об определении глубины проникновения магнитного поля в оксидные сверхпроводники методом отражения поляризованных нейтронов

Д.А.Корнеев, Л.П.Черненко

На основе квантово-механической модели, описывающей процесс зеркального отражения нейтронов от поверхности тонкой сверхпроводящей пленки, рассчитаны спинзависящие коэффициенты отражения $R_+(k_\perp)$, $R_-(k_\perp)$ для пленки $YBa_2Cu_3O_7$, напыленной на подложку из $SrTiO_3$, где $k_\perp$ – нормальная к поверхности компонента волнового вектора нейтронов. Проанализирована зависимость функции $S(k_\perp)=R_+(k_\perp)/R_-(k_\perp)$ от глубины проникновения магнитного поля в сверхпроводник Λ, величины внешнего магнитного поля H и толщины пленки d. Обоснована возможность постановки эксперимента по определению Λ в условиях, выгодно отличающихся от условий экспериментов с керамическими образцами высокотемпературных сверхпроводников.

Работа выполнена в Лаборатории нейтронной физики ОИЯИ.

Recently the results[1] on determination of the magnetic field penetration depth in $YBa_2Cu_3O_7$ obtained by polarized neutron reflection have been published. The polarized neutron reflection method compared with the other ones[2,3] has demonstrated a significant divergence (by 10 times) from estimation of Λ. As yet, the reasons of such divergence are not clear.

It should be noted that basically, under definite conditions, the polarized neutron reflection at low energies allows one to determine the dependence of a magnetic field value on a depth. The possibility of interpreting the obtained results in the frame of the problem of neutron reflection from a medium surface should be referred to such conditions. The high density and substance magnetization homogeneity along the surface (the absence of pores, multiphase states and other inhomogeneities) is the most essential requirement. Thus, it follows that the whole of the sample must be in the Meissner phase. The density of superconducting ceramics differs from the crystallographic one. Hence, those ceramics bear a significant structure inhomogeneity. This fact to some extent may reduce the evidence of the Λ estimations on the base of experiments on polarized neutron reflection from the surface of mass samples. Besides, microscopic divergences from ideal planeness, i.e. surface undulations of a ceramic sample $YBa_2Cu_3O_7$ at the experiment[1] have led to the fact that the uncertainty $\Delta\theta$ represents 25% of the mean value of a grazing angle θ. Clearly the great value of a parameter $(\Delta\theta/\theta)$ reduces the sensitivity of the method and it is connected with some hypotheses of the surface quality.

Below we analyse the chance of carrying out an experiment to determine Λ by means of polarized neutron reflection under more clear conditions using a thin film of identical composition; the film is made by spraying on monocrystal base. It goes without saying that high homogeneity of a film and the quality of its surface provided by a monocrystal base should essentially improve the reliability of the Λ estimation for the following reasons: firstly, due to the adequacy of a real reflection process and a model forming the data handling basis; secondly, because of an increase of a method sensitivity through a decrease of $(\Delta\theta/\theta)$. It is known from[4] the pattern of magnetic field distribution in a thin superconducting film differs from the one in a half-infinite sample in the case that a penetration depth is comparable to a film thickness d. According to[4] the dependence of induction on a coordinate z normal to a film surface is of the from

$$B(z) = H \cdot \frac{Ch((2z-d)/\Lambda)}{Ch(d/2\Lambda)}, \tag{1}$$

where H is the value of an external magnetic field parallel to a film surface. In order to handle experimental data on polarized neutron reflection from a superconducting film surface the method of calculation of values R_+ and R_- is essential. Here R_+ and R_- are reflection coefficients of neutrons polarized "up" and "down" the field H, respectively. We consider the induction B(z) in a film is inhomogeneous and it is described by the equation (1). The film is applied on the base of the known composition.

The calculation method developed in [5] allows one to estimate reflection coefficients $R_+(k_\perp)$ and $R_-(k_\perp)$ ($k_\perp$ — is a normal component of a wavevector of incident neutrons to the surface) and thus, to determine the value of expected discrepancy between $R_+(k_\perp)$ and $R_-(k_\perp)$ according to Λ, d, H; it also permits to judge a sensitivity of the method with relation to the change of $(\Delta\theta/\theta)$.

The total effective potential of a medium is written in the form of:

$$U = 4\pi \frac{\hbar^2}{2m} N(b_n \pm b_M(z)), \tag{2}$$

where m is a neutron mass, N is a number of nuclei in a unit of volume, b_n is a mean length of coherent neutron-nucleus scattering, and $b_M(z)$ is calculated by the formula

$$b_M(z) = \frac{2.31 \cdot 10^{-10}}{N} (B(z) - H). \tag{3}$$

In (3) the dimensions of quantities are as follows: b_M — Å; N — Å^{-3}; B,H — gausses.

So, a superconductor without ferromagnetic ordering in the external field can be thought of as a magnetized medium with some effective "magnetic" length of neutron scattering related to the induction and external field by the formula (3); in this case the total neutron scattering length has two values of opposite polarizations in an incident beam:

$$b^{\pm}(z) = b_n \mp b_M(z).$$

In the table given below we present the values being used hereafter and calculated on the basis of tabulated and crystallographic data:

	Film ($YBa_2Cu_3O_7$)	Base ($SrTiO_3$)
b_n (Å)	$0.631 \cdot 10^{-4}$	$0.42 \cdot 10^{-4}$
N(Å^{-3})	0.0747	0.0837
b_M (Å)	$3.06 \cdot 10^{-9}$ (B(z) - H)	0.0
k_0 (Å^{-1})	$7.7 \cdot 10^{-3}$	$6.64 \cdot 10^{-3}$
λ_0 (Å)	814	946

where B and H are being measured in gausses; $k_0 = (2\pi/\lambda_0)$ is the value of a normal component of a wavevector of incident neutrons obtained if:

$$\frac{\hbar^2 k_0^2}{2m} = U_n .$$

In brief, the principle of the method is that a continuous potential is substituted for a discrete quasipotential:

$$U(z) = \frac{\hbar^2}{2m} \sum_{i=1}^{n} b_z(z_i)\, \delta(z - z_i) . \tag{4}$$

The neutron interaction in $z = z_i$ is proportional to the value of $b_z(z_i)$, which is a mean value of a neutron scattering length on the whole plane of $z = z_i$. A neutron wave function is chosen at each section between z_i and z_{i-1} as a sum of plane waves moving in both directions (a positive and a negative one) with corresponding amplitudes: $A^{(i)}(\vec{k}_\perp)$ and $A^{(i)}(\overleftarrow{k}_\perp)$. By this means the substitution of the written wave function into a Schrödinger equation with a quasipotential (4) reduces it to a system of bounded algebraic equations in relation to $A^{(i)}$. Using this method one may find all $A^{(i)}(\vec{k}_\perp)$ and $A^{(i)}(\overleftarrow{k}_\perp)$ $(i = 1, 2, ..., n+1)$ for any model dependence of $b_z(z_i)$, and thus find out a wave function in an inhomogeneous medium, reflection coefficients $R(k_\perp) = |A^{(1)}(\overleftarrow{k}_\perp)|^2$ and transmission coefficients $T(k_\perp) = |A^{(n+1)}(\vec{k}_\perp)|^2$ of neutrons (here n is a number of points where a potential (4) is given). A continuous potential corresponding to a discrete one is defined for a homogeneous medium (b_z = const, $\Delta z = z_{i+1} - z_i$ = const) by the following expression:

$$U = 4\pi \frac{\hbar^2}{2m} \left(\frac{b_z}{\Delta z}\right) . \tag{5}$$

The latter expression may serve as a determination of a potential for a one-dimensional homogeneous problem. A particular recalculation of "three-dimensional" scattering lengths in "one-dimensional" ones is done taking this simple condition as the base: the potential of one- and three-dimensional problem must agree very closely.

The results of experiments on the polarized neutron reflection are accepted to be presented in the following form:

$$S_\theta(k) = \frac{N_\theta^+(k)}{N_\theta^-(k)} , \tag{6}$$

where $N_\theta^+(k)$, $N_\theta^-(k)$ are the intensities of the narrowly collimated

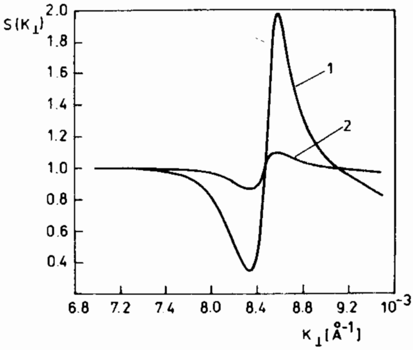

Fig.1. S($k_\perp$) *for cases: 1 – Λ =200 Å; 2 – Λ=1000 Å, when the field* H=420 *ga-usses for a film 1000 Å thick.*

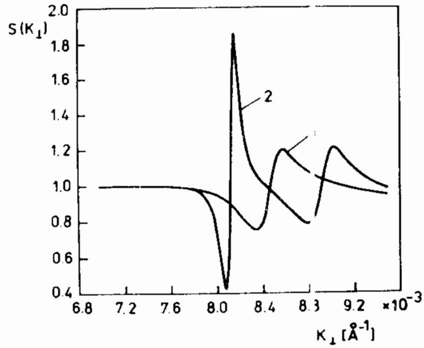

Fig.2. S($k_\perp$) *for cases: 1 –* d = *=1000 Å; 2 –* d *=1500 Å when the field* H=*105 gauses and* Λ=*200 Å.*

neutron beam reflected at a grazing angle θ, k is a wavevector of incident neutrons. It should be noted that $k_\perp = k \cdot \theta$. Signs – and + show that neutrons have been registered with the help of a spin-flipper being switched on and switched off, respectively. A spin-flipper is the device reversing the polarization vector $\vec{P}$ about the vector $\vec{H}$ in an incident beam. In the general case P = P(k). The probability f of the polarization reverse with a spin-flipper is also the function k, i.e. f = f(k).

Now we turn our attention to the discussion of calculated values of $S(k_\perp) = R_+(k_\perp)/R_-(k_\perp)$ for a model superconducting film with the values of neutron-optical parameters given in the Table.

Figures 1÷3 show calculation results of the S($k_\perp$) for an ideal reflectometer, i.e. $(\Delta\theta/\theta)=0.$; $(\Delta k/k)=0.$; P = 1.; f = 1.

Figure 1 presents S($k_\perp$) for a film with a thickness of d = 1000 Å in the region of values $k_\perp \gtrsim k_0$. Two cases are given: 1) when Λ= 200 Å (curve 1) and when Λ = 1000 Å (curve 2) if an external field is equal to 420 gausses. S($k_\perp$) is of oscillating character (also see fig.2). It is seen that as Λ decreases the effect increases.

Fifure 2 demonstrates the differences of S($k_\perp$) for films with a thickness of 1000 Å and 1500 Å, respectively. A film thickness increase has led to an increase in a number of oscillations in a picked interval $k_\perp$.

The comparison of curve 1 in Figs. 1 and 2 allows one to evaluate the dependence S($k_\perp$) on an external field value: as a field decreases the effect also decreases being available for measurement when fields are $\gtrsim$ 50 gausses.

Figure 3 presents a specific case, i.e. when a film with a substrate δ thick does not transfer to a superconducting state. The deficiency

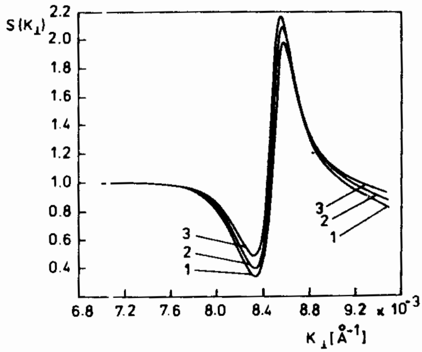

Fig.3. $S(k_\perp)$ *shows the existence of a film layer with the deficiency of oxygen. In a layer* δ *thick on the surface of a film* $B(z) = H = const.$ *Cases: 1 –* $\delta = 0$ *Å; 2 –* $\delta = 100$ *Å; 3 –* $\delta = 200$ *Å. A film 1000 Å thick in the field* $H = 420$ *gausses,* $\Lambda = 200$ *Å.*

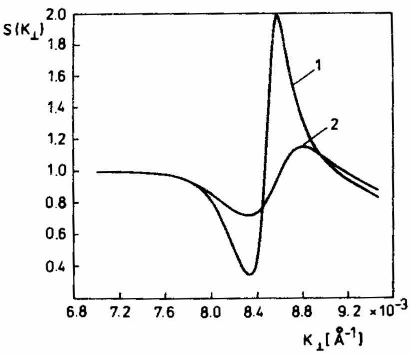

Fig.4. $S(k_\perp)$ *for an ideal reflectometer (curve 1) and considering finite resolution (curve 2). A film with a thickness of 1000* $\mathring{A}_o$ *in a field* $H=420$ *gausses and* $\Lambda=200$ *Å.*

of oxygen near a film surface may cause the existence of such a layer. Figure 3 demonstrates the manner in which $S(k_\perp)$ depending on δ is changing.

The finite reflectometer resolution transforms $S(k_\perp)$ into $S_\theta(k)$; the latter function is equal to $S_\theta(k_\perp)$ at a fixed value of parameter θ when $k = k_\perp/\theta$.

Curve 2 in Fig.4 shows $S_\theta(k_\perp)$ at $\theta = 5 \cdot 10^{-3}$; $(\Delta\theta/\theta) = 4 \cdot 10^{-2}$ and $P(k) = 1 - c/k^4$ ($c = 6.28 \cdot 10^{-3}$ Å^{-4}). The dependence $P(k)$ has been taken from /7/. Curve 1 in Fig.4 is an ideal case. One may see that taking into account the reflectometer real parameters we observe a significant decrease in the effect.

It should be noted that at first sight it seems advantageous to increase the parameter θ because at $(\Delta\theta/\theta)$ it tends to zero. But θ will be confined by $k = (k_o/\theta) \gtrsim k^*$, i.e. $\theta \lesssim (k_o/k^*)$ which comes from the ordinary requirement: the k values must get to the region of k^* values where the spectral density of thermal neutron flux is rather high, in order to provide the statistic precision in measuring $S(k_\perp)$. Thus, for example, the typical value of k^* for thermal beam of the pulsed reactor IBR-2 of JINR is $k^* = (2\pi/\lambda^*) \simeq 1.7$ Å^{-1} ($\lambda^* \simeq 4 \div 5$ Å). That corresponds to $\theta \leq k_o/k^* \simeq 5 \cdot 10^{-3}$.

Conclusions:

1. The experiment on the determination of Λ in film high-temperature superconductors by polarized neutrons will allow one to get the Λ using more precise conditions compared to those used for investigations on thick samples. The estimation of Λ becomes more reliable.

2. The calculation method has been created for handling experimental spectra of neutrons reflected from a thin superconducting film, applied on a mass base and placed in the magnetic field H, to determine the Λ and the thickness of the substrate having no superconducting properties.

3. Neutron-optical parameters for the $YBa_2Cu_3O_7$ film and $SrTiO_3$ base are such that the effect might be statistically observable in the region of values of $k \gtrsim k_0 = 7.7 \cdot 10^{-3}$ Å^{-1} at a grazing angle of $\theta \lesssim 5 \cdot 10^{-3}$. In this case the value of the very effect grows with an increase of the field H and with a decrease of the Λ. The region of $0 \lesssim \Lambda \lesssim 2000$ Å for fields $\simeq 400$ gausses is considered to be available for measurements of the Λ. When a field reduces, this region gets narrower. In real conditions of the experiment the values of $H \lesssim 50$ gausses, apparently, might not provide one with a reliable determination of a Λ at different values. If the first critical fields is $H_1 < 50$ gausses, the latter condition limits the correctness of the experiment interpretation in the frame of a one-dimensional neutron reflection model.

4. Film thickness at which advantages of the thin-film sample $YBa_2Cu_3O_7$, connected with a characteristic non-monotone behaviour of $S(k_\perp)$, are apparent lie in the interval of $1000 \div 1500$ Å.

5. The uncertainty in the reflectometer parameter $(\Delta\theta/\theta) \sim 5\%$ and consideration of incomplete neutron beam polarisation preserve all characteristic peculiarities of the $S(k_\perp)$, reducing the effect by approximately two times.

6. The experiments with monocrystal films allow one to determine the value of Λ along definite crystallographic direction determined by the behaviour of a film growth in the process of its preparation. The experiments with polycrystal films give information on the Λ averaged over crystallographic directions considering the degree of a reciprocal crystal disorder. The comparison of experiments on films with a different degree of a mosaic structure will permit one to estimate crystallographic anisotropy of Λ.

References

1. Felici R. et al. — Nature, 1987, 329, p. 523.
2. Ted Forgan. — Nature, 1987, 329, p. 483.
3. Cava R.J. et al. — Phys.Rev. Lett., 1987, 58, p.1676.

4. Buckel W. Superconductivity. M., Mir, 1975.
5. Korneev D.A., Chernenko L.P. JINR Communications, P4-87-460, Dubna, 1987.
6. Blokhintsev D.I. The Base of Quantum Mechanics. M., Nauka, 1976.
7. Korneev D.A. et al. JINR Communications, P3-81-547, Dubna,1981.

Received on June 8, 1988.

Краткие сообщения ОИЯИ №4 [30]-88　　*JINR Rapid Communications No.4 [30]-88*
УДК 538.945 + 538.955 + 539.126.334

μSR-INVESTIGATION OF THE HIGH-T_c SUPERCONDUCTOR $HoBa_2Cu_3O_{7-\delta}$

V.N.Duginov, I.E.Graboj[1], V.G.Grebinnik, I.I.Gurevich[2], A.R.Kaul[1], B.F.Kirillov[2], E.P.Krasnoperov[2], A.B.Lazarev, B.A.Nikolsky[2], V.G.Olshevsky, A.V.Pirogov[2], V.Yu.Pomjakushin[2], A.N.Ponomarev[2], S.N.Shilov, V.A.Suetin[2], V.A.Zhukov

A high-T_c superconductor $HoBa_2Cu_3O_{7-\delta}$ (T_c ~93 K) has been investigated by the μSR-method in a zero external magnetic field, the sample being cooled from the temperature much higher than T_c to T=4.2 K. The fast increasing of the muon spin depolarization in the temperature range 10-4.2 K is observed, which indicates the fluctuating production of the magnetic ordering in this sample.

The investigation has been performed at the Laboratory of Nuclear Problems, JINR.

Исследование высокотемпературного сверхпроводника $HoBa_2Cu_3O_{7-\delta}$ μSR-методом

В.Н.Дугинов и др.

Исследован μSR-методом высокотемпературный сверхпроводник $HoBa_2Cu_3O_{7-\delta}$ (T_c ~93 К) в нулевом внешнем магнитном поле при охлаждении образца от температуры, значительно превышающей T_c, до температуры T= 4,2 К. В области температур 10-4,2 К наблюдается быстрая деполяризация спина мюона, свидетельствующая о флуктуационном образовании магнитоупорядоченного состояния в исследуемом соединении $HoBa_2Cu_3O_{7-\delta}$.

Работа выполнена в Лаборатории ядерных проблем ОИЯИ.

Nowadays the phenomena in high-T_c superconductors like $RBa_2Cu_3O_{7-\delta}$, R being the rare-earth elements with high atomic magnetic moments, arouse great interest /1, 2/.

In our experiment a high-T_c superconductor $HoBa_2Cu_3O_{7-\delta}$ has been investigated by the μSR-method. The experiment was perfor-

---

[1] *Moscow State University*

[2] *I. V. Kurchatov Institute of Atomic Energy, Moscow*

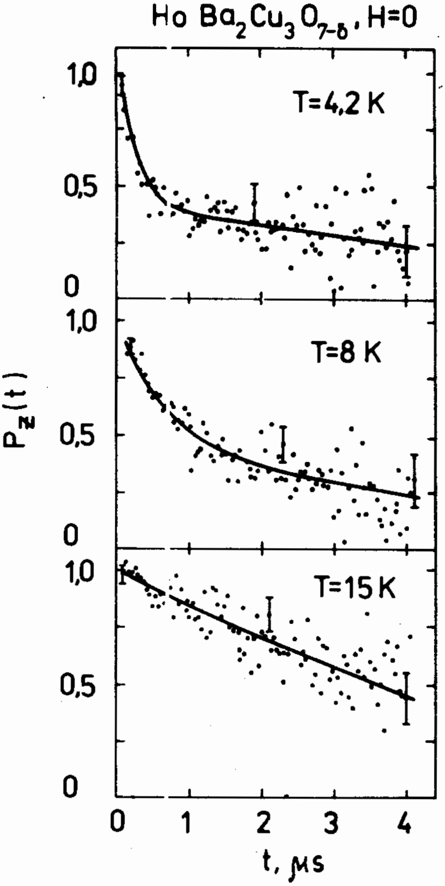

Fig.1. Muon spin relaxation functions in $HoBa_2Cu_3O_{7-\delta}$ at different temperatures in the zero external magnetic field. The solid curves are plotted according to formula (1).

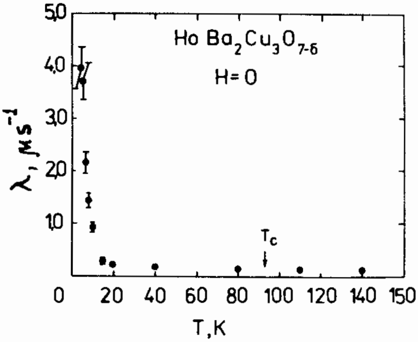

Fig.2. Temperature dependence of the muon spin relaxation rate λ in the zero external magnetic field.

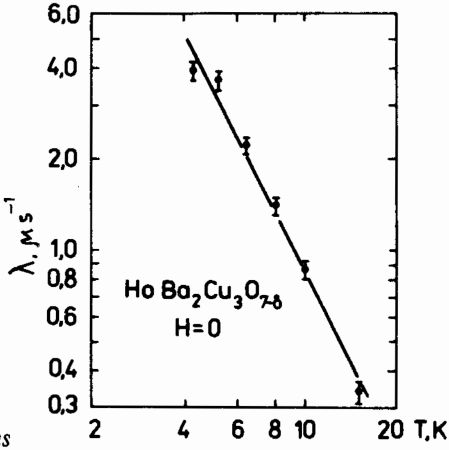

Fig.3. Temperature dependence of λ(T) in the temperature range 4.2-15 K. The solid line is plotted according to formula (2).

med at the Laboratory of Nuclear Problems (JINR, Dubna) in the phasotron muon beam. The sample was a disk ~40 mm in diameter and ~10 mm thick. The disk's face was perpendicular to the direction of the muon beam polarization. The superconducting transition temperature, determined in resistivity measurenents, was about 93 K. Investigations of the sample were performed in a zero external magnetic field in the temperature range 4.2-140 K.

To fit the experimental data the relaxation function was taken to be:

$$P_z(t) = \frac{1}{a_\Sigma}[a e^{-\lambda(T)\cdot t} + (a_\Sigma - a) e^{-\sigma^2 t^2}], \tag{1}$$

where a is the decay asymmetry of the μ^+-fraction stopped, as we suppose, at the sites nearest to Ho-atoms; $\lambda(T)$ is the muon spin relaxation rate for this fraction; a_Σ is the total decay asymmetry determined in the experiment at $T \gg T_c$ in the magnetic field $H_\perp$ transversal to the initial muon polarization; σ is the muon spin relaxation rate for the muon fraction stopped at the sites far from Ho-atoms. It was assumed that a, a_Σ and σ are constant at all temperatures ($a = 0.097 \pm 0.002$; $a_\Sigma = 0.155$; $\sigma = 0.182 \pm 0.008$). Values of $\lambda(T)$ were selected individually for each spectrum. Figure 1 shows the experimental dependences $P_z(t)$ and those computed by eq.(1).

The muon spin relaxation rate $\lambda(T)$ as a function of the temperature is plotted in Fig.2. As is seen, there is no visible change in λ from $T = 140$ K up to $T \sim 15$-20 K. This means, that there are no signs of magnetic ordering above ~ 15-20 K. However, the fast increasing of λ is observed below ~ 15-20 K, which can be explained by the fluctuating formation of magnetic ordering (ferro- or antiferromagnetic) in the paramagnetic phase of the superconductor near the magnetic phase transition temperature. The dependences $P_z(t)$ in Fig.1 also indicate the fast increasing of the muon spin relaxation rate when the temperature approaches 4.2 K.

The analysis of the $\lambda(T)$-dependences at $T < 15$ K showed (Fig.3), that the observed increasing of λ with decreasing temperature can be expressed as:

$$\lambda(T) = \frac{C}{(T - T_{cr})^\beta}, \tag{2}$$

where $T_{cr} = (0 \pm 1)$ K, $\beta = 1.9 \pm 0.3$.

The magnetic ordering in $HoBa_2Cu_3O_{7-\delta}$ is connected with holmium atoms whose unfilled 4f-shell has a magnetic moment of $10\,\mu_B$. In pure holmium these moments are ordered at $20 \le T \le 132$ K as helicoidal antiferromagnetic and at $T < 20$ K as helicoidal ferromagnetic. The magnetic ordering in the high-T_c superconductor $HoBa_2Cu_3O_{7-\delta}$ observed in the experiment points to coexistence of superconductivity and magnetism in this substance.

The same result was obtained in Ref.[3], where the magnetic phase transition was observed in $GdBa_2Cu_3O_{7-\delta}$ at 2.3 K.

We thank V.Yu.Yushankhaj for helpful discussions and I.A.Gaganov for assistance in measurements.

References

1. Thomson J.R. et al. — Phys.Rev., 1987, v. B36, p.718.
2. Thomson J.R. et al. — Phys.Rev., 1987, v. B36, p.836.
3. Golnic A. et al. — Phys.Lett.A, 1987, v. 125, p.71.

Received on May 10, 1988.

Краткие сообщения ОИЯИ №4 [30]–88 *JINR Rapid Communications No.4 [30]–88*
УДК 538.945

POSITRON ANNIHILATION IN A HIGH-TEMPERATURE SUPERCONDUCTOR $YBa_2Cu_3O_{7-\delta}$

J.Wawryszczuk, T.Goworek[1], A.I.Ivanov[2], M.Lewandowski, P.Mazurek[1], V.N.Rybakov, I.F.Uchevatkin[2], I.A.Yutlandov

Positron annihilation as a function of temperature in high-temperature superconductors $YBa_2Cu_3O_{7-\delta}$ has been investigated. It is shown that a change in the annihilation character at the transition into superconducting state is relatively small. The change of τ_1 and τ_2 positron lifetimes as well as of the intensity of the component with $\tau_2 - J_2$ and Doppler broadening S parameter allows one to assume that transition into superconducting state is accompanied with a certain decrease in electron density and with decreasing number of defects or increasing their size.

The investigation has been performed at the Laboratory of Nuclear Problems, JINR.

Аннигиляция позитронов в высокотемпературном сверхпроводнике $YBa_2Cu_3O_{7-\delta}$

Я.Ваврыщук и др.

Изучена аннигиляция позитронов в образцах высокотемпературной сверхпроводящей керамики $YBa_2Cu_3O_{7-\delta}$. Показано, что изменение характера аннигиляции при переходе в сверхпроводящее состояние относительно невелико. Изменения времен жизни позитронов τ_1 и τ_2, а также интенсивности компоненты J_2 и допплеровского уширения аннигиляционной γ-линии (параметра S) позволяют предполагать, что переход в сверхпроводящее состояние сопровождается некоторым уменьшением электронной плотности и уменьшением числа или увеличением размеров дефектов кристаллической решетки.

Работа выполнена в Лаборатории ядерных проблем ОИЯИ.

Nowadays superconductors like La-Ba-Cu-O /1/ have been intensely studied by all available methods, including the positron annihilation method which is especially sensitive to the structure of a sub-

[1] *Institute of Physics of Curie-Sklodowska University, Lublin*
[2] *All-Union Mendeleev Research Institute of Metrology, Leningrad*

stance. Usually, the parameters describing the annihilation process (positron lifetime, electron momentum distribution width[2]) significantly change in the phase transition point. Despite the disappointing results obtained with common metal superconductors in the 50-s[3-5], it seems reasonable to follow the behaviour of the annihilation parameters in the transition region (T_c) of high-temperature superconductors. In the first paper[6] dealing with this problem the Doppler broadening of the 511 keV annihilation γ-line was measured for La-Sr-Cu-O and Y-Ba-Cu-O systems. In further experiments[7,8] positron lifetimes were also measured for Y-Ba-Cu-O system. Ambiguity and sometimes discrepancy of the results obtained make it necessary to continue the investigations.

This paper presents the results of positron lifetime measurements for $YBa_2Cu_3O_{7-\delta}$ and Doppler broadening measurements for the annihilation γ-line in the temperature interval 80-130 K.

Experimental Technique

Positron lifetimes were measured by means of a $\gamma\gamma$-coincidence time spectrometer with two BaF_2 crystalls 38x25 mm in size. The energy resolution of both scintillators with photomultiplyers XP2020Q was 7% for the ^{60}Co 1333 keV line. To eliminate distortions of the time spectrum shape at large loads in the coincidence selection circuits, blocks were used to reject overlapping pulses. Under the experimental conditions (for 1274 and 511 keV γ-quanta) the time resolution of the spectrometer was $2\tau_0$ = 220 ps. The shape of the instantaneous coincidence curve for ^{60}Co corresponded to one Gaussian distribution up to 0.001-th of its full maximum. The time scale was graduated to 22.0(1) ps/channel.

The Doppler broadening of the 511 keV annihilation γ-line (S-parameter) was measured by an X-ray Ge(Li)-detector of volume 1 sm^3 and energy resolution 1.02 keV for the ^{106}Ru 512 keV line. The energy value of the channel was 0.080 keV. Instability of the 511 keV line position during measurements did not exceed one channel.

For measurements at different temperatures the $YBa_2Cu_3O_{7-\delta}$ samples were placed in a cylinder-shaped liquid-nitrogen-cooled vacuum cryostat ($p \simeq 10^{-3}$ Torr), diameter 18 mm. Temperature was changed by heating the intermediate hollow copper cylinder by current flowing through a double-wound winding around this cylinder. Inside it there was a small copper cylinder with the sample tightly inserted in a slot. The temperature of the sample was measured in relation to liquid nitrogen temperature by means of a copper-constantan thermocouple. The voltage from the thermocouple was also used for temperature stabilisation (winding current correction). The stabilisation system we had developed allowed a constant temperature of the sample to an accuracy better than 0.3 K in the interval 79-200 K.

The positron source of activity $\sim 30\ \mu K$ was prepared by evaporating the aqueous solution of $^{22}NaCl$ on nikel foil 1.2 μm thick coated with a gold layer 50 Å thick. The source area was $\sim 8\ mm^2$.

The time spectra were processed by the programme POSITRONFIT[9] in a microcomputer of the type IBM XT which is part of the measurement apparatus. Correction for positron annihilation in the nickel foil ($\sim 8\%$) was not taken into account. The time resolution of spectrometer $2\tau_0$ was also regarded as a fitting parameter. The values of $2\tau_0$ obtained in the fitting were within 222-225 ps. There were $\gtrsim 1.2 \cdot 10^6$ coincidences registered for each time spectrum.

To follow the annihilation γ-line shape varying with the sample temperature, the S parameter was calculated, which is the ratio of the number of counts in 14 channels of the central part of the 511 keV peak to the sum of counts in two windows (18 channels each) on the peak's left and right slopes.

$YBa_2Cu_3O_{7-\delta}$ Samples

The samples to be investigated were prepared by sintering Y_2O_3, BaO_2, CuO in the Laboratory of Nuclear Problems, JINR (sample 1) and by sintering Y_2O_3, $BaCO_3$, CuO in the Institute of Physics of the Curie-Sklodowska Lublin University (samples 2, 3). The sintering temperature was 950°C, the superconducting transition temperatures T_c were 96, 86, 95 K, respectively. The behaviour of the function R(T) allowed an assumption that all three samples were not single-phase ones.

Results of Measurements and Discussion

The components with $\tau_1 \simeq 180$ ps, $\tau_2 \simeq 350$ ps and $\tau_3 \simeq$ $\simeq 1.9$ ns can be singled out in the positron lifetime spectra of the samples under investigation. The intensity of the longest-lived component τ_3 did not exceed 0.55% and J_2 varied from a sample to a sample within the range of 8%-17%. The attempts to single out only two components lead to a significantly worse reduced χ^2 (~ 1.3 at two components instead of ~ 1.1 at three components) and to $\tau_1 \simeq 190$ ps,

$\tau_2 \simeq 480$ ps. Since no variations of τ_3 were found in the temperature range investigated, the final analysis of all time spectra was performed at a fixed averaged value of this parameter.

Our measurements in the temperature range of 80-130 K and at room temperature showed that the change in the positron annihilation character in our samples at their transition to the superconducting state is relatively small. The transition to the superconducting state is seen to lead to larger τ_1 and τ_2, to a small intensity of J_2 and parameter S (Figure).

If one considers that the component with $\tau_1 \approx 180$ ps is related to the free positron annihilation in the space between lattice points, the small increase in τ_1 observed at the supperconducting transition of the sample may indicate a change in the electron structure which leads to a lower electron density. The component with $\tau_2 \simeq 350$ ps typical of annihilation of positrons captured by lattice defects should be perhaps associated with oxygen vacancies. A decrease in intensity of J_2 and parameter S at $T < T_c$ allows an assumption that the number of these defects reduces in the superconducting state. A larger τ_2 can be associated with the decreasing electron density or the increasing size of the defects. The weak component with $\tau_3 \simeq 1.9$ ns is probable due to positronium production in the porous structure of the metal-oxide ceramics.

It is state in Ref. /7/ that the lifetime τ_1 (139 ± 7 ps) does not depend on the sample temperature, the lifetime τ_2 (~210 ps) noticeably decreases at the superconducting transition while J_2 (~30%) increases. It is strange, however, that the parameter S in the superconducting state decreases as in our experiments. A possible reason for discrepancy between our results and those of Ref. /7/ is a difference in the composition of the samples investigated.

In the experiments /6/ only the Doppler broadening of the annihilation line was studied. The results for the Y-Ba-Cu-O system do not contradict our data.

An abnormal behaviour of τ_1, τ_2 and J_2 aroung T_c was observed in Ref. /8/. The lifetimes τ_1 and τ_2 have a sharp maximum of half-width ~1 K while J_2 has a deep minimum. However, the values of τ_1 and τ_2 below and above T_c agree with our results for the case of resolving the time spectrum into 2 components. Besides, an unusual increase in the positron thermalisation time t_0 (by ~130 ps) was observed in Ref. /8/ at T_c. An anomaly like this was found neither in our paper, nor in Ref. /7/.

Having compared the above results one may say that: (a) the superconducting transition of Y-Ba-Cu-O systems affects positron annihilation character; (b) quite probably, annihilation process is

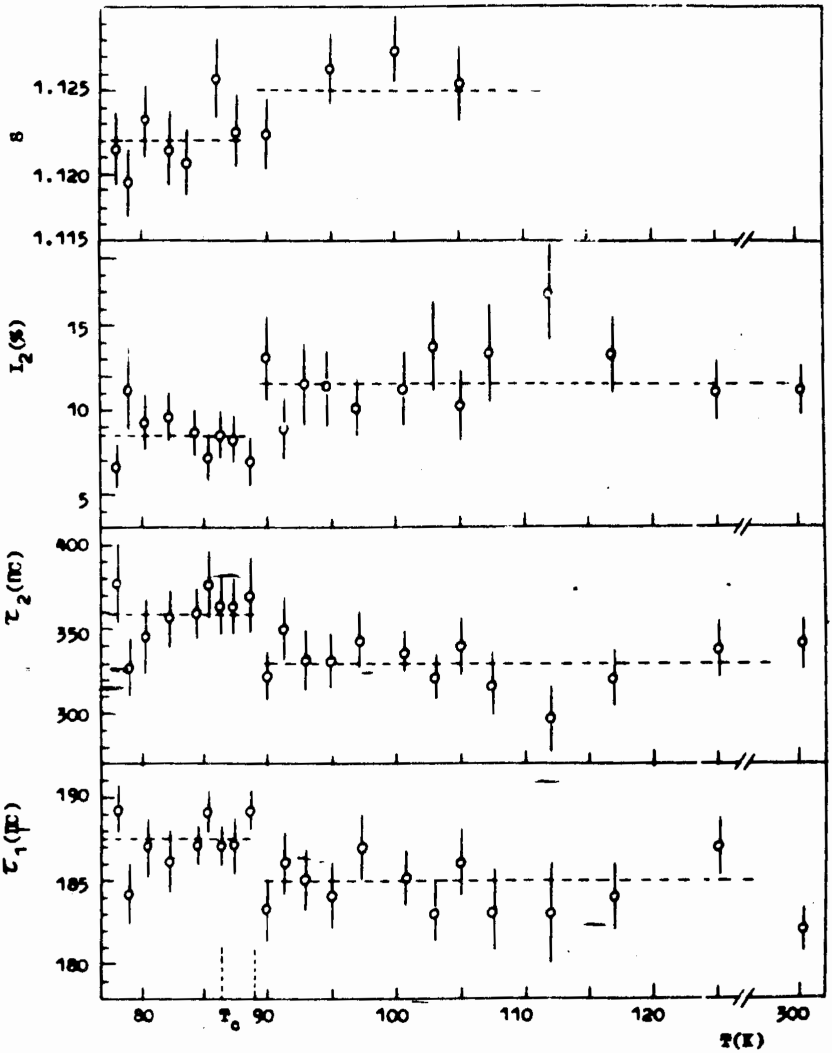

Figure. Temperature dependence of the parameters τ_1, τ_2, J_2 *and S. Dashed lines denote the mean parameter values in regions below and above* T_c.

very sensitive to the internal structure details of the samples and to their preparation technique. It is proved by the opposite temperature dependence of τ_2 and J_2 in this paper and Ref. /7/, and by their different absolute values.

In conclusion the authors express their gratitude to Prof. K.Ya.Gromov and Prof. Ts.Vylov for the constant and stimulating interest in the work, to Z Skorzynski, A.K.Kachalkin and A.I.Akatov for technical assistance in setting up an experiment.

The authors are also thankful to the leader of the programme CPBP 01.09, Poland for assistance in carrying out this investigation.

References

1. Bednorz J.C., Müller K.A. — Z. Phys. B, 1986, v.64, p.189.
2. Positrons in Solids, Ed. P.Hautojärve, Springer—Verlag, 1979, Chapter 1.
3. Stump R., Tally H.E. — Phys. Rev., 1954, v.96, p.904.
4. Green B., Modansky L. — Phys. Rev., 1956, v.102, p.1014.
5. Shafroth S.M., Marcus J.A. — Phys. Rev., 1956, v.103, p.585.
6. Ishibashi S. et al. — Jap. J. Appl. Phys., 1987, v.26, p.L688.
7. Jean Y.C. et al. — Phys. Rev. B, 1987, v.36, p.3994.
8. Teng M.-K. et al. — Phys. Lett. A, 1987, v.124, p.363.
9. Kirkegaard P. et al. — Comput. Phys. Commun., 1981, v.23, p.307.

Received on April 18, 1988.

УДК 538. 945

EFFECT OF HIGH ENERGY RADIATION ON CRITICAL PARAMETERS OF SUPERCONDUCTING CERAMICS $YBa_2Cu_3O_7$

A.S.Alexandrov, A.A.Astapov, V.M.Drobin, L.N.Zaitsev, A.V.Kuznetsov, V.I.Lushchikov, E.I.Diachkov, E.A.Protasov, G.P.Reshetnikov, V.V.Sikolenko, V.I.Smirnov, V.N.Trofimov, S.V.Chernov, A.L.Shishkin

Critical temperature (T_c) and critical current density (j_c) of high temperature superconducting (HTSC) ceramics $YBa_2Cu_3O_7$ were measured as functions of dose from $5x10^3$ Gy to $3x10^8$Gy. Samples were irradiated at room temperature by protons with energies 0.66 and 8.09 GeV and by ^{12}C with energy 3.65 GeV/nucleon. Radiation degradation of critical parameters j_c and T_c of HTSC-ceramics is stronger than in the NbTi alloy based superconductors and is obviously connected with the formation of disordered regions, leading to the electron localization and to the infractions of Josephson contacts between ceramics grains.

The investigation has been performed at the Laboratory of High Energies, JINR.

Влияние излучений высокой энергии на критические параметры сверхпроводящей керамики $YBa_2Cu_3O_7$

А.С.Александров и др.

Измерены зависимости критической температуры (T_c) и плотности критического тока (j_c) высокотемпературной сверхпроводящей (ВТСП) керамики $YBa_2Cu_3O_7$ от дозы в диапазоне $5 \cdot 10^3$–$3 \cdot 10^8$ Гр. Облучение проведено при комнатной температуре протонами с энергией 0,66 и 8,09 ГэВ и ядрами ^{12}C с энергией 3,65 ГэВ/нуклон. Радиационная деградация критических параметров j_c и T_c ВТСП-керамики сильнее, чем у сверхпроводников на основе NbTi сплава, и связана, по-видимому, с образованием разупорядоченных областей, приводящих к локализации электронов и нарушению джозефсоновских контактов между гранулами.

Работа выполнена в Лаборатории высоких энергий ОИЯИ.

Samples and Conditions of Irradiation

Single-phase samples of $YBa_2Cu_3O_7$ ceramics were prepared as described in ref.(1) and had dimensions not exceeding 1x4x15 mm.

Such sample size was determined mainly by ceramics mechanical strength, by the construction of current and potential contacts, and by the cross section of extracted beam from a synchrophasotron and phasotron of JINR in the region of irradiation.

Samples were irradiated at room temperature directly by protons with energy E_p = 660 MeV and ^{12}C nuclei with energy E = = 3.65 GeV/nucleon, and also by protons with energy E_p = 8.09 GeV through a copper target. Dose fractions after the samples successive irradiations (D) are presented in the table.

At D $\lesssim 10^5$ Gy the doses were determined both directly, using the coloured film dosimeters (12), and by fluence (ϕ) of the beam through the samples. At D $\gtrsim 10^5$ Gy the doses were determined by the fluence only (taking into account nuclear interactions) by measuring the activation from the $^{27}Al(p,3p3n)^{22}Na$ reaction of the aluminium foils the samples were rapped in. Transition coefficients from ϕ to D are:

$$K_p(E_p = 0.66\ \mathrm{GeV}) = 2.9 \times 10^{-10}\ \mathrm{Gy \cdot sm^2};$$

$$K_{^{12}C}(E = 3.65\ \mathrm{GeV/nuc}) = 17 \times 10^{-10}\ \mathrm{Gy \cdot sm^2}.$$

In all cases the dose determination error did not exceed 20%. Following ref. (3), for the protons with E_p = 0.66 GeV the number of displacements per atom was calculated as $C_d = 6.4 \times 10^{-21}$ per unit fluence.

Effect of Irradiation on j_c and T_c

Measurements of the volt-ampere characteristics (VAC) and resistance of samples R(T) after each irradiation fraction were carried out independently on three different apparatuses by using the standard 4 contact method. As a rule, with increasing dose the regular growth of specific resistance was observed at room temperature.

The relative change in critical current density caused by a dose $j_c(D)/j_{co}(D)$ for all the irradiated samples of $YBa_2Cu_3O_7$ ceramics (3) and for the NbTi alloy based superconductors (1 and 2) is shown in fig. 1. Data on samples, primarily different in quality and specific resistance under normal conditions and then irradiated by protons, are in good enough agreement and lie on a common curve (3). At irradiation with heavy charged particles (in our case carbon nuclei) the degradation curve shifts to the region of smaller doses. It should be

Table

Doses at successive irradiation of HTSC-ceramics $YBa_2Cu_3O_7$, Gy

N	Sample code and symbol of experimental points in figs. 1 and 2		Type of radiation and energy of particles						Sum of dose
			p, E_p=8.09 GeV irradiation through target	p, E_p=8.09 GeV irradiation through target	^{12}C, E_{12_C}=3.65 GeV/n	p, E_p=0.66 GeV	^{12}C, E_{12_C}=3.65 GeV/n	p, E_p=0.66GeV	
			1	2	3	4	5	6	
1	M1	⊕	$5.2\cdot10^4$	$4.8\cdot10^4$	-	$3.5\cdot10^5$	-	-	$4.6\cdot10^5$
2	M2	◊	-	-	$5\cdot10^3$	-	$1.3\cdot10^4$	-	$1.8\cdot10^4$
3	D1	□	10^5	$4.8\cdot10^4$	$2.6\cdot10^3$	$3\cdot10^6$	$3.5\cdot10^4$	-	$3.2\cdot10^6$
4	D2	▽	-	10^4	$8\cdot10^2$	-	-	$3.5\cdot10^5$	$3.6\cdot10^5$
5	D3	◊	-	$3\cdot10^4$	$8\cdot10^3$	-	-	-	$3.8\cdot10^4$
6	D6	◊	-	-	-	$2.2\cdot10^5$	-	$1.7\cdot10^8$	$1.7\cdot10^8$
7	D8	○	-	-	$6\cdot10^4$	-	$3.4\cdot10^4$	-	$9.4\cdot10^4$
8	D10	▽	-	-	-	$1.5\cdot10^7$	-	$2.9\cdot10^8$	$3.1\cdot10^8$
9	D11	△	-	-	-	$4.4\cdot10^5$	$2.8\cdot10^4$	-	$4.7\cdot10^5$
10	B1	◧	-	$1.6\cdot10^4$	$2\cdot10^2$	-	$3\cdot10^4$	-	$4.6\cdot10^4$
11	B2	⊗	-	$8\cdot10^4$	$1.5\cdot10^3$	$5\cdot10^6$	$1.5\cdot10^4$	$1.6\cdot10^8$	$1.6\cdot10^8$
12	B3	●	-	-	-	$3\cdot10^4$	$3.5\cdot10^4$	$4.4\cdot10^5$	$5\cdot10^5$
13	B4	▲	-	-	-	$1.5\cdot10^4$	-	$2\cdot10^8$	$2\cdot10^8$
14	B5	◩	-	-	-	$2\cdot10^4$	$3.2\cdot10^4$	-	$5.2\cdot10^4$

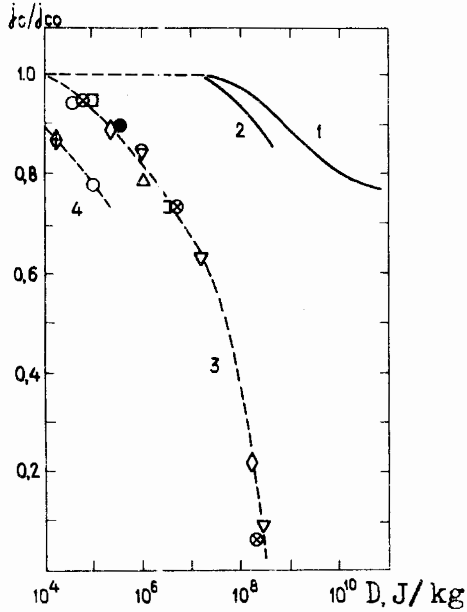

Fig. 1. Dependence $j_c(D)/j_{co}(D)$ for the low temperature NbTi superconductors irradiated by reactor neutrons (1) and protons with energy 30 GeV (2), and for the HTSC-ceramics $YBa_2Cu_3O_7$ irradiated by protons with energy 0.66 and 8.09 GeV (3) or nuclei ^{12}C with energy 3.65 GeV/nucleon (4). Denotions are indicated in the table.

noted that the irradiation under similar conditions of a monocrystal of a $YBa_2Cu_3O_7$ compound investigated in work (4) has increased j_c by 2-3 times, while the reported here HTSC-ceramics are by 1-2 orders of magnitude less radioresistant than the NbTi superconductors, which are also sensitive to the type of irradiation at equal doses.

Figure 2 shows the dependence of the relative critical temperature of the given HTSC ceramics on the doses $T_c(D)/T_{co}(D)$ in comparison with the results on irradiation of Chevrel phases and A-15 structures (6). Data on different samples lie also on a common curve and are in agreement with earlier data (7,8). The observed in work (4)

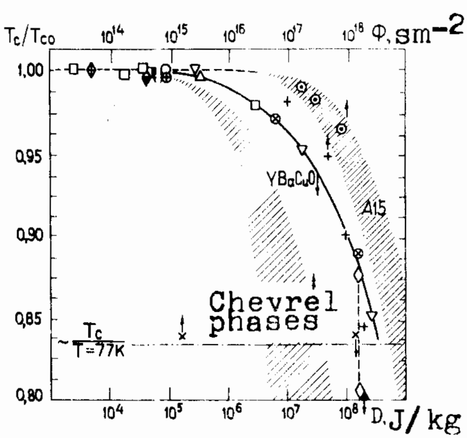

Fig. 2. Dependence $T_c(D)/T_{co}(D)$ for the HTSC-ceramics $YBa_2Cu_3O_7$ under irradiation: a) by protons and ^{12}C nuclei (solid curve with experimental points on it, symbols being explained in the table; b) by neutrons with $E_n > 0.1$ MeV (the data on single-phase ceramics (+) and monocrystal (O) are given); c) by α-particles with $E_α = 6.1$ MeV (the results are obtained with a film 1-2 μm thick (∇)).

degradation of T_c at irradiation of a monocrystal $YBa_2Cu_3O_7$ by fast neutrons is as yet difficult to explain.

Conclusions

Under irradiation the disorder regions seem to arise in a $YBa_2Cu_3O_7$ compound. Spontaneous recombination of initially knocked out atoms due to thermally activated (in track) zones of disorder in a crystal with a dielectric layer allows the use of the dose dependence of critical parameters in place of the dependence on the number of displacements per atom.

References

1. Cava R.J. — Phys. Rev. Lett., 1987, v.58, No.4, p.408.
2. Astapov A.A. et al. JINR Report 14-88-57, Dubna, 1988.
3. Koptelov E.A., Staviski U.I. Preprint INR P-0053, M., 1977.
4. Umerava A. et al. — Phys. Rev. B, 1987, v.36, No.13, p.7151.
5. Zaitsev L.N. Radiation Effects in Accelerator Structures, M.: Atomizdat, 1987, p.116.
6. Maskidashvili I.A. Questions of Atomic Science and Technology. Series: Physics Radiation Damages and Radiation Material Study. Issue 4(18), 1981, p.19.
7. Antonenko S.V. et al. Pis'ma ZhETF, 1987, v.46, issue 9, p.362.
8. Egner B. et al. XVIII Int. Conf. on Low Temperature Physics, LT18, Aug. 20-26, 1987, Kyoto, Japan, 1987, v.III, p.2141.

Received on Jule 22, 1988.

Краткие сообщения ОИЯИ №4 [30]-88 *JINR Rapid Communications No.4 [30]-88*
УДК 538.945

НАМАГНИЧЕННОСТЬ КЕРАМИКИ $YBa_2Cu_3O_{7-x}$ ПОСЛЕ ОБЛУЧЕНИЯ РЕЛЯТИВИСТСКИМИ ЯДРАМИ УГЛЕРОДА

И.Н.Гончаров, О.Е.Омельяновский *

Проведены измерения R(T), χ(T) и M(B) образцов керамики $YBa_2Cu_3O_{7-x}$, облученных релятивистскими ядрами фтора и углерода (максимальный флюенс $6{,}3 \cdot 10^{12}$ яд./см^2). Кривые R(T) и χ(T) облученных образцов не отличаются от кривых для исходного образца. В то же время разница между M_- и M_+, а следовательно, и величина внутризеренной плотности тока j_c, проходят через максимум, лежащий при флюенсах, меньших $2 \cdot 10^{12}$ яд./см^2 (для случая, когда магнитное поле параллельно трекам).

Работа выполнена в Лаборатории высоких энергий ОИЯИ.

Magnetization of $YBa_2Cu_3O_{7-x}$ Ceramics after Irradiation with Carbon Relativistic Nuclei

I.N.Goncharov, O.E.Omelyanovsky

R(T), χ(T) and M(B) of samples of $YBa_2Cu_3O_{7-x}$ ceramics were measured after irradiation with relativistic nuclei of fluorine and carbon (maximum fluence of $6.3 \cdot 10^{12}$ nucl./cm^2). The curves of R(T) and χ(T) for irradiated samples do not differ from those for an initial sample. At the same time the difference between M_- and M_+ and, consequently, the value of intragrain current density j_c pass via maximum located at the fluences less than $2 \cdot 10^{12}$ nucl./cm^2 (for the case when magnetic field is parallel to tracks).

The investigation has been performed at the Laboratory of High Energies, JINR.

Исследовать влияние облучения на свойства ВТСП важно как с точки зрения получения существенной, порой уникальной, информации о физике этого явления, так и с точки зрения использования этого нового класса сверхпроводящих материалов в радиационных полях (ускорители, термоядерные реакторы, космические аппараты и т.д.).

---

* *Физический институт им. П.Н.Лебедева АН СССР, Москва*

В различных лабораториях мира уже выполнены первые исследования свойств ВТСП, облученных нейтронами /1–4/ и ионами /5–9/. Прежде всего, обнаружено, что они гораздо более чувствительны к облучению, чем соединения типа А15 (Nb_3Sn, Nb_3Ge, V_3Si) — для снижения критической температуры до определенной доли от исходной требуются в 10-20 раз меньшие величины флюенсов частиц. При этом утверждается, что облучение сильнее влияет на межзеренную связь, чем на внутреннюю область зерна ВТСП-керамики. В ряде работ /2–6, 8, 9/ получены очень интересные и неоднозначные результаты о влиянии облучения нейтронами и ионами на критическую плотность тока ВТСП. Транспортный критический ток, измеренный либо пропусканием через образец тока от внешнего источника, либо путем наведения его в кольце, неизменно снижался в результате облучения Что же касается внутризеренной плотности тока j_c в керамике или j_c в монокристалле, вычисленных из измерений магнитного момента, то они заметно возрастали при флюенсах нейтронов, соответствующих началу падения T_c, свидетельствуя о повышении пиннинга вихревых нитей (по-видимому, на образовавшихся в результате облучения многочисленных микрообластях с ухудшенными сверхпроводящими параметрами).

В настоящей работе проведены измерения намагниченности образцов ВТСП-керамики до и после облучения релятивистскими ядрами с целью обнаружить его влияние на внутризеренную критическую плотность тока.

Образцы изготавливались по методу твердотельной диффузии /10/ с многократным перетиранием, прессованием и отжигом их. Для окончательного отжига в печь были помещены одновременно несколько спрессованных дисков одинаковой массы. В окончательном виде образцы имели вид дисков диаметром 5 мм и толщиной 1,6 мм.

Облучение образцов проводилось при комнатных температурах на выведенном пучке синхрофазотрона ОИЯИ (падавшем перпендикулярно плоскости дисков) при энергии 3,65 ГэВ/нукл. Образец II·1 облучен ядрами ${}^{19}_{9}F^{9+}$ с флюенсом 0,002 · $\cdot 10^{12}$ яд./см^2, а образцы II·2, II·3, II·4 и II·5 облучены ядрами углерода ${}^{12}_{6}C^{6+}$ с флюенсами соответственно 3,4; 2,9; 2,0; 6,3 · 10^{12} яд./см^2. Флюенсы определялись по изменению плотности цветного пятна пленочных радиохромных детекторов, которые были прокалиброваны гамма-излучением во ВНИИФТРИ, с использованием расчетных данных по ионизационным потерям ядер углерода в пленке данного состава*. Эпизодический дополнительный контроль за параметрами пучка осуществлялся путем измерений с ионизационными камерами (многопроволочными — для определения профиля пучка и с двумя большими электродами для определения полного потока ядер). Точность в определении соотношения флюенсов не хуже 10%, а точность в определении абсолютной величины не хуже 35%.

Для всех образцов проводились измерения кривых перехода по сопротивлению и по магнитной восприимчивости. Результаты представлены на рис. 1. Облучение не привело к изменению кривых перехода (в пределах 1%).

Намагниченность измерялась с помощью чувствительного вибрационного магнитометра /10/ при температуре 4,2 К путем медленного увеличения и последующего уменьшения магнитного поля $B \leq 8$ Тл. Эпизодически развертка магнитного поля останавливалась и определялось равновесное значение $|M(B)|$, которое было на 8-9% ниже, чем в случае ненулевой развертки. Кривые

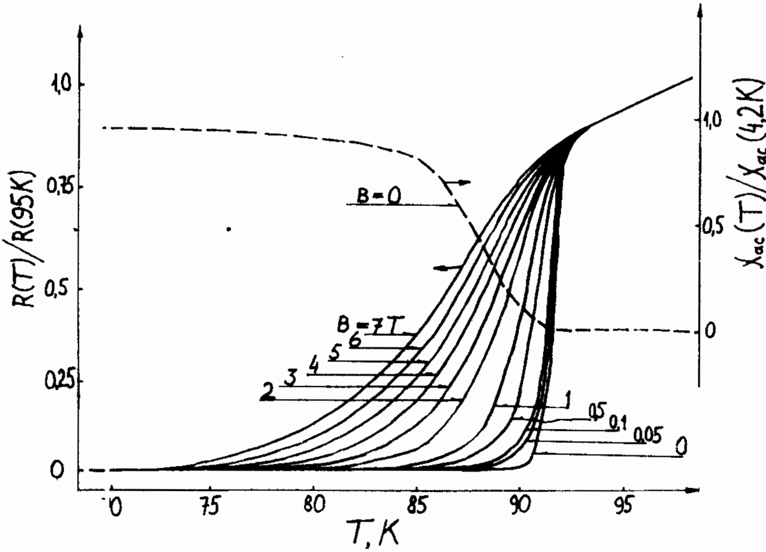

Рис. 1.Температурные кривые перехода необлученного образца из нормального в сверхпроводящее состояние по сопротивлению и восприимчивости.

** Авторы выражают признательность В.В.Генераловой, А.А.Громову и М.Н.Гурскому за помощь при калибровке детекторов, а также А.П.Череватенко, выполнившему расчеты ионизационных потерь.*

-M(B) имели характерный вид с максимумом и очень малым изменением при $B > 4$ Тл (см., например,[10]). Критическая плотность тока пропорциональна $\Delta M = M_- - M_+$, где M_+ и M_- — равновесные значения магнитных моментов образца соответственно при вводе и выводе поля. Так как геометрические размеры зерен в образцах (а также и самих образцов) не меняются при облучении, то изменение ΔM отражает изменение внутризеренной критической плотности тока[11]. Величины $\Delta M^i/m^i$, нормированные к этим же величинам для необлученного образца*, представлены на рис. 2 (здесь m^i — масса соответствующего образца). Измерения проводились в условиях, когда поле параллельно трекам (т.е. параллельно оси дисков) и перпендикулярно им. Соответствующие поля обозначим как $B_{||}$ и $B_{\perp}$.

Анализ результатов показывает, что в случае $B_{||}$, т.е. когда пиннинг на треках наиболее эффективен, кривые намагниченности, а следовательно, и внутризеренной плотности тока j_c в зависимости от флюенса проходят через максимум, лежащий, очевидно,

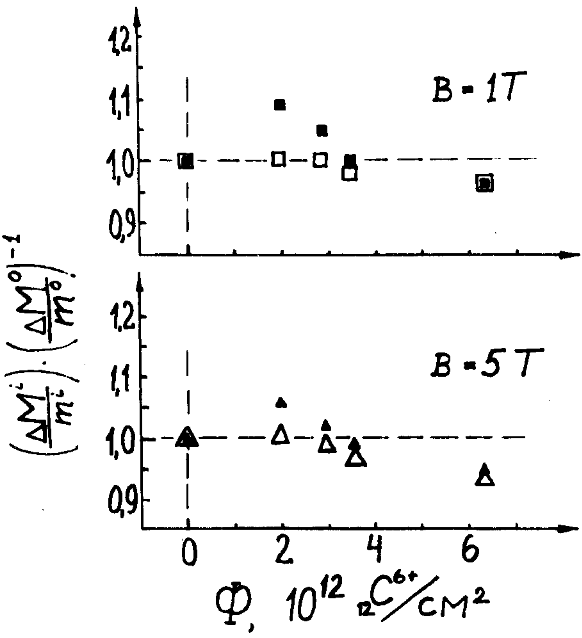

Рис.2. Зависимость внутризеренной критической плотности тока от флюенса для случаев, когда магнитное поле параллельно трекам (сплошные значки) и перпендикулярно им.

** Заметим, что после облучения ядрами фтора с малым флюенсом ($2 \cdot 10^9$ яд./см^2) указанное отношение для образца II · 1 и исходного образца II · 0 не отличалось от единицы, свидетельствуя о надежности выбранной нормировки.*

при флюенсах, меньших $2 \cdot 10^{12}$ яд./см^2 (когда средние расстояния между треками оказываются не менее 70 Å). И хотя величина максимума неизвестна, знаменательным является то, что впервые для образцов ВТСП наблюден пиннинг на отдельных треках. Это подтверждается и тем, что в случае $B_{\perp}$ никакого роста j_c не обнаружено, как и следовало ожидать. Естественно предположить, что облучение частицами с более высокими линейными передачами энергии (например, более тяжелыми или менее быстрыми ионами) при тех же флюенсах приведет к более заметному увеличению j_c таких образцов.

Что касается уменьшения j_c при флюенсах, превышающих $3 \cdot 10^{12}$ яд./см^2 (как для $B_{||}$, так и для $B_{\perp}$), то, видимо, здесь начинают превалировать процессы, приводящие в конце концов к полному исчезновению высокотемпературной сверхпроводимости вследствие массированного облучения таких материалов /1-8/.

Литература

1. Воронин В.И. и др. — Письма в ЖЭТФ, 1987, т.46 (приложение), с.165.
2. Sekula S.T. et al. — Proc. of LT 18, 1987, v.2, p.1185, Kyoto.
3. Küpfer H. et al. — Z. Phys. B — Condensed Matter, 1987, v.69, p.167.
4. Umèzawa A. et al. — Phys. Rev., 1987, B36, No.13, p.7151.
5. Geerk J. et al. — Z. Phys. B — Condensed Matter, 1987, v.67, p.507.
6. Egner B. et al. — Proc. of LT 18, 1987, v.3, p.568.
7. Антоненко С.В. и др. — Письма в ЖЭТФ, 1987, т.46, в.9, с.362.
8. Астапов А.А. и др. Сообщение ОИЯИ 14-88-57, Дубна, 1988.
9. Антоненко С.В. и др. — Письма в ЖЭТФ, 1988, т.47, в.5, с.260.
10. Карасик В.Р. и др. Препринт ФИАН № 271, М., 1987.
11. Карасик В.Р. и др. Препринт ФИАН № 296, М., 1987.

Рукопись поступила 22 июля 1988 года.

Краткие сообщения ОИЯИ №4 [30]-88 *JINR Rapid Communications No.4 [30]-88*
УДК 537.312 + 541.15 + 548.539

THE STABILIZATION OF HIGH-TEMPERATURE SUPERCONDUCTOR $Y_1Ba_2Cu_3O_{7-\delta}$ SURFACE

S.A.Korenev, D.Valentovič, V.I.Lushchikov

A technique is suggested for stabilization of a high-temperature superconductor $Y_1Ba_2Cu_3O_{7-\delta}$ surface by means of a high-current pulsed electron beam (J = 12.5 ÷ 65 A/cm^2, E = 70 ÷ 200 keV, t = 300 ns, P = 0.001 Pa). The quality of the remelted surface film is characterized and first experimental results are discussed. It is shown that within 50 days after the electron beam processing, no dielectric film was developed at superconductor surface and superconductor characteristics did not change.

The investigation has been performed at the Scientifical-Methodical Division, JINR.

Стабилизация поверхности высокотемпературного сверхпроводника $Y_1Ba_2Cu_3O_{7-\delta}$

С.А.Коренев, Д.Валентович, В.И.Лущиков

Обсуждается метод стабилизации высокотемпературного сверхпроводника $Y_1Ba_2Cu_3O_{7-\delta}$ путем оплавления его поверхности импульсным сильноточным электронным пучком и приводятся первые экспериментальные результаты. В экспериментах использовался электронный пучок с параметрами: плотность тока 12,5÷ ÷65 А/см^2, кинетическая энергия электронов 70 ÷ 200 кэВ, длительность импульса тока пучка ~ 300 нс. Облучения проводились в вакуумных условиях при давлении остаточного газа Р ~ 10^{-3} Па. Экспериментально показано, что в течение 50 суток после облучения на поверхности керамики $Y_1Ba_2Cu_3O_{7-\delta}$ отсутствует диэлектрическая пленка, а сверхпроводящие характеристики образца не ухудшаются.

Работа выполнена в Общеинститутском научно-методическом отделении ОИЯИ.

Y-Ba-Cu-O high-temperature ceramic superconductive materials are investigated in many laboratories throughout the world /1/. However, a certain progress has been achieved in fabricating superconductive high-temperature ceramics having stable superconductive characteristics. It must be mentioned that $Y_1Ba_2Cu_3O_{7-\delta}$ surface is degraded during storing superconductive samples in atmospheric environment. Apparently the surface degradation is caused by development of a surface dielectric layer composed of metal hydrooxides [2]. The existence of such a film may cause surface unstability problems.

In this rapid communication a method of the superconductor surface stabilization by means of a high current pulsed electron beam surface remelting is suggested, and our first experimental results are presented.

The surface thermoprocessing of many materials using concentrated pulses of high power beams (laser, electron, etc.) results in a stable protective layer [3].

In accordance with [3], for the case of pulsed electron beam used for the surface thermoprocessing it is necessary to have the beam power density higher than 10^6 W/cm^2 and the surface freezing velocity of material higher than 10^5 K/sec.

Analysing the model of the nanosecond electron beam interaction with material surface [4] it may be shown that the physical phenomena which are taking place during the electron pulse beam stabilization of the $Y_1Ba_2Cu_3O_{7-\delta}$ surface may be characterized as the adiabatic ones.

Due to lack of data in literature we have used approximative thermophysical data for our material and we have estimated the time constant of the e-beam remelted surface freezing as 10^{-4} sec. Thus the superconductor surface may be modified by our electron beam up to penetration depth of the electrons. (See fig. 1). The details of experiments with our electron beam source may be found in [5]. The ceramic samples which had been processed were placed behind e-beam source anode (cathode-anode-sample). The vacuum in the apparatus used was 10^{-3} Pa.

The dimensions of our experimental $Y_1Ba_2Cu_3O_{7-\delta}$ superconductive samples were 25x5x1 mm^3 and they were prepared in the Laboratory of Neutron Physics of the JINR at Dubna. The converted dielectric surface layer was mechanically removed directly prior to the electron beam processing. The surface of our experimental samples prior to and after the e-beam processing may be seen in SEM pictures (fig. 2). The picture of remelted surface is in fig. 2b. Using the results of [3] we have estimated the maximum surface temperature within the interval of 1500-2000° C during sample processing by means of e-beam.

The depth of modified layer estimated from SEM pictures (not shown) as 50-60 μm corresponds to fig. 1, penetration depth of electrons being 200 keV.

We have measured the electric resistance R of the samples immediately after the e-beam processing and 50 days after. The simple measu-

Fig. 1. Depedence of penetration dept h on energy of electrons E for $Y_1Ba_2Cu_3O_{7-\delta}$ material.

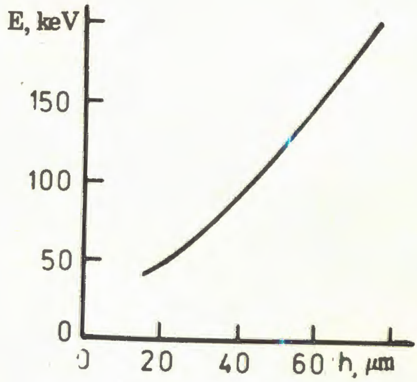

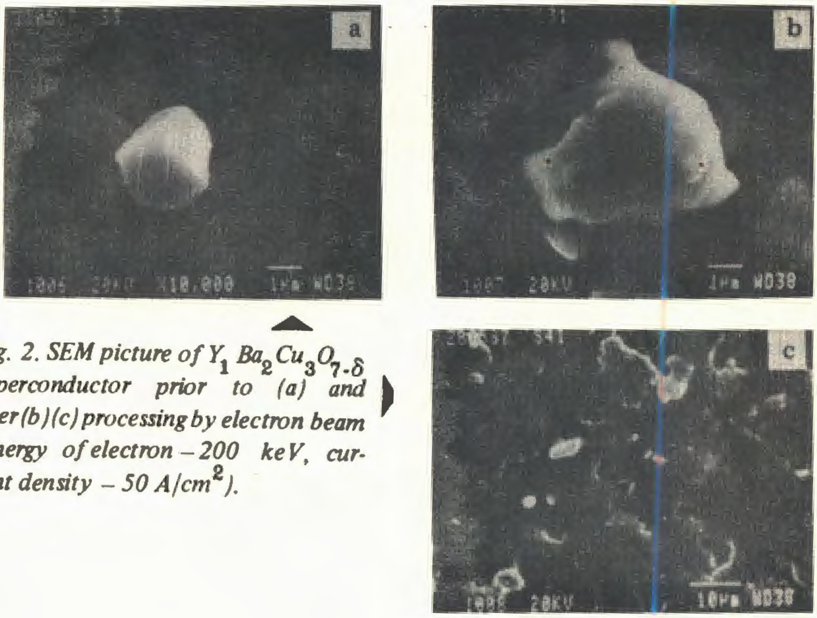

Fig. 2. SEM picture of $Y_1Ba_2Cu_3O_{7-\delta}$ superconductor prior to (a) and after (b)(c) processing by electron beam (energy of electron – 200 keV, current density – 50 A/cm^2).

Fig. 3. Measuring scheme of resistance R along the sample length: CK – superconducting ceramics, Э – electrode, N – number of electron pulses applied along length of sample, In – Indium layer, Cu – Cu electrode.

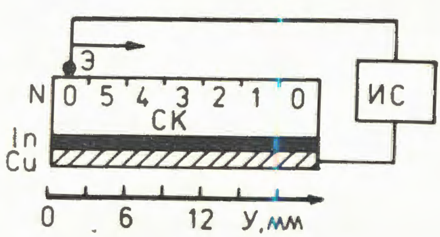

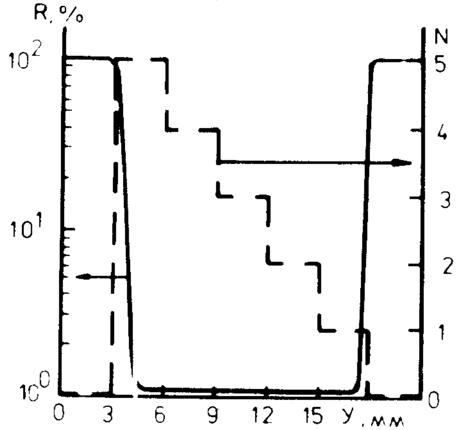

Fig. 4 The resistanse R along sample length Y dependence on number N of electron pulses applied (histogramm).

ring scheme is shown in fig. 3; and the results, in fig. 4. It may be seen that the resistance R of the surface processed is about two orders of magnitude lower than the resistance of unprocessed regions, R does not depend on the number of e-beam pulses applied subsequently—N, and R remains the same within 50 days after processing at least.

The analogic results were obtained for Nb_3Ge in [6] where characteristics of the surface did not depend on N too.

The evidence of a dielectric layer present on unprocessed $Y_1Ba_2Cu_3O_{7-\delta}$ surface was proved by impedance measuring. Originally all our samples had capacitive impedance but, after the e-beam processing the impedance was pure ohmic. The ohmic impedance was checked on the samples immediately after their dielectric film was removed mechanically but, it became capacitive few hours after again.

We believe that the high power pulsed electron beam stabilization of $Y_1Ba_2Cu_3O_{7-\delta}$ superconductive surface should be one of the new possibilities in the high temperature superconductivity technology.

We should like to express our thanks to O.L.Orelovich, V.A.Altynov, S.V.Kostuchenko for their help and B. V. Vasiliev for useful discussions.

References

1. Bednors J.G., Muller K.A. — Z. Phys., 1986, v.B64, p.189.
2. Somekh R.E. et al. — Nature, 1987, v.326, p.857.
3. Kraposhin V.S. Results of Science and Technology. Physical Metallurgy and Thermal Treatment. Moscow, VINITI, 1987, v.21, p.144.
4. Fracis M. et al. — J. Appl. Phys., 1967, v.38, No.2, p.627.
5. Korenev S.A. JINR 9-87-313, Dubna, 1987.
6. Vavra I., Korenev S.A. JINR P13-86-860, Dubna, 1986.

Received on April 26, 1988.

Краткие сообщения ОИЯИ №4 [30]-88 *JINR Rapid Communications No.4 [30]-88*
УДК 537.312 + 541.15 + 548.539

THE EMISSION CHARACTERISTICS OF $Y_1 Ba_2Cu_3O_{7-\delta}$ CATHODE

S.A.Korenev

The results are presented of experimental investigation of the electron beam in diode with cathode on the base of $Y_1 Ba_2Cu_3O_{7-\delta}$. After corresponding cathode training, the cathode made from $Y_1 Ba_2Cu_3O_{7-\delta}$ material may be practicable of stable current electron beam yeild. It is shown experimentally that at the voltage of diode of about 100÷÷300 kV there exists an evident possibility of forming the electron beams with the current density of 70 A ÷ 380 A/cm^2. The motion velicity of cathode plasma in the direction of anode for this material of a cathode amounts to $(1 \div 3) \cdot 10^6$ cm/s.

The investigation has been performed at the Scientifical-Methodical Division, JINR.

Эмиссионные характеристики катода из $Y_1 Ba_2Cu_3O_{7-\delta}$

С.А.Коренев

Приводятся результаты экспериментального исследования формирования электронных пучков в диоде с катодом со взрывной эмиссией на основе $Y_1 Ba_2Cu_3O_{7-\delta}$. После тренировки катода, изготовленного из $Y_1 Ba_2Cu_3O_{7-\delta}$, можно осуществлять стабильный токоотбор пучка электронов. Экспериментально показано, что при напряжении на диоде 100÷300 кВ можно формировать электронные пучки с плотностью тока ~70÷380 А/см^2. Скорость движения катодной плазмы в сторону анода для этого материала катода составляет ~ $(1 \div 3) \cdot 10^6$ см/с.

Работа выполнена в Общеинститутском научно-методическом отделении ОИЯИ.

In high temperature superconductor research, attention is paid to the emission characteristics of superconductors /1/ .

In this rapid communication the experimental results of the electron emission from the $Y_1Ba_2Cu_3O_{7-\delta}$ superconductor cathode working in explosion regime are given.

The experiments have been performed on high-current electron beam source /2/. The electron source consists of a high-voltage Arkadiev — Marx pulse generator (peak voltage ~ 100-300 kV, pulse duration 300-1000 ns) and vacuum diode. The anode was made from stainless steel grid having transmission coefficient ~ 0.6. The cylindrical $Y_1Ba_2Cu_3O_{7-\delta}$ cathode fixed on a liquid nitrogen cooled support has diameter 6 mm and the tip radius 3 mm.

The emission characteristics of 3 cathodes (having resistivities ρ ~ 2 $\Omega \cdot$cm; 10^{-1} $\Omega \cdot$ cm; $2.5 \cdot 10^{-2}$ $\Omega \cdot$ cm) have been investigated. The cathode temperature prior to impulse starting was measured by a Cu-constantan thermocouple. The apparatus vacuum pressure was $5 \cdot 10^{-5}$ Tor. The electron beam current was registered by an integrating Rogowski transformer and a Faraday cup; the voltage, by high resistance pulse attenuator.

In fig. 1 the voltage-current characteristics (v.c.ch.) of diodes having the plasma initiation regime temperature T_1 ~ 300 K (fig.1a) and T_2 ~ 79 K (fig. 1b) are displayed. The cathode-anode distance is 1 cm. As one can see analysing the v.c.ch., the current yield of diode does not depend on the cathode resistivity at both temperatures T_1 and T_2. The experimental results could be explained as following. Due to the cathode surface geometrical microinhomogeneities the explosive cathode plasma is formed under the high voltage pulse influence. The cathode plasma here is the electron emitter. As can be seen in fig. 2a, where the part of cathode is shown, the cathode has a large

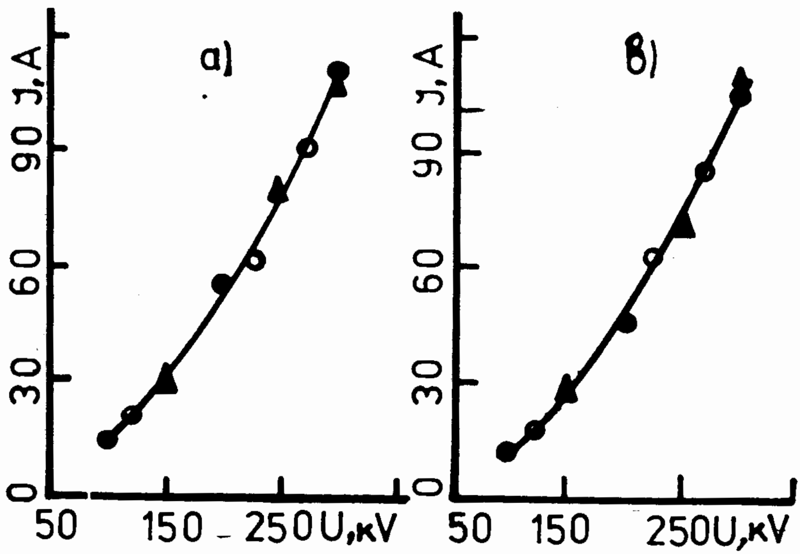

Fig. 1. Voltage-current characteristics of electron source diode with cathode made of $Y_1Ba_2Cu_3O_{7-\delta}$ for t_1 ~ 300 K (a) and t_2 ~ 79 K (b) and for: o – ρ ~ 2.5 × $\times 10^{-2}$ $\Omega \cdot$cm; ● – ρ ~ 10^{-1} $\Omega \cdot$cm; ▲ – ρ ~ 2 $\Omega \cdot$cm.

amount of different inhomogeneities on its surface, causing effects of local electric field shielding in the primary flare region, so the electron current oscillates. However, after dozens of pulses (the cathode training) these oscillations disappear, as a result of melting of the cathode surface by cathode plasma. The SEM picture of such a cathode surface (after 10 pulses, 300 keV, 300 ns) is presented in fig. 2b.

As can be seen in fig. 1, the v.c.ch. of the electron current yield corresponds to the Child-Langmuir law.

The velocity of cathode plasma may be calculated from the commutation characteristics of diode. We have calculated $V_{c.p.} \sim 3 \times 10^6$ cm/s for material resistivity $\rho \sim 2.5 \cdot 10^{-2} \div 10^{-1}$ $\Omega \cdot$ cm and $V_{c.p.} \sim 10^6$ cm/s for $\rho \sim 2$ $\Omega \cdot$cm. In comparison with the other cathode materials, of carbon fiber, for example, having $V_{c.p.c.f.} \sim 5 \cdot 10^6$ cm/s, an $Y_1Ba_2Cu_3O_{7-\delta}$ cathode permits us to enlarge the electron pulse beam duration approximatily 1.7 ÷ 5 times. This pulse enlarging permits one to construct planar source working at microsecond regime, having such a cathode with anode-cathode distance ~ 1 cm and pulse duration ~ 1 μs.

Conclusion

1. After corresponding cathode training, the cathode made from $Y_1Ba_2Cu_3O_{7-\delta}$ material may be used for construction of high current pulsed electron beam sources giving stable and homogeneous electron beam pulses. The electron current yield satisfies the Child-Langmuir law.

Fig. 2. SEM picture of $Y_1Ba_2Cu_3O_{7-\delta}$ cathode surface prior to (a) and after (b) cathode training (10 pulses, U ~ 300 kV, τ_p ~300 ns).

2. The electron beam of microsecond duration can be formed in the planar diode, which is possible due to the use of $Y_1Ba_2Cu_3O_{7-\delta}$ cathode.

I would like to express my gratitude to D.Valentovic, O.G.Zamolodchikov, S.P.Kobeleva, O.K.Smirnova for giving me kindly their superconductive $Y_1Ba_2Cu_3O_{7-\delta}$ ceramic material for construction of the above discussed cathodes.

References

1. Mecayc V.G., Shkuratov S.I. In: Problems of High-Temperature Superconductivity. P.I. Sverdlovsk, Publishing House of Academy of Sciences USSR, 1987, p.248.
2. Korenev S.A. JINR, 9-81-703, Dubna, 1981.

Received on April 26, 1988.

Краткие сообщения ОИЯИ №4 [30]-88 *JINR Rapid Communications No.4 [30]-88*
УДК 538.945

ИЗМЕРЕНИЕ КРИТИЧЕСКОГО ТОКА КОЛЬЦЕВЫХ ОБРАЗЦОВ ВЫСОКОТЕМПЕРАТУРНОГО СВЕРХПРОВОДНИКА БЕСКОНТАКТНЫМ МЕТОДОМ

В.И.Дацков, Л.Миу, И.Н.Гончаров

Описан метод бесконтактного измерения критического тока в кольцевых образцах высокотемпературного сверхпроводника (ВТСП). Показана схема созданного штока, погружаемого в гелиевый дьюар с широким горлом. Диапазон измерения критического тока в образце 5÷ 4000 А в интервале регулируемой температуры образца 4,2÷ 150 К. Показаны результаты измерения критического тока образца ВТСП из $Y_1Ba_2Cu_3O_{7-\delta}$.

Работа выполнена в Лаборатории высоких энергий ОИЯИ.

The Measurement of Critical Current in HTSC Ring Probes by the Noncontact Method

V.I.Datskov, L.Miu, I.N.Goncharov

The method of noncontact measurement of critical current in the ring probes of high-temperature superconductor (HTSC) is described. The construction of a created rod inserted in a helium storage dewar with a wide neck is presented. The range of critical current measurement in a probe is 5÷4000 A, and the range of controlled temperature for a probe is 4.2÷150 K. The results of the critical current measurements for the HTSC of $Y_1Ba_2Cu_3O_{7-\delta}$ probe are shown.

The investigation has been performed at the Laboratory of High Energies, JINR.

Известный метод 4-контактного измерения критического тока образцов ВТСП обладает определенным недостатком. В местах подвода тока к керамике имеются резистивные участки, в которых при больших токах возможен нагрев керамики, ведущий к искажению результатов измерения. С другой стороны, известна работа/1/ по измерению критических токов обычных сверхпроводников бесконтактным методом, исключающим разогрев образца.

Авторы настоящей методики создали шток для бесконтактного измерения критического тока образцов ВТСП. Принципиальная схема измерительной части штока показана на рис. 1. Кольцевой образец 1 насаживается на трубку 2 и поджимается прижимом 3 таким образом, чтобы середина образца 1 оказалась на одном уровне с плоскостью датчика Холла 4. Вся сборка помещена в квазиадиабатическую измерительную камеру 5, температура которой с помощью внешнего электронного терморегулятора, нагревателя 7 и термометра 6 может изменяться от 4,2 до 150 К. Температура образца измеряется с помощью термометра 8 на основе угольного резистора типа ТВО. Измерительная камера 5 помещена в сверхпроводящий соленоид 9, необходимый для создания экранирующего тока в кольцевом образце. На рис. 2 показана блок-схема аппаратурного обеспечения методики. Данная методика работает следующим образом. Шток с установленным в нем кольцевым образцом вставляется в гелиевый дьюар с широким горлом

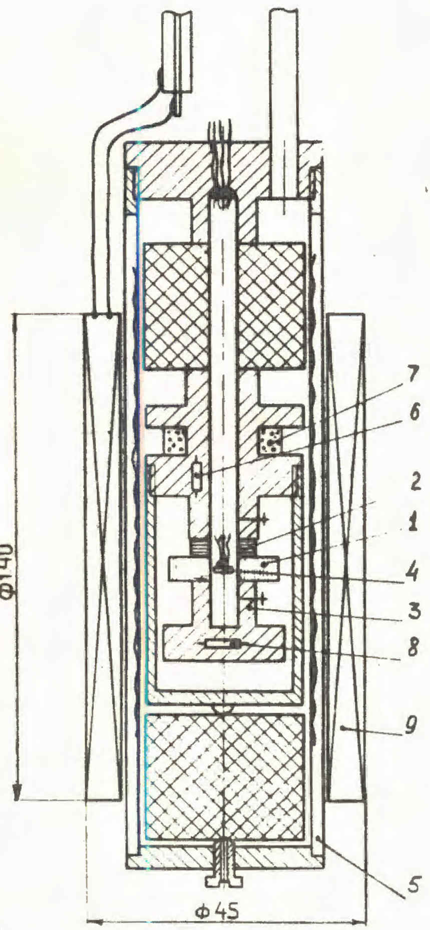

Рис. 1. Схема измерительной части штока.

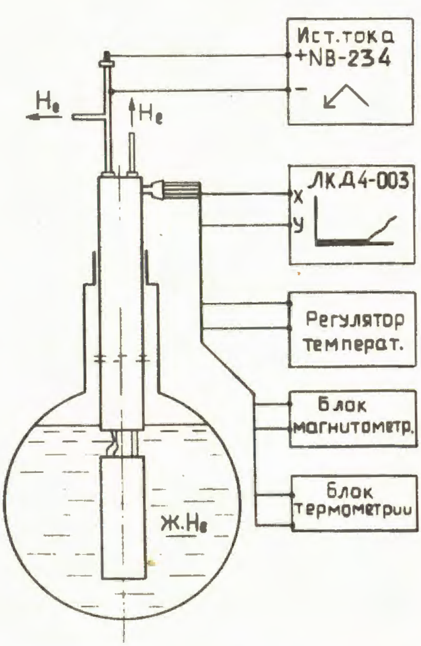

Рис. 2. Блок-схема аппаратурного обеспечения методики.

Рис. 3. Зависимость показаний датчика Холла от тока соленоида штока: 1 – без образца ВТСП; 2 – с образцом ВТСП.

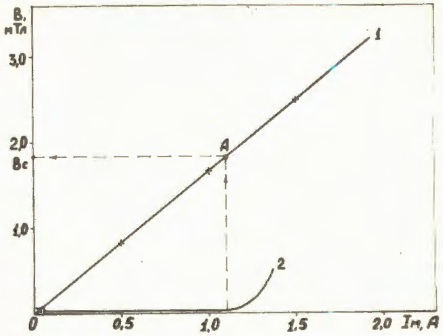

диаметром ≥ 45 мм. Затем после охлаждения с помощью терморегулятора устанавливается необходимая температура образца. Измерительный ток датчика Холла $= 100$ мА стабильностью 10^{-4}. При введении тока в соденоид (рис. 3) поле в нем нарастает по зависимости 1, сигнал с датчика Холла соответствует зависимости 2. В это время в кольцевом образце ВТСП наводится экранирующий ток, препятствующий проникновению магнитного поля соленоида в отверстие с датчиком Холла. При достижении критической величины экранирующий ток в образце начинает разрушаться, и датчик Холла показывает проникновение поля соленоида во внутреннее отверстие образца. Величина магнитного поля соленоида в данный момент соответствует положению точки А на зависимости I и равна B_c. Критический ток I_c кольцевого образца можно определить по формуле:

$$I_c = K \cdot I_M' , \qquad (1)$$

где I_M' — ток соленоида в момент перехода кольца, К — коэффициент пропорциональности, получаемый экспериментально при калибровке. Калибровка заключается в замене образца ВТСП на разрезное медное кольцо с теми же размерами и введении в него такого тока, чтобы получить аналогичное показание датчика Холла $\approx B_c$ (рис. 3). После каждого перехода кольца ВТСП необходимо его подогревать до температуры выше критической ($\sim 100 \div 150$ К) для снятия остаточных замороженных токов и затем охлаждать до нужной температуры.

На данном штоке был испытан кольцевой образец ВТСП из $Y_1Ba_2Cu_3O_{7-\delta}$, приготовленный Л.Миу. Размеры образца и полученная зависимость $I_c = f(T)$ показаны на рис. 4. Шток имеет второй сменный соленоид, позволяющий вставлять его в апертуру (~ 40 мм) большого сверхпроводящего соленоида в гелиевом криостате. В большом соленоиде можно испытывать образцы в магнитном поле $0 \div 8$ Тл.

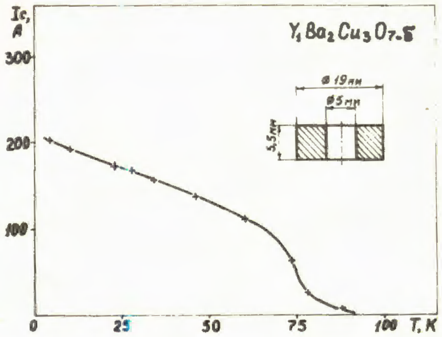

Рис. 4. Зависимость критического тока I_c кольцевого образца из $Y_1Ba_2Cu_3O_{7-\delta}$ от температуры T.

Технические характеристики методики:

1. Диапазон регулирования температуры 4,2 ÷ 150 К с точностью ~ 0,05 ÷ 0,1 К.

2. Стабильность поддержания внешнего магнитного поля с большим соленоидом в криостате 0 ÷ 8 Тл с точностью 0,01 Тл;

3. Диапазон измеряемых критических токов кольцевых образцов ~ 5 ÷ 4000 А с точностью 0,5 А.

4. Размеры кольцевых образцов:

— внутренний диаметр 5 мм;

— внешний диаметр ~10 ÷ 19 мм;

— высота кольца ~5 ÷ 10 мм.

Авторы считают своим долгом выразить благодарность Е.В.Митьковскому за помощь при изготовлении штока, Ю.А.Шишову, В.М.Дробину за полезные обсуждения.

Литература

1. Kim Y.B., Heampstead C.F., Strnad A.R. — Phys.Rev.Lett., 1962, 9, p.306; — Phys.Rev., 1963, 129, p.528.

Рукопись поступила 4 мая 1988 года.

Краткие сообщения ОИЯИ №4 [30]-88 *JINR Rapid Communications No.4 [30]-88*
УДК 538. 945

TEMPERATURE DEPENDENCE OF CRITICAL CURRENT AND I-V CHARACTERISTICS (IVC) IN THE $YBa_2Cu_3O_7$ (Y) AND $Bi_2Sr_2CaCu_2O_8$ (Bi) CERAMICS

V.M.Drobin, E.I.Dyachkov, V.N.Trofimov

The temperature dependence of the transport critical current I_{cr} and the I-V characteristics (IVC) for Y and Bi ceramic samples has been measured. For $0.05 \le T/T_{cr} < 1$, it was found that $I_{cr} \sim (T_{cr} - T)^{\alpha}$ for both the types of high -T_c superconductors, with $\alpha = 1.24$ and 1.48 (two samples) for Y and $\alpha = 2.58$ for Bi. For the low voltage region of the IVC ($V \le 1$ mV), voltage and current could be naturally normalized so that for the nondimensional quantites $U = i^{\gamma(T)}$ both for Bi and Y. At the same time a great discrepancy in the temperature dependence of the characteristic parameters of the IVC fit point to a quite different process of transport current dissipation in Y and Bi.

The investigation has been performed at the Laboratory of High Energies, JINR.

Температурная зависимость критического тока и ВАХ керамик $YBa_2Cu_3O_7$(Y) и $Bi_2Sr_2CaCu_2O_8$(Bi)

В.М.Дробин, Е.И.Дьячков, В.Н.Трофимов

Измерена зависимость от температуры транспортного критического тока $I_{кр.}$ и ВАХ образцов из керамик Y и Bi. В диапазоне $0,005 \le T/T_{кр.} < 1$ для обоих типов ВТСП $I_{кр.} \sim (T_{кр.} - T)^{\alpha}$, где для Y $\alpha = 1,24$ и 1,48 (2 образца), для Bi $\alpha = 2,58$. Для начальных участков ВАХ ($U \le 1$ мВ) можно естественным образом ввести нормировку U и I так, что в безразмерных величинах $U = i^{\gamma(T)}$, как для Bi, так и для Y. В то же время большая разница в зависимости от T характерных параметров позволяет сделать вывод, что механизмы диссипации транспортного тока в этих керамиках весьма различны.

Работа выполнена в Лаборатории высоких энергий ОИЯИ.

The four-terminal measurement of $I_{cr}(T)$, R(T) and the IVC were taken in the set-up which cryogenic part is shown in fig. 1. The ambient magnetic fields were not compensated. Two samples made of one Y pellet and one sample of Bi were used. The superconducting ceramics were prepared by a standard ceramic sintering process, but

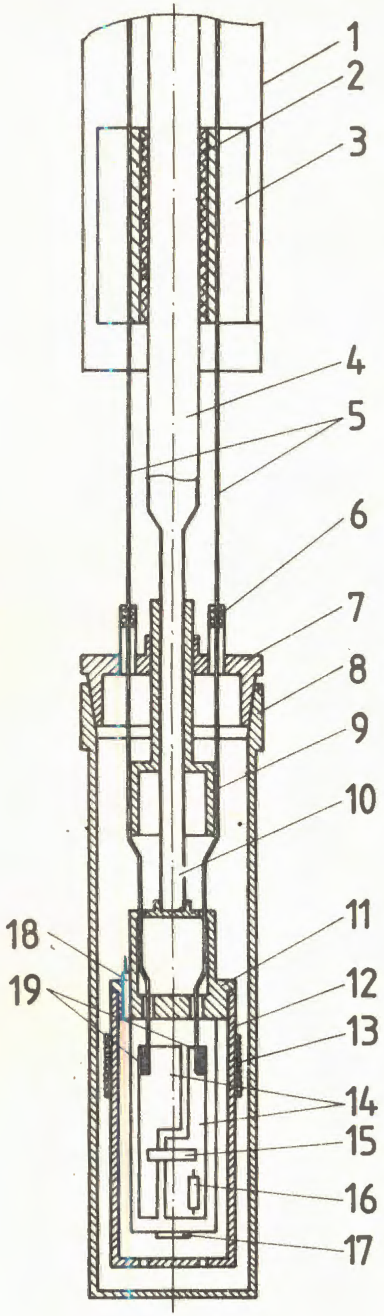

Fig. 1. The lower part of the set-up. 1 – external stainless tube, 2 – insulating gasket 3 – heat drain for terminals and current leads, 4 – constructive stainless tube, 5 – current leads, 6 – leak-tight inlets of current leads, 7, 8 – chamber, 9 – heat drain, 10 – pumping tube, 11 – sample holder, 12 – heat screen, 13 – heater, 14 – current electrodes, 15 – sample, 16 – TVO thermometer, 17 – Hall's sensor, 18 – capacitive thermometer, 19 – current lead soldering.

without pressure before the final sintering for Bi. The dimensions of sample were about 10x2x1 mm^3. The sample chamber (7, 8, fig. 1) is leakproof due to a very suitable cone-cone connection. All measuring wires and current leads pass through LHe or LN_2 and so keep the longitudinal heat conductivity of the insert away. The temperature of the sample holder (11) is stabilized by a capacitive thermometer (18) and the thermostabilizer CT-201 (Intermagnetics) better than about 0.1 K within the whole measuring range from 4.2 K up to T_{cr}. When the lower part of the insert is immersed in LHe, a power of 1.5 W is needed to warm the holder with the sample (15) up to 60 K. The temperature was measured by a TVO-thermoresistor (16) with an absolute accuracy better than 0.7 K at 77 K and 0.05 K at 4.2 K. Two current directions were used to measure the IVC with a voltage resolution of 0.1 μV. The contacts were made in the following way: a thin Ag film was formed initially at Y1 and then the leads were soldered by the Wood's alloy, for Y2 and Bi the contacts were prepared by rubbing in the Wood's alloy and the liquid alloy In-Ga-Sn ($T_m = +10.3°$ C), respectively. The resistance of a single current contact is:

R, Ohm / T, K	Y1	Y2	Bi
293	1,3	≤ 2	2
10	≤ 0.1	5	≤ 0.15

The critical current was estimated graphically from the IVC at a voltage level of 1 μV and is denoted as $I_{cr.\,1}$. Over the range $0.05 \leq$ $\leq T/T_{cr} < 1$ the results can be well expressed by the formula

$$I_{cr.\,1} = A(T_{cr} - T)^{\alpha}, \qquad (1)$$

where $T_{cr} = 86.3$ K for Y and $T_{cr} = 78$ K for Bi. In the $\ln I_{cr}$ - $\ln(T_{cr}$ - -$T)$ plot the straight line corresponds to (1), as shown in fig. 2 (the current unit is mA). The points marked with arrows were obtained with the samples directly immersed in LHe. Two points in the circle demonstrate the overheating effect for Y2 with high resistivity contacts at low temperatures, where the thermal power dissipated in each contact was about 100 mW. As is seen in fig.3, the critical temperature estimated from fitting $I_{cr}(T)$ by (1) coincides for Bi with that one obtained graphically from R(T) and differs by 1.7 K for Y. In accordance with (1) and fig. 2, the critical current density can be expressed as:

$$\begin{aligned}
&\text{Y1} \quad I_{cr.\,d.}(T) = 3.12 \cdot 10^{-3}(T_{cr} - T)^{1,48} \quad [A \cdot cm^{-2}] \\
&\text{Y2} \quad I_{cr.\,d.}(T) = 2.98 \cdot 10^{-2}(T_{cr} - T)^{1,24} \quad [A \cdot cm^{-2}] \qquad (2) \\
&\text{Bi} \quad I_{cr.\,d.}(T) = 3.28 \cdot 10^{-4}(T_{cr} - T)^{2,58} \quad [A \cdot cm^{-2}] .
\end{aligned}$$

The difference in $I_{cr.\,d.}$ and in α for Y1 and Y2 may be caused by heating Y1 while forming the Ag-contacts ($\simeq$ 300° C, 5 sec). For the IVC—measurements a previously fixed current was supplied for a while of 1-3 sec and the voltage was measured by a digital voltmeter. For these data processing the IVC were expressed in a double logarithmic plot $\ln U$ - $\ln(I - I_{cr})$, where the units of U and I were in μV and mA, respec-

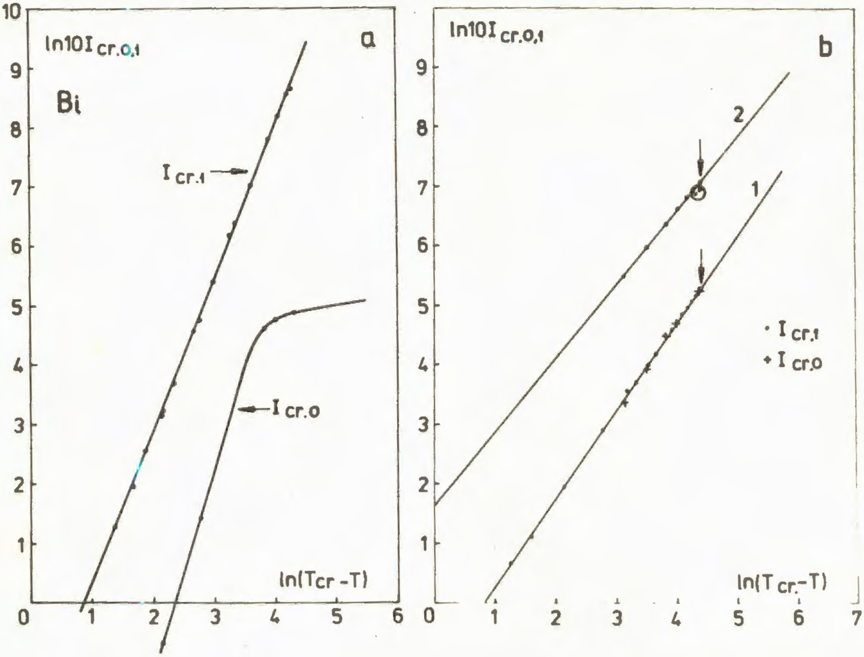

Fig. 2. $I_{cr.1}$ *and* $I_{cr.0}$ *VS temperature: a) Bi, b) 1 – Y1, 2 – Y2.*

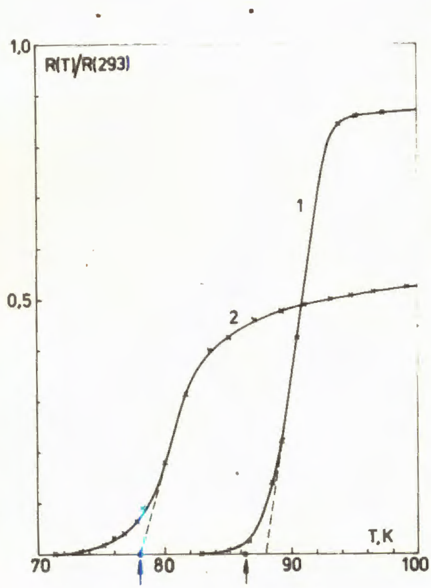

tively. The value of $I_{cr.1}$ was used as a first approximation for I_{cr}. A certain value of I_{cr} was found to exist for each $T < T_{cr}$, when the corresponding IVC can be expressed in such a plot by a straight line. This current is denoted as $I_{cr.o}$. It is obvious that $I_{cr.o}$ will be the critical current for $U \to 0$, if the $U(I)$ – dependence can be extrapolated to $U < 1\,\mu V$. Thus, a number of straight lines can be obtained

Fig. 3. SN – transition of the samples. 1 – Y1, 2 – Bi. The arrows show critical temperatures obtaind from fitting $I_{cr.}(T)$.

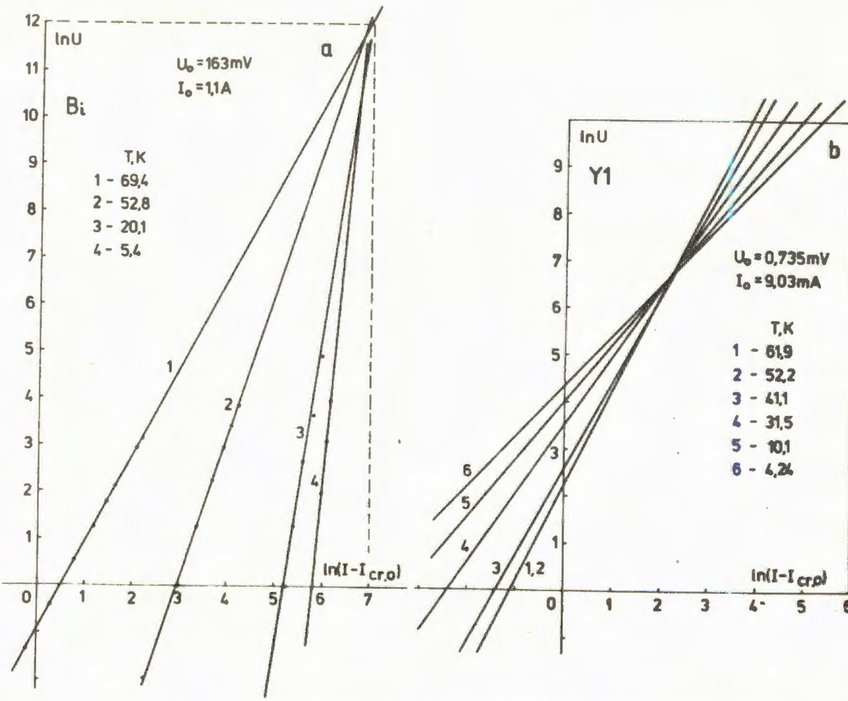

Fig. 4. The low voltage (U < 1 mV) parts of the IVC: a) Bi, b) Y1.

for different temperatures (fig. 4). As is seen, these lines pass through nearly one point and so the normalized quantities can be used: $u = U/U_o$ and $i = (I - I_{cr,o})/I_o$, where $U_o = 163 \cdot 10^3\ \mu V$, $I_o = 1{,}1 \times 10^3$ mA for Bi and $U_o = 735\ \mu V$, $I_o = 9.03$ mA for Y1. In the new ln u — ln i coordinates all the IVC pass through the origin and the expression for the IVC is extremely simple:

$$u = i^{\gamma(T)} \quad (3)$$

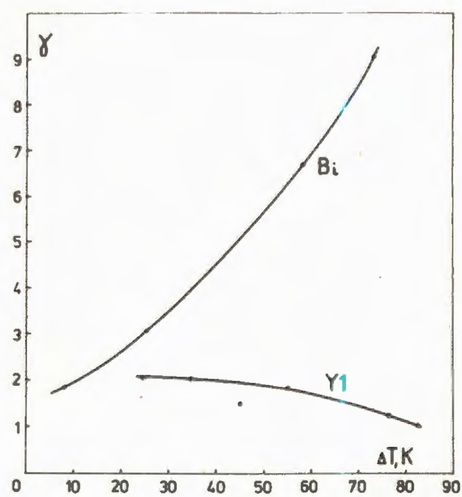

Fig. 5. γ VS temperature.

The temperature dependences of $I_{cr.o}$ and γ are shown in fig. 2 and 5, respectively. A great difference in these curves for Bi and Y is quite obvious.

Conclusions

For both the types of high-T_c superconductors $I_{cr.tr} = A(T_{cr} - T)^{\alpha}$ over the range $0.05 \leq T/T_{cr} < 1$, but for Y $\alpha < 2$ while for Bi $\alpha > 2$. It is known that $\alpha = 2$ corresponds to a SNS-type weak link and so the transport critical current is probably limited by different reasons in these ceramics. Although the IVC for Y and Bi can be expressed by the same formula (3), the temperature dependences of $I_{cr.o}$ and γ for these ceramics are not similar. This points to different processes of current dissipation in accordance with the previous conclusion.

We are indebted to O.Zamolodchikov for the ceramics samples and E.Fischer for usefull discussions.

Received on June 1, 1988.

УДК 538. 945

SQUID OPERATING AT LIQUID NITROGEN TEMPERATURES

V.F.Bobrakov, B.V.Vasiliev, V.N.Polushkin

A two-hole rf-squid fabricated from high-temperature superconducting yttrium-based ceramic is described. Squid operates at liquid nitrogen temperatures and demonstrates all principal features of rf-squid signal. At high frequency the noise level of the high-T_c squid is only three times as much as the corresponding level of the commercial helium rf-squid. The 1/f-noises begin from approximately 100 Hz so that at low frequencies the high-T_c squid sensitivity is by 1.5 order less than the helium squid sensitivity.

The investigation has been performed at the Laboratory of Neutron Physics, JINR.

Сквид, работающий при азотной температуре

В.Ф.Бобраков, Б.В.Васильев, В.Н.Полушкин

Описан двухиндуктивный радиочастотный сквид, изготовленный из высокотемпературной керамики $Y_1Ba_2Cu_3O_7$. Сквид функционирует при температуре жидкого азота, проявляя все основные особенности сигнальной характеристики, присущие радиочастотному сквиду. Уровень шумов высокотемпературного сквида в диапазоне высоких частот примерно в три раза превышает соответствующий уровень низкотемпературного сквида. Шумы типа 1/f начинаются примерно от 100 Гц так, что на низких частотах чувствительность высокотемпературного сквида примерно на полтора порядка хуже чувствительности низкотемпературного сквида.

Работа выполнена в Лаборатории нейтронной физики ОИЯИ.

1. Introduction

The conventional low-temperature squids are the most sensitive devices used for precision measurement of magnetic fields, magnetic field gradients, voltage and other parameters that can be transformed into magnetic ones. However, the wide practical use of such squid is limited because its operation requires liquid helium.

The high-temperature superconductors (HTS) discovery has promised to make a revolution in the measurement technique by widespread application of high sensitive squid-based devices operating at liquid nitrogen temperatures. Therefore, the efforts in creating the HTS squids were made at several laboratories of many countries. The first success in this area was the development of the so-called bulk-squid [1-4] that is a lump of HTS ceramic with rf-coil wrapped round it. The magnetic field generated by the coil destroys a number of weak links between the superconductor grains which causes the reaction similar to response of conventional rf-squid, though it is accompanied by very large noises. These noises are at the level of 10^{-9} T/Hz$^{1/2}$ that is some four orders more than low-temperature squid noises which makes this squid interesting only as a demonstration model.

The more sensitive low-temperature squids are the thin-film dc-squids [5]. Nevertheless the high-temperature thin-film squids are not created up to date. In spite of the efforts made in this area the best thin-film squids operate below 60 K with the same sensitivity as the bulk-squids [6].

To date the most widely applied are low-temperature rf-squids that combine high sensitivity (up to 10^{-13} T/Hz$^{1/2}$ in the white noise region) with reliability and ease of operation. At present there are created the HTS rf-squids operating at 78 K with sensitivity level of 10^{-11} - 10^{-12} T/Hz$^{1/2}$ [7,8].

The purpose of this paper is to describe the HTS rf-squid with sensitivity approximating to 10^{-13} T/Hz$^{1/2}$.

2. Squid Preparation

This squid was made from $Y_1Ba_2Cu_3O_7$ ceramic obtained by standard proceedings through solid-state reaction method [9]. Temperature dependence of the ceramic sample resistance measured by usual four-contact method have shown that it becomes fully superconductive at temperature about 90 K (fig. 1).

Before the last annealing this ceramic powder was pressed into pellets. In these pellets for squid preparation there were drilled holes a little more than 1 mm in diameter and there was filed a weak-junction of about 10 microns thick. In this way there were made both one-hole and two-hole squids. Approximately every fifth squid was operating well.

The squid parameters were measured on standard equipment designed for conventional low-T_c squids and fabricated by the Experimental Physics Facilities Division (EPFD) of our Institute [10]. The measurements were performed in a standard transport liquid nitrogen dewar. For elevated temperature mesurement the squid attached at the

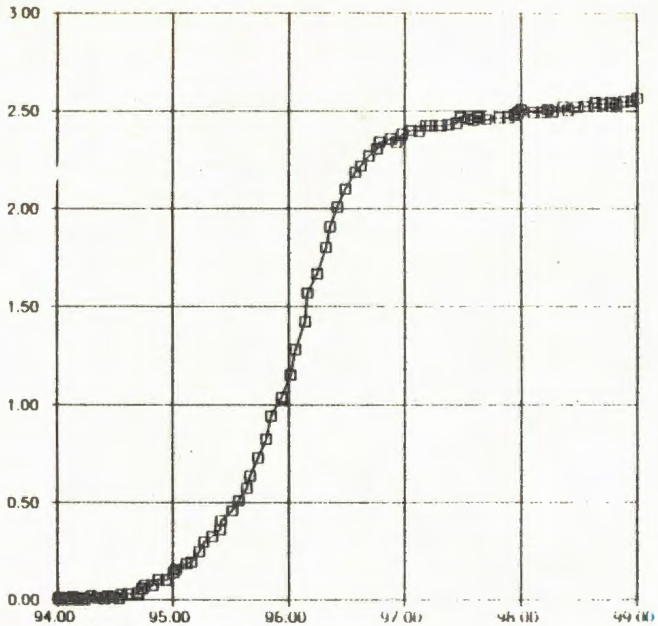

Fig. 1. Temperature dependence of yttrium-based ceramic resistance. X-axis – temperature, K. Y-axis – resistance, arbitrary units.

measurement rod was just lifted to the dewar's neck. In order to protect squid from moisture during the measurement it was placed in a sealed valve. All these proceedings have provided ceramic squid operation for several cooling-heating cycles. There was observed some degradation of the contact critical current after cycling, but such squids have lasted for 10 cycles and more. Some of the squids have operated well only at elevated temperature, its critical current at nitrogen temperature being too large.

In order to suppress the external noise influence squid in nitrogen dewar was screened by mu-metall magnetic shield that reduced earth magnetic field to 10^{-8} T and the external noise to a low enough level. However, it was observed earlier that the magnetic field within the shield had a slow drift and fluctuated, so the squid sensitivity measured in such conditions could be found lower influenced by these fluctuations.

3. Results

In order to test the squid there were measured its voltage-current characteristics first. There was as usual modulated squid pumping amplitude which gave a standard knee-picture well known for low-temperature rf-squids and permitting to optimise with the "naked eye" squid-circuit coupling. For example, fig. 2 shows 2-hole ceramic squid voltage-current characteristic received at liquid nitrogen temperature. The squid applied magnetic field modulation at optimal pumping gave the conventional "triangular pattern". This triangular signal with about $1.6 \cdot 10^{-9}$ T period and amplitude about 10 μV received in a bandwidth 1kHz at first three plateaus in a 2-hole ceramic squid at 78 K is shown in fig. 3. These measurements have shown large portion of 1/f – noises in the spectrum originating at much higher frequencies than 1/f-noises of low-temperature rf-squid. Figure 4 shows Fourier-spectrum for 2-hole ceramic rf-squid noises received at liquid nitrogen temperature (upper curve). At the same figure there is shown for comparison Fourier-spectrum of standard (made in EPFD of JINR) 2-hole helium-temperature rf-squid (lower curve). The noise measurements were carried out under different conditions: niobium squid was screened by perfect superconducting shield and ceramic one screened by mu-metal shield which could affect the measurements.

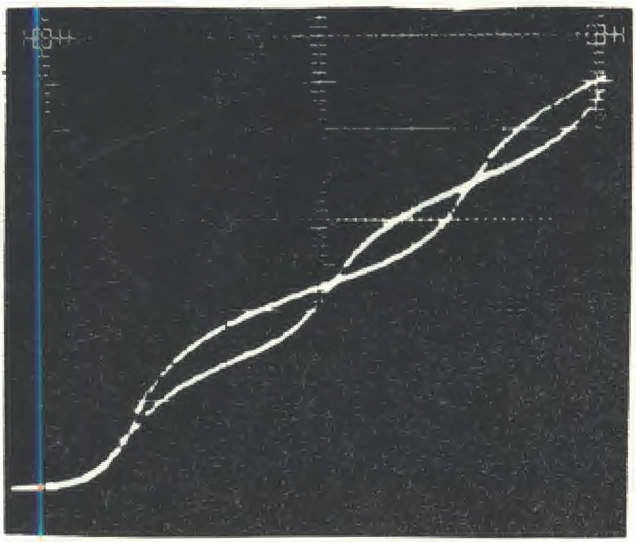

Fig. 2. Voltage-current characteristic of ceramic 2-hole rf-squid, operating at 78 K. X-axis – squid pumping amplitude. Y-axis – squid signal amplitude.

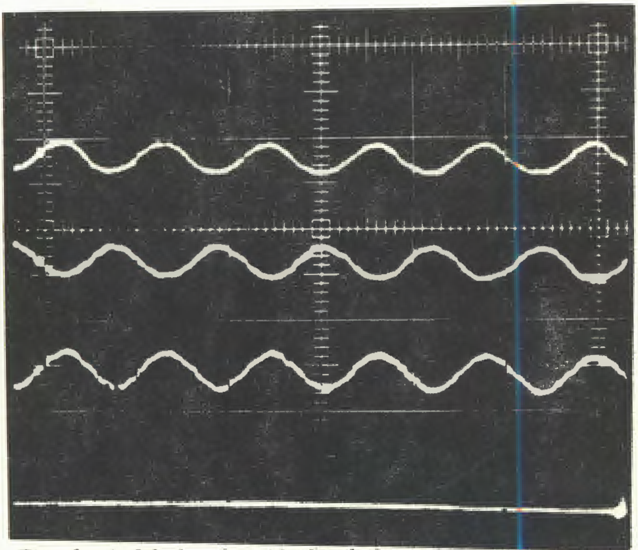

Fig. 3. A 2-hole rf-squid signal dependence on applied external magnetic field, recieved in the first 3 plateaus. Operating temperature – 78 K. Bandwith – 1KHz. X-axis – magnetic field, 3.1 nT/div. Y-axis – squid signal, 20 μV/div.

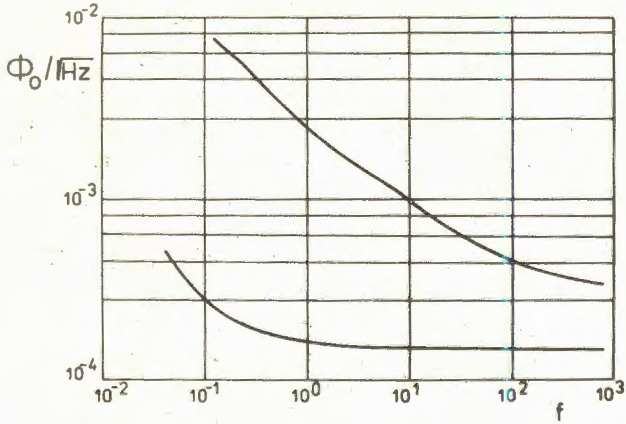

Fig. 4. Fourier-spectrum of ceramic 2-hole rf-squid at 78 K (upper curve) and of standard low-temperature 2-hole rf-squid at 4 K (lower curve). X-axis – frequency, Hz. Y-axis – noise density, $\phi_0/Hz^{1/2}$.

4. Conclusions

The ceramic squid 1/f-noises are so large because the weak-link area has probably a number of intergrain contacts switching quite at random alike the bulk-squid.

The fact that at high frequencies the ceramic squid noise level at liquid nitrogen temperatures is about $3 \cdot 10^{-4}$ flux quantum (about $5 \cdot 10^{-13}$ $T/Hz^{1/2}$) which is about rf niobium squid noise level at liquid helium temperature is not surprising, because it is well known that the white noise level of niobium squid (about 10^{-4} flux quantum) is defined by its preamplifier.

It should be noted in conclusion that despite a lower sensitivity of the described squid in comparison to its low-temperature analogue, especially at low frequencies, its development has demonstrated that the extremely sensitive HTS squid will be created in the near future. On the other hand the reported squid can be applied because of its rather high sensitivity and ease of operation, for instance, in field trial for earth magnetic field anomaly measurements. Furthermore, it seems that making use of method described above one can develope a 2-hole squid with unequal holes. Such squid can be used to handle several problems in solid-state physics and probably in magnetic cardiography.

References

1. Colclough M.S. et al. — Nature, 1987, 328, p.47.
2. Pedrum C.M. et al. — Appl. Phys. Lett., 1987, 51, p.1364.
3. Tichy R. et al. — Jnl. Low Temp. Phys., 1988, 70, p.187.
4. Gallap J.C. et al. — Phys. Lett., 1988, to be published.
5. Tesche C.D. et al. IEEE Trans. on Magn. 1985, No.2,. v.Mag-21, p.1932.
6. Koch R.H. et al. — Appl. Phys. Lett., 1987, 51, p.200.
7. Zimmermen J.E. et al. — Appl. Phys. Lett., 1987, 51, p.617.
8. Harrop S. et al. — Materials of $HTSM^2$ S-Interlaken, March, 1988.
9. Васильев Б.В., Лущиков В.И., Сиколенко В.В. Краткие сообщения ОИЯИ, №2 [28] -88, Дубна, 1988.
10. Бобраков В.Ф., Васильев Б.В. ОИЯИ, Р13-85-20. Дубна, 1985.

Received on April 26, 1988.